Graduate School ETD Form 9
(Revised 12/07)

PURDUE UNIVERSITY
GRADUATE SCHOOL
Thesis/Dissertation Acceptance

This is to certify that the thesis/dissertation prepared

By Ann Marie Goulding

Entitled
BIOCHEMICAL APPLICATIONS OF DSRED-MONOMER UTILIZING FLUORESCENCE AND METAL-BINDING AFFINITY

For the degree of Doctor of Philosophy

Is approved by the final examining committee:

Dr Sapna K Deo
Chair

Dr Kyungsoo Oh

Dr Amy Davidson

Dr Garth Simpson

To the best of my knowledge and as understood by the student in the *Research Integrity and Copyright Disclaimer (Graduate School Form 20)*, this thesis/dissertation adheres to the provisions of Purdue University's "Policy on Integrity in Research" and the use of copyrighted material.

Approved by Major Professor(s): Dr Sapna K Deo

Approved by: Dr Martin O'Donnell May 20, 2010
Head of the Graduate Program Date

Graduate School Form 20
(Revised 1/10)

PURDUE UNIVERSITY
GRADUATE SCHOOL

Research Integrity and Copyright Disclaimer

Title of Thesis/Dissertation:

BIOCHEMICAL APPLICATIONS OF DSRED-MONOMER UTILIZING FLUORESCENCE AND METAL-BINDING AFFINITY

For the degree of Doctor of Philosophy

I certify that in the preparation of this thesis, I have observed the provisions of *Purdue University Teaching, Research, and Outreach Policy on Research Misconduct (VIII.3.1)*, October 1, 2008.*

Further, I certify that this work is free of plagiarism and all materials appearing in this thesis/dissertation have been properly quoted and attributed.

I certify that all copyrighted material incorporated into this thesis/dissertation is in compliance with the United States' copyright law and that I have received written permission from the copyright owners for my use of their work, which is beyond the scope of the law. I agree to indemnify and save harmless Purdue University from any and all claims that may be asserted or that may arise from any copyright violation.

Ann Marie Goulding

Printed Name and Signature of Candidate

May 20, 2010

Date (month/day/year)

*Located at http://www.purdue.edu/policies/pages/teach_res_outreach/viii_3_1.html

BIOCHEMICAL APPLICATIONS OF DSRED-MONOMER UTLIZING FLUORESCENCE AND METAL-BINDING AFFINITY

A Dissertation
Submitted to the Faculty
of
Purdue University
by
Ann Marie Goulding

In Partial Fulfillment of the
Requirements for the Degree
of
Doctor of Philosophy

August 2010
Purdue University
Indianapolis, Indiana

ACKNOWLEDGEMENTS

I would like to thank Dr Sapna Deo, for her guidance, brilliance and patience, while serving as my advisor; I could not have succeeded without her. Additionally, everyone who has also worked in this research group has assisted me in completing the work presented in this thesis. Specifically, David Broyles, Kyle Cissell and Eric Hunt have offered advice, information, and an extra pair of hands, which has been invaluable. The staff in the chemistry department, Beverly Hewitt and Kitty O'Doherty, have also offered immeasurable help with the many administrative questions that have arisen throughout. I would like to also thank Dr Amy Davidson, Dr Garth Simpson, and Dr Kyungsoo Oh for serving on my thesis committee, and all of their help and suggestions throughout this process. Finally I need to thank my friends and family for all of their support and love and patience for the last five years. My parents; James and Janet, Mark and Alix, Brooke, Lenny and Christian, Dallas, and Kristin for allowing me to be as crazy as I needed to be while offering me free food, wine, advice, love, and distractions, I appreciate every minute.

TABLE OF CONTENTS

Page

LIST OF TABLES

Table Page

LIST OF FIGURES

Figure Page

Figure Page

LIST OF ABREVIATIONS

GFP	Green Fluorescent Protein
RFP	Red Fluorescent Protein
ε	Extinction Coefficient
$\lambda_{excitation}$	Excitation wavelength maxima
$\lambda_{emission}$	Emission wavelength maxima
τ_0	Lifetime of the fluorophore
pSKD1	Plasmid coding for DsRed-Monomer
pSKD104	Plasmid coding for CaM-DsRed-Monomer
pSKD104TEV	Plasmid coding for CaM-TEV-DsRed-Monomer
pSKD105	Plasmid coding for M13-DsRed-Monomer
pVUC-1	Plasmid coding for spinach calmodulin
CaM	Calmodulin
M13	Skeletal muscle light chain kinase peptide
TEV	Tobacco etch virus
kDa	Kilo-Daltons
K_d	Dissociation constant
K_{sv}	Stern-Volmer constant
K_q	Quenching rate constant

ABSTRACT

Goulding, Ann Marie. Ph.D., Purdue University, August 2010. Biochemical Applications of DsRed-Monomer Utilizing Fluorescence and Metal-Binding Affinity. Major Professor: Sapna K. Deo.

The discovery and isolation of naturally occurring fluorescent proteins, FPs, have provided much needed tools for molecular and cellular level studies. Specifically the cloning of green fluorescent protein, GFP, revolutionized the field of biotechnology and biochemical research. Recently, a red fluorescent protein, DsRed, isolated from the *Discosoma* coral has further expanded the pallet of available fluorescent tools. DsRed shares only 23 % amino acid sequence homology with GFP, however the X-ray crystal structures of the two proteins are nearly identical. DsRed has been subjected to a number of mutagenesis studies, which have been found to offer improved physical and spectral characteristics. One such mutant, DsRed-Monomer, with a total of 45 amino acid substitutions in native DsRed, has shown improved fluorescence characteristics without the toxic oligomerization seen for the native protein. In our laboratory, we have demonstrated that DsRed proteins have a unique and selective copper-binding affinity, which results in fluorescence quenching. This copper-binding property was utilized in the purification of DsRed proteins using copper-bound affinity columns.

The work presented here has explored the mechanism of copper-binding by DsRed-Monomer using binding studies, molecular biology, and other biochemical techniques. Another focus of this thesis work was to demonstrate the applications of DsRed-Monomer in biochemical studies based on the copper-binding affinity and

fluorescence properties of the protein. To achieve this, we have focused on genetic fusions of DsRed-Monomer with peptides and proteins. The work with these fusions have demonstrated the feasibility of using DsRed-Monomer as a dual functional tag, as both an affinity tag and as a label in the development of a fluorescence assay to detect a ligand of interest. Further, a complex between DsRed-Monomer-bait peptide/protein fusion and an interacting protein has been isolated taking advantage of the copper-binding affinity of DsRed-Monomer. We have also demonstrated the use of non-natural amino acid analogues, incorporated into the fluorophore of DsRed-Monomer, as a tool for varying the spectral properties of the protein. These mutations demonstrated not only shifted fluorescence emission compared to the native protein, but also improved extinction coefficients and quantum yields.

CHAPTER 1. FLUORESCENT PROTEINS

1.1 Fluorescent Proteins

In recent years a number of optically active proteins have been isolated and examined. These proteins have revolutionized the field of biotechnology and biochemical research. Such proteins emit fluorescence and bioluminescence in a number of ways including autocatalytic chromophore formation, and addition of an interacting substrate. One such family of proteins forms a fluorescently active chromophore from a tri-peptide sequence surrounded by a beta-barrel. These chromoproteins include a green fluorescent protein, GFP, and a red fluorescent protein, DsRed, and their mutants. While fluorescent proteins have offered many advantages to various fields of research, a number of disadvantages have been identified. Many of these proteins form oligomeric structures upon maturation, causing slow maturation and often, cellular toxicity. Additionally many of these naturally occurring proteins show poor extinction coefficients and quantum yields. Various mutagenesis studies have been done on fluorescent proteins, including directed evolution and point mutations, to address these issues, often resulting in improved biological and spectral properties. Fluorescent proteins have been utilized for a number of biochemical and detection studies including cell tracking studies, to explore folding pathways, as qualitative reporters, and labels for analytical applications.

1.2 DsRed

1.2.1 Discovery and Spectral Properties of DsRed

DsRed is a naturally occurring red fluorescent protein, initially isolated in 1999, by Lukyanov and colleagues [1]. The gene for this protein was isolated from the Indo-Pacific sea anemone *Discosoma striata.* It was speculated that such corals contain fluorescent pigments to protect them from harmful UV radiation. This fluorescence also permits conversion of blue light to a longer wavelength suitable for photosynthesis by algal endosymbionts. Organisms living in deeper ocean environments, where ambient light is depleted of low-energy components, need this conversion mechanism from short to longer wavelength light. Therefore the presence of fluorescence activity in coral is crucial to the survival of sea organisms. While corals utilize the red pigments as sunscreen against damaging radiation, we can use these pigments for a number of biochemical studies, based on their red emission spectra.

Lukyanov and coworkers successfully isolated six brightly fluorescent proteins [2], from a number of body parts of the coral. This work resulted in the isolation of genes for six proteins with 26-30 % amino acid sequence identity to GFP. Of the six proteins isolated five of them were green emitting and one red emitting, DsRed. DsRed is composed of 225 amino acid residues with a molecular mass of 25.4 kDa, with an excitation and emission wavelength maximum of 558 and 583 nm, respectively. DsRed shares 26 % amino acid sequence identity with GFP, while the excitation and emission maximum are far red-shifted, indicating distinct differences in the chromophore structures of the two proteins (Table 1).

Table 1: Spectroscopic properties of green fluorescent protein (GFP), tetrameric DsRed-Express, and DsRed-Monomer

	Size (kDa)	$\lambda_{excitation}$ (nm)	$\lambda_{emission}$ (nm)	ε ($M^{-1}cm^{-1}$)	Quantum Yield (%)
GFP	26.9	488	509	55,000	0.60
DsRed-Express	89.0	557	579	38,000	0.40
DsRed-Monomer	26.8	556	586	35,000	0.04 – 0.25

While DsRed demonstrates a number of desirable properties: resistance to photobleaching, pH insensitivity over a wide pH range, stable conformation, and red region emission, a number of limitations have also been identified for this protein. For practical laboratory purposes the most problematic issues of these characteristics include the slow maturation, green emitting intermediate and oligomerization. The chromophore of the tetrameric DsRed takes several days to fully mature, limiting its possible use as a reporter for gene expression studies [3]. DsRed also demonstrates high molecular weight aggregates, as seen for other Anthozoan GFP-like proteins. It has been suggested, based on computational studies that these aggregates form as a result of electrostatic interactions between the negatively charged protein surface and the positively charged, basic, residues at the N-terminus. These limitations described for DsRed have been addressed through a number of mutation studies, utilizing both random and site-directed mutagenesis techniques.

1.2.2 Maturation and Oligomerization of DsRed

The DsRed chromophore is extremely slow to mature, taking several days at room temperature to reach full red expression. This red chromophore forms through a green intermediate, which is seen at about 7 hours post induction. After 48 hours this green

emission completely disappears and red fluorescence reaches > 90 % maximal intensity [3].

Crystallographic studies of DsRed reveal that it exists as a tetramer even at nanomolar concentration. This oligomerization has been the speculated cause of the slow maturation seen for DsRed; since it requires more time for all four chromophores within the tetramer structure to fully mature. It has also been suggested that this tetrameric form may be responsible for DsRed's resistance to photobleaching, which is four to fivefold greater than that of GFP [4, 5].

The DsRed tetramer, based on X-ray crystallography studies, forms from four individual units, each made up of an 11-stranded β barrel with a central helix (Figure 1). This central helix consists of the chromophore and α helical caps on each of the ends of the barrel [6]. Although, as previously stated, DsRed shares only 26 % amino acid sequence identity with GFP, their three dimensional structures are nearly identical. The superimposed structures reveals that the loops in DsRed are shorter than those in GFP, due to a reduced number of amino acids in the comparable loop regions and higher hydrophobicity of the residues present. Further, a pronounced bulge is seen centered around Ser146 in DsRed, a similar bulge is not seen for GFP in this region. Finally residues 97-100 and 140-145 are significantly closer to the chromophore in DsRed, compared to GFP, which probably impacts chromophore formation.

Figure 1: X-ray crystal structure of DsRed [7]

1.3 DsRed-Monomer

1.3.1 Construction of DsRed-Monomer

Since the discovery of DsRed, work has been done to address the limitations seen for the native tetrameric protein; much of this work has focused on the need to create a monomeric mutant. Yanushevich *et al*. [8] developed the first commercially available non-aggregating mutant of DsRed, in 2002. This group focused on mutations at the charged N-terminus of a number of previously described mutants, E57 (V105A, I161T, S197A) [9], E5 (V105A, S197T) [10], and ds/drFP616 [11]. From the results of these initial N-terminally focused studies, further substitutions; R2A, K5E, and K9T, in

different combinations were examined. The R2A showed the greatest effect on the aggregation of the E57 mutant. However, mutant E57-NA with all three of these mutations showed the best results with regard to aggregation and spectroscopic properties, which are comparable to E57. This E57-NA mutant became the first commercially available non-aggregating DsRed, DsRed2.

While Yanushevich's DsRed2 was the first commercially available non-aggregating mutant of DsRed, Campbell *et al.* [4] produced a further monomeric DsRed shortly after. Campbell initially reduced the tetrameric DsRed to a dimer via a single point mutation, I125R. This mutation however led to a decrease in the red fluorescence of the protein with an increase in the green intermediate component, and increased maturation time. Utilizing directed evolution Campbell *et al.* identified mutants of this dimer, which showed the desired optical and physical properties. From this pool of mutants Dimer2 was isolated with 16 additional mutations. These 17 mutations are located at a number of sites within the final protein structure, specifically eight internal to the β-barrel, two at the AB interface, four surface mutations and three that are known to reduce aggregation. From this Dimer2 a tandem dimer, tdimer2, was produced, via a polypeptide linker of 12 amino acids, which demonstrated excitation and emission identical to Dimer2 with an improved extinction coefficient. This increased extinction coefficient was attributed to the presence of the two absorbing chromophores. Through a series of point mutations in this tdimer2, a first generation monomer, mRFP.1, was identified. Further use of directed evolution yielded mRFP1, the first true monomer of DsRed with 33 amino acid substitutions in native DsRed.

This mRFP1 mutant was further improved by Shaner *et al.* [12] through a series of mutation studies and screened both manually and by fluorescence-activated cell sorting (FACS)-based screening. From these mutation studies a number of mutants were isolated which showed differing emission maxima, increased tolerance to N- and C-terminal fusions, improved extinction coefficients, quantum yields and high photostability. While individual improvements were seen for all of the mutants no one mutant showed improvement in all of these areas. This was addressed by a further series of amino acid substitutions, focusing on the residues around the chromophore, leading to

mutant mRFP1.1. The sensitivity of this mutant to N-terminal fusion was addressed by replacing the first seven amino acids with MVSKGEE followed by a four amino acid linker, NNMA (6a-6d). The C-terminal of the protein was also replaced with the last seven residues of GFP (mRFP1.3). Two additional point mutations in this mutant created mRFP1.4, which showed improved chromophore folding.

The work of Yanushevich, Shaner, Campbell and others, described above, lead to the optimized monomeric DsRed, DsRed.M1 described by Strongin *et al.* [13]. This protein DsRed.M1, or DsRed-Monomer, is now commercially available through Clontech. DsRed-Monomer contains 45 amino acid substitutions in native DsRed; it overcomes the oligomerization seen for the native protein. This non-aggregating species was verified via a number of methods, which led to an obtained molecular weight of ~28kDa, consistent with a single DsRed unit. The DsRed monomers generated by both directed evolution and site-specific mutagenesis of amino acid residues have an almost ideal set of properties for biological sensing and analytical applications. A more detailed discussion of the work, which led to the creation of this monomeric DsRed variant, is presented in Appendix A.

1.3.2 Spectral Properties of DsRed-Monomer

While the spectral properties of DsRed-Monomer are less ideal than those seen for the tetrameric DsRed, DsRed-Express (Clontech, Palo Alto, CA), the maturation is much faster. The chromophore of this protein fully matures within hours of induction and shows none of the parasitic green florescence reported for the native DsRed. DsRed-Monomer displays a fluorescence excitation maximum at 556 nm and emission at 586 nm, however the range of quantum yields reported, by a number of groups, for this protein is much lower (Table 1) [4, 13].

1.3.3 X-ray Crystal Structure of DsRed-Monomer

The chromophore of DsRed-Monomer is formed internally from a tripeptide sequence composed of Gln66-Tyr67-Gly68. This chromophore is autocatalytically formed via cyclization and dehydrogenation of the tripeptide (Figure 2). The environment around this chromophore is more polar than that of GFP, consisting of charged residues such as lysine (residues 70, 83, and 163) and glutamine (residue 148) which closely interact with the chromophore [6]. The phenolate oxygen of the chromophore interacts with Ser146 and Lys63, while Gln223 and Asn42 form hydrogen bonds with Gln66. These interactions help position the Gln66, necessary for red fluorescence.

The crystal structure of DsRed-Monomer was generated by Strongin *et al.* [13], the results of these studies are presented in Table 2 and displayed in Figure 3. The crystallized DsRed-Monomer displays spacegroup $P2_12_12_1$ with one molecule in the asymmetric unit. Since native DsRed is a naturally occurring tetramer, as previously discussed, the intermolecular contacts in the DsRed-Monomer crystal lattice differ significantly from those of DsRed, specifically the intermolecular interactions that define the 222 symmetry of the tetramer are completely disrupted. Additionally, the intersubunit distances and orientations are different from those in the tetramer. Regardless of the numerous amino acid substitutions in this monomer, a total of 45, the structure reveals no gross distortion of the GFP-like fold, seen in the units of the tetramer. The largest conformational distortions appear in the loop regions. There are several surface mutations that disrupt intramolecular interactions in the tetramer and that actually form interactions in the monomer. These include Arg153 and Lys158, which mediate interactions in the polar and hydrophobic interfaces. In the monomer this 153 residue is replaced with a Gln disrupting the salt bridge with Glu100 and forming a new intramolecular hydrogen bond between Gln153 and Lys158. In DsRed-Monomer the Tyr26 fills a void by packing against the service and forming hydrogen bonds with Glu28.

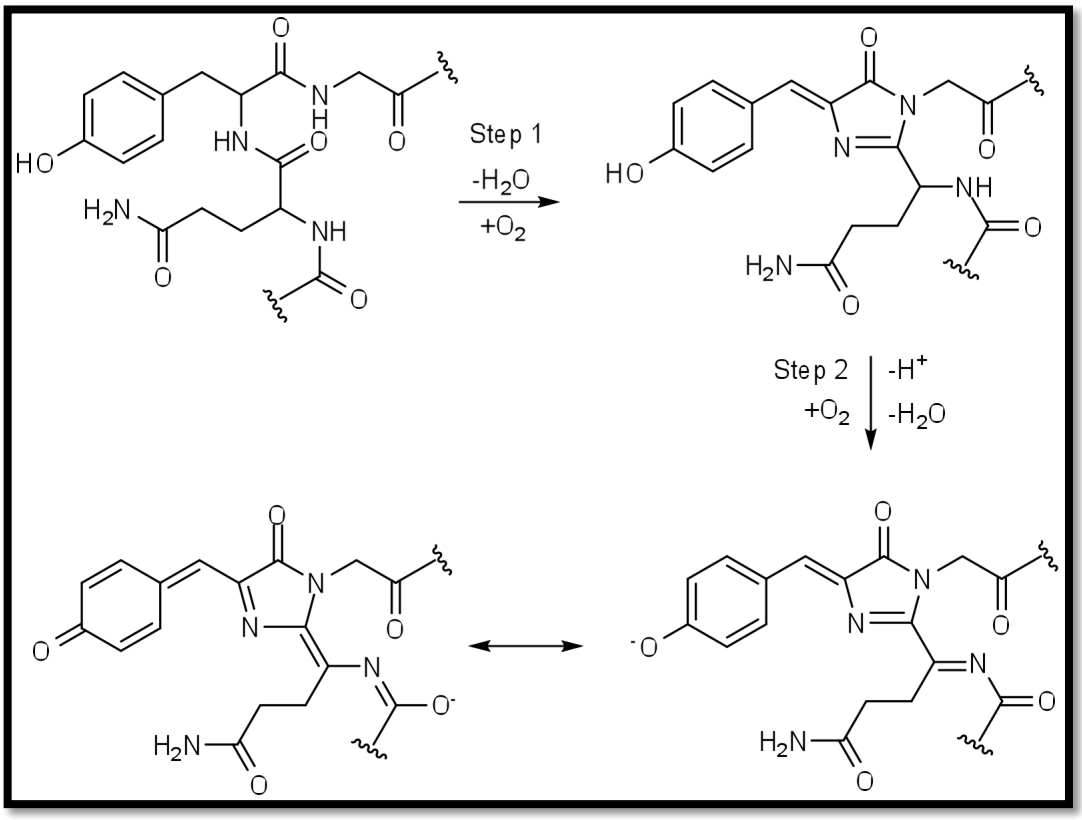

Figure 2: The chromophore of DsRed, generated autocatalytically in the presence of molecular oxygen from the Gln66-Tyr67-Gly68 tripeptide [6]

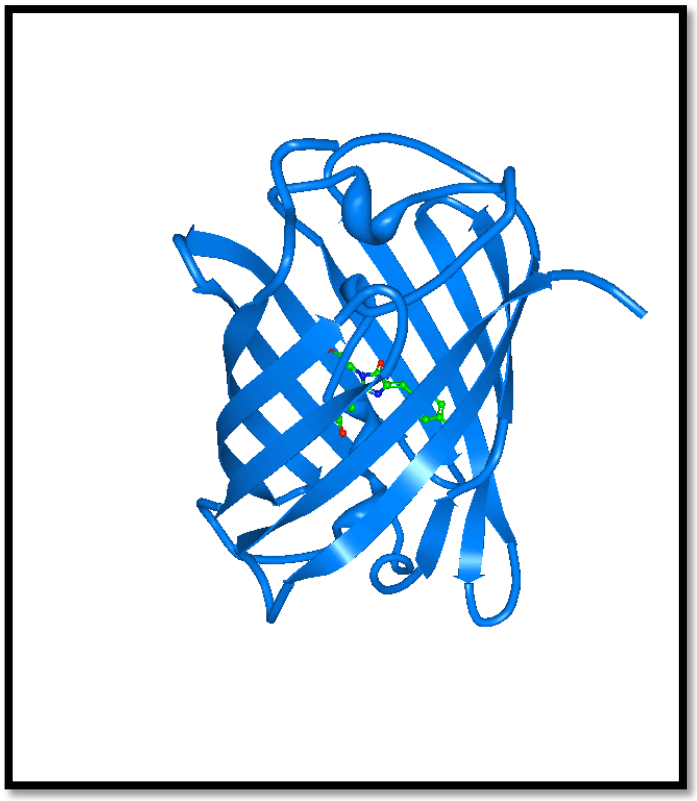

Figure 3: X-ray crystal structure of DsRed-Monomer [13]

Table 2: X-ray crystal structure data for DsRed (wild type) and DsRed-Monomer [7, 13]

	DsRed (wild type)	DsRed-Monomer
Space group	$P2_1$	$P2_12_12_1$
Unit cell dimensions (Å)	a=55.7, b=127.2, c=57.1 β=100.4°	a=38.9, b=62.2, c=81.9 α=β=γ=90°
Molecules per asymmetric unit	4	1
X-ray source	ALS beamline 5.0.1	APS 14BM-C
Wavelength (Å)	1.000	0.900
Resolution range (Å)	40-1.4 (1.45-1.40)	50-1.59 (1.65-1.59)
Total/unique observations	363894/148353	181 013/27 397
Completeness (%)	96.8 (93.2)	99.7 (99.6)
<I/sigI>	18 (1.9)	43.7 (6.7)
R_{sym} (%)	5.1 (35.7)	5.5 (39.7)

Further deviations in structure from the tetramer were seen in and around the chromophore of the DsRed-Monomer. Specifically a +10 degrees and -11 degrees deviation from coplanarity from the phenolate plane is seen for the chromophore of the monomer. Additionally the Lys70 no longer interacts with Glu215 or Ser197; instead this residue forms a salt bridge with Glu148. Replacing this Lys70 side chains, a water molecule mediates a network of hydrogen bonds between Glu215, Ser197 and the repositioned Lys70. This Lys residue may also adopt multiple conformations and sweep out in an arc above the chromophore. This Lys70 may also be further modulated by the V71A and S179T.

1.3.4 Advantages of DsRed-Monomer

Through the use of point mutations and directed evolution a true monomer of DsRed, DsRed-Monomer, is now commercially available. This protein offers a variety of spectral characteristics with advantages and disadvantages compared to the commercially available tetramer of DsRed. This protein offers strong emission in the red region of the spectrum, ideal for use as markers for gene expression and protein localization in biological systems, due to decreased background signal in the red region of the spectrum, as compared to the green, for most organisms. Additionally this monomer demonstrates no aggregation or oligomerization and allows for full maturation of the chromophore within hours.

1.4 Copper-Binding Characteristics of DsRed and its Variants

DsRed and its mutants have demonstrated the ability to bind copper ions, resulting in a quenching of their fluorescence [14, 15]. Kopelman and colleagues [15] developed a sensitive fluorescent probe for the detection of mono- and divalent copper ions, utilizing wild type DsRed. Copper ions are important for numerous biological and biosynthesis pathways, copper-containing proteins are key players in the human nervous system and many neurological conditions are linked to defects in copper homoeostasis. For example Menkes' and Wilson's disease, both neurological disorders, are caused by an inability to metabolize copper. Additionally copper has been widely used in industrial processes and is a source of pollution in the environment, micromolar amounts of copper are toxic within a biological environment. The availability of copper detection methods for biological and environmental samples is of great significance.

The work of Kopelman and colleagues yielded a nanomolar detection limit, with 90 % fluorescence quenching at 2.5 μM Cu^{2+} and 75 % at 2.5 μM Cu^{+}. K_d values for this tetrameric DsRed from this work were found to be 540 ± 90 nM and 450 ± 60 nM for Cu^{2+} and Cu^{+} respectively. The binding, and subsequent fluorescence quenching, was

also found to be very selective to copper ions, compared to Mn^{2+}, $Fe^{2+/3+}$, Co^{2+}, Ni^{2+}, Cd^{2+}, Ag^{2+}, Hg^{2+}, Pb^{2+}, Mg^{2+}, and Ca^{2+}. Finally, studies indicated that this quenching was reversible, with up to 90 % of fluorescence retrieved, within two minutes, upon the addition of a metal chelator such as ethylenediaminetetraacetic acid (EDTA). Such studies indicate that the tetrameric DsRed contains a copper-binding site, which is not present in other fluorescent proteins, for example GFP.

Further studies by Eli and Chakrabartty [14] explored the metal binding affinity of red shifted DsRed mutants. One mutant, tetrameric Rmu13 (F91L, V105A) demonstrated copper sensitivity with a binding constant of ~11 μM for this mutant and ~15 μM for DsRed. Eli *et al.* demonstrated that their copper sensor, utilizing the Rmu13 mutant, could reliably detect Cu^{2+} at concentrations between 0.1 and 100 μM, *in vitro* or *in vivo.* Initial work in our laboratory has demonstrated the selective copper-binding affinity and fluorescence quenching of DsRed-Monomer. Rahimi *et al*. reported that the fluorescence of DsRed-Monomer was quenched by greater than 90 % in the presence of 500 μM of copper ions (Figure 4). This work lead to a detection limit for Cu^{2+} of 0.8 μM [16], indicating that DsRed-Monomer can be used in the development of a copper sensor. This study also demonstrated that the metal affinity seen for DsRed-Monomer was selective for copper, compared to a number of other mono- and divalent metals, namely calcium, magnesium, iron, cobalt, nickel, zinc, and barium [17].

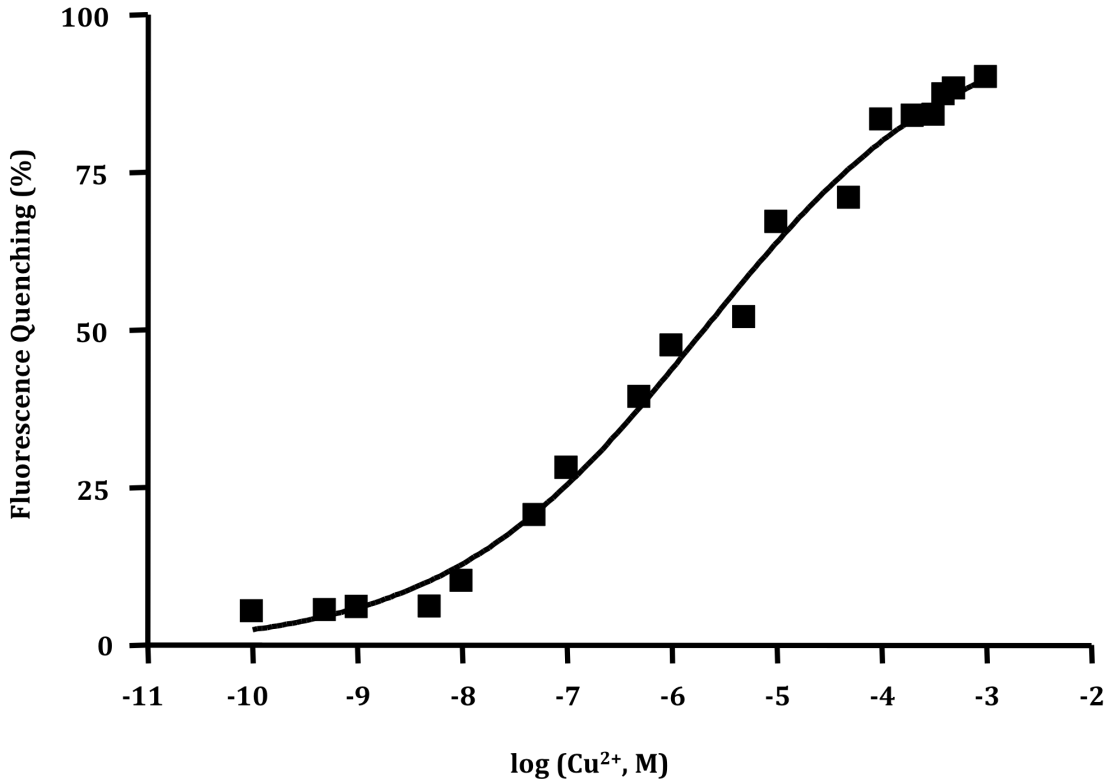

Figure 4: Fluorescence quenching of DsRed-Monomer in the presence of increasing concentrations of Cu^{2+} [17]

Further, this copper-binding affinity has also been utilized by Rahimi *et al.* [16] as an efficient purification strategy for DsRed-Monomer. The crude DsRed-Monomer was bound to an immobilized copper charged column and eluted with an imidazole-containing buffer (Figure 5). Purification of DsRed-Monomer, using this strategy, demonstrated greater than 95 % purity of recovered protein, and 95 % recovery of total protein [16]. Subsequent work, presented in this thesis, has been done to determine the mechanism of this quenching and to utilize this, and other properties of DsRed-Monomer, for sensing and detection applications.

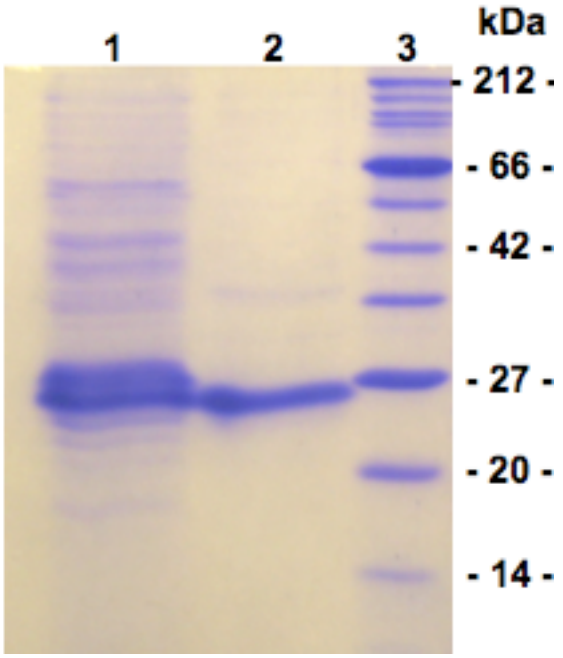

Figure 5: SDS-PAGE gel of copper-affinity purified DsRed-Monomer, crude DsRed-Monomer (lane 1), pure DsRed-Monomer (lane 2), molecular weight protein marker (lane 3) [16]

1.5 Copper-Binding Proteins

Copper is an essential trace element in living organisms. It plays a critical role in the activation of a variety of proteins with functions including electron transfer, oxygen transport in the body and oxygen insertion into a substrate [18]. However, in addition to these necessary functions, free copper ions within the cellular environment can be toxic, even at μM concentrations. As reported by us and other groups DsRed proteins show a unique and selective copper-binding affinity, however in addition to this fluorescent protein a number of naturally occurring copper-binding proteins have also been identified which control these levels of free copper within the cell, restricting their movement. Such proteins are frequently employed within the cellular environment to bind free copper ions, guiding them to their appropriate locations in the cell. Copper-binding proteins can be classified by a number of characteristics, including spectral properties, function, binding site, and binding affinity [19, 20]. These proteins demonstrate a wide

range of copper dissociation constants from 10^{-6} – 10^{-17} M. One such group of copper-binding proteins, the copper chaperones, is divided into three types.

Type 1 "blue" copper proteins have a visible absorption band near 600 nm. These copper enzymes generally contain a four-coordinated, distorted tetrahedral, copper ion. However a five-coordinated copper ion has also been seen for a limited group of these proteins. The structural motif at the active site consists of a $(His)_2CysX$ sequence, where X is normally a Met residue (Figure 6). Type 2 "non-blue" copper proteins, have a visible absorption band between 350 and 420 nm. The copper in this type of proteins is usually found in a square planar or tetragonal coordination. These proteins form their copper-binding site through a number of motifs including $(Cys)_4$, $(His)_4H_2O$, $(His)_2(Tyr)_2(H_2O)$, or $(His)_2(Tyr)_2$ with the copper coordinated to N, O, or S of these residues (Figure 7). Type 3 "binuclear" copper proteins have a strong absorption band near 330 nm. These are characterized by an antiferromagnetically-coupled pair of copper ions (Figure 8), each coordinated by three His residues.

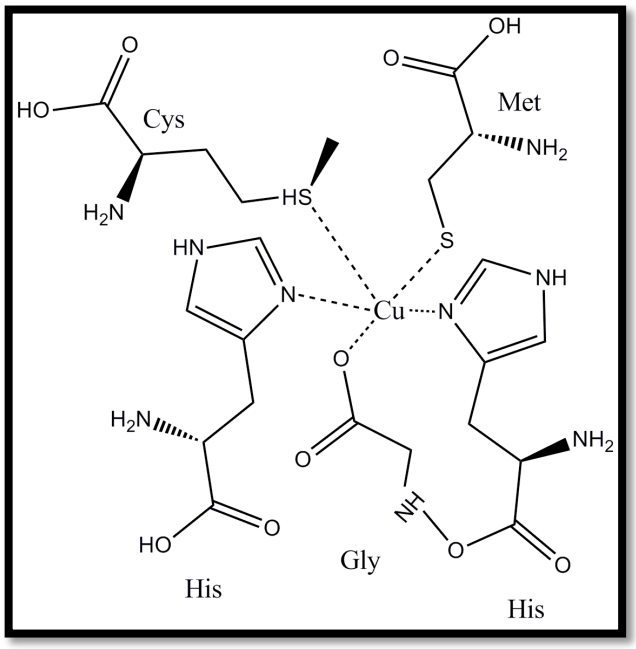

Figure 6: Copper-binding site of azurin, a type 1 copper chaperone [21]

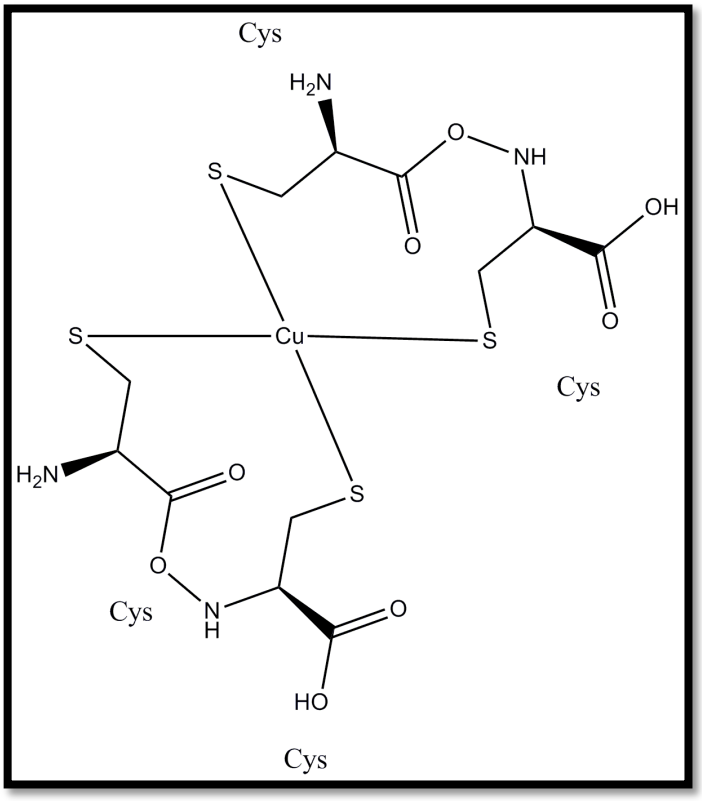

Figure 7: Copper-binding site of HAH1 (Atx1), a type 2 copper chaperone [19]

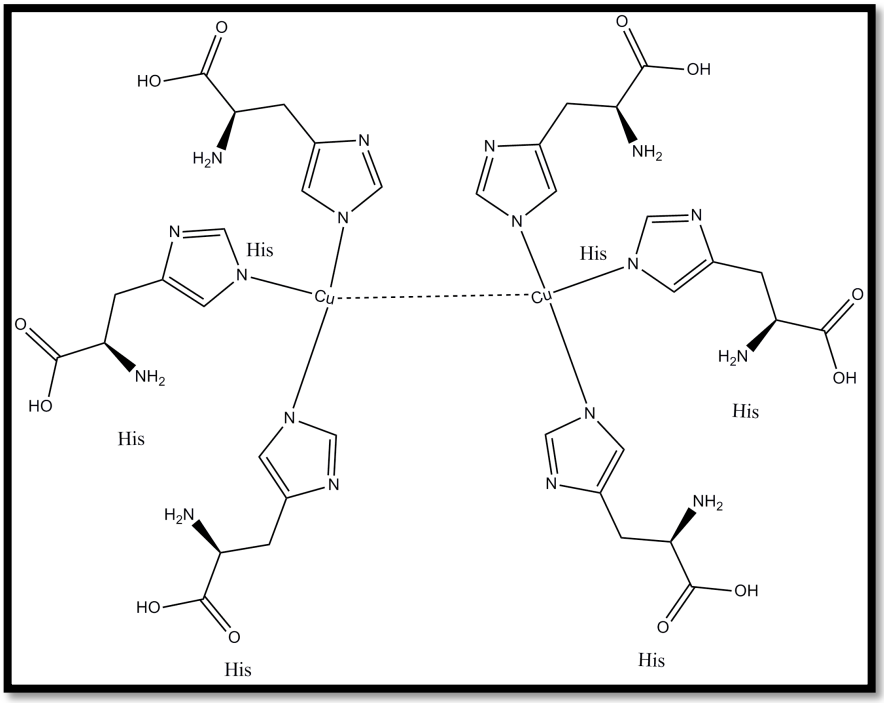

Figure 8: Copper-binding site of hemocyanin, a type 3 copper chaperone, demonstrating the binuclear copper complex [19]

In addition to the binding motifs described above, more complex cooper-binding sites have also been identified for copper chaperones. These copper-binding sites, with di and trinuclear copper centers, display properties indicative of both type 2 and 3 copper chaperones. For example trinuclear copper centers, such as those seen for blue oxidases, which demonstrate type 2 and type 3 properties as well as dinuclear copper centers seen for cytomchrome c oxidase have been described. Copper-binding proteins have been shown to utilize both single and combinations of multiple copper-binding motifs within a single protein. The proteins and binding motifs described above belong to the group commonly referred to as copper chaperones, a second group of copper-binding proteins, so called prion proteins, also demonstrate copper-binding affinity within the cellular environment. These prion proteins form complexes with the copper ions in a 4 coordinated structure, similar to that seen for the type 1 blue copper proteins, from a HGGGQ peptide sequence. A variety of dissociation constants have been reported for prion proteins from 0.03 nM – 100 nM [22-24]. A further copper-binding site, frequently referred to as the copper-binding peptide, demonstrates one of the lowest dissociation

constant of these copper-binding proteins, 1 x 10^{-17} M. This simple tripeptide acts as a quadridentate ligand to create complexes with copper through an amino group, two deprotonated amide groups and an imidazole pyridine nitrogen (Figure 9) [25]. The initial work in this thesis has focused on defining the mechanism of the unique fluorescence quenching seen for DsRed-Monomer in the presence of copper ions. In addition to defining this mechanism, further work aimed at identifying the binding site of this protein has also been explored.

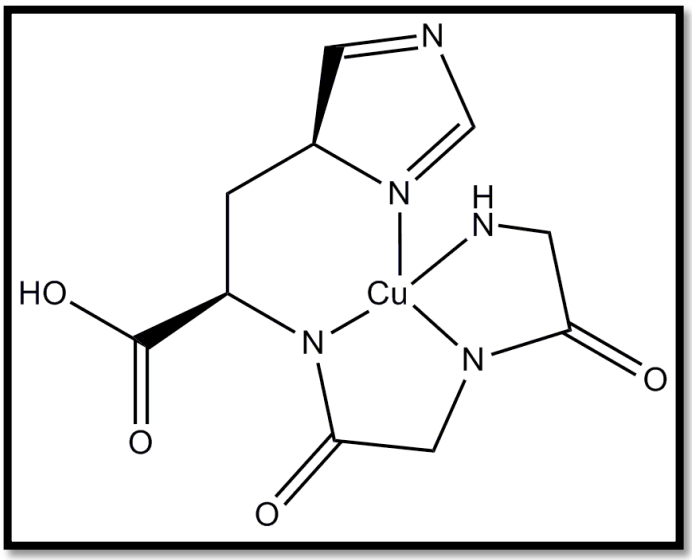

Figure 9: Copper-binding site of the copper-binding peptide, GlyGlyHis

CHAPTER 2. MECHANISM OF COPPER INDUCED FLUORESCENCE QUENCHING OF RED FLUORESCENCE PROTEIN, DSRED-MONOMER

2.1 Introduction

As discussed in the previous chapter, a number of fluorescent proteins have recently been isolated and explored. Isolation and characterization of these proteins has expanded the possible applications of fluorescent proteins into multi-color labeling, resonance energy transfer, and intracellular tracking studies [26-29]. To date, red fluorescent proteins have been mainly employed as genetically encoded fluorescent probes for cellular applications. However, other fluorescent proteins have also been employed in novel applications, for example GFP was employed as an intracellular calcium detector, as a chloride indicator, as a pH indicator and in ligand monitoring using receptor inserted GFPs [30-35]. Only recently we, and others, have found that red fluorescent proteins, namely DsRed and its variants, bind copper ions selectively in the presence of other divalent cations resulting in a quenching of their native fluorescence [14-17]. By relating fluorescence quenching of DsRed with copper concentration, *in vitro* biosensing systems for copper determination have been developed [15, 17]. Moreover, this ability to bind copper ions can now be utilized in the intracellular detection of copper, at μM levels based on the fluorescence of DsRed.

Copper is an important cofactor of several enzymes and plays a significant role in several cellular pathways and disease pathogenesis [36-38]. Therefore, the availability of genetically encodable probes such as DsRed, which can be targeted to specific organelles for detection of copper, would prove highly beneficial. Furthermore, this copper-binding can serve as a unique tool for affinity purification, as well as for cooper sensing. In that

regard, it is essential to understand the binding of copper to DsRed, its mechanism of quenching, and the spectral changes in DsRed proteins in the presence of copper.

In the work presented in this chapter, we have characterized the mechanism of fluorescence quenching of DsRed-Monomer in the presence of copper, using spectroscopic tools. We have also performed studies to identify possible amino acid residues involved in this binding. Sequence comparison with known copper-binding proteins and computational studies have been used to explore possible copper-binding motifs within the protein. DsRed-Monomer was selected for this study because our laboratory has, previously, developed biosensors for copper detection utilizing this DsRed variant [39]. In addition, other copper-binding DsRed proteins, specifically, DsRed2, native DsRed, and Rmu13 share > 80 % identity with DsRed-Monomer, suggesting that DsRed-Monomer may serve as a representative member of the copper-binding family of DsRed proteins.

2.2 Materials and Methods

2.2.1 Protein Expression and Purification

Expression and purification of DsRed-Monomer was performed using previously established protocols. Briefly, the plasmid DsRed-Monomer was obtained from Clontech. This plasmid was transformed into *E. coli*, JM107 and expressed in LB broth. LB media containing 100 μg mL^{-1} ampicillin was prepared. A 5 mL sample of LB was inoculated with the *E. coli* containing the plasmid pSKD1 and incubated overnight in a shaker at 37 °C. The culture was transferred to a 200 mL sample of LB and grown to an OD_{420} of 0.5 and induced with isopropyl-β-D-thiogalactoside (IPTG, 0.5 mM final concentration), and grown for a further 5 h, with shaking, 250 r.p.m., at 37 °C and collected by centrifugation, 4000 r.p.m., for 30 min at 4 °C. The pellet was dissolved in the PBS-binding buffer (100 mM Na_2PO_3, 50 mM NaCl, pH 7.0) and sonicated for 5 min to lyse the cells.

The protein was purified using a Ni Sepharose high-performance affinity column, charged with copper [16]. A volume of 1.5 mL of the Ni Sepharose high-performance beads was centrifuged and the storage ethanol poured off. The beads were resuspended in sterile water and applied to the column. A volume of 2 mL of the stripping buffer (0.02 M sodium phosphate, 0.5 M NaCl, 0.05 M EDTA, pH 7.4) was applied to the column. The column was rotated overnight to fully remove the Ni from the beads. The column was washed with multiple column volumes of sterile water, and 1.5 mL copper sulfate (0.1 M) was applied. The column was again rotated, for at least 2 h to assure full binding of the Cu^{2+} ions to the beads. The column was washed with up to 10 column volumes of PBS-binding buffer to remove all unbound copper. A volume of 1.5 mL aliquots of the crude protein was applied to the column, with the column being rotated for 2 h between additions. The column was again washed with up to 10 column volumes of PBS-binding buffer to remove anything not bound to the copper immobilized column. Wash buffers (0.05 M sodium phosphate, 0.3 M NaCl, ph 8.0, containing 0.001 to 0.01 M imidazole) were used to wash the column. The protein was eluted by the final wash step, with the buffer containing 0.01 M imidazole (0.05 sodium phosphate, 0.3 M NaCl, pH 8.0). The purified protein was collected and dialyzed to remove the imidazole, using PBS buffer (0.05 M sodium phosphate, 0.05 M NaCl, pH 8.0). Protein purity was determined via SDS-PAGE gel electrophoresis and concentration by BioRad assay.

2.2.2 Determination of Dissociation Constant for Cu^{2+}

The purified protein was dialyzed against 20 mM MOPS buffer, pH 7.4, to remove the imidazole. The imidazole-free protein solution was passed through a Chelex-100 column to remove any trace levels of Cu^{2+}. For the binding study 100 μL of different concentrations of a copper solution were added to 100 μL of 1 μM of DsRed-Monomer. The fluorescence readings were obtained and buffer corrected. The fluorescence intensity ratio, $[F/F_0]$, was plotted against the copper concentration to obtain the copper dissociation constant for DsRed-Monomer. This fluorescence was measured

(Varian Cary Eclipse Fluorescence Reader, Palo Alto, CA) by exciting the sample at 556 nm and reading the emission at 597 nm.

2.2.3 Stern-Volmer Plots

A volume of 100 μL of different concentrations of Cu^{2+} solution was added to 100 μL of 1 μM protein in 20 mM MOPS, pH 7.4, in an individual microtiter well. After the addition of the copper, the sample was incubated at a number of different temperatures (16, 25 and 30 °C). Fluorescence readings were recorded for each temperature at each concentration, as described above. Again the results were buffer corrected and plotted.

2.2.4 Spectroscopic Studies

The CD spectrum was obtained for the DsRed-Monomer. A volume of 250 μL of 3.3 μM protein in 20 mM MOPS, pH 7.4, was placed in a 0.2 cm cell and the CD absorption spectra obtained, at room temperature (Jasco J-720 Spectropolarimeter, Tokyo, Japan). A volume of 10 μL of copper was added to the protein to a final concentration of 0.5 mM and the spectra recorded. The collected spectra were again buffer corrected.

The UV-visible spectra were also obtained for DsRed-Monomer. A volume of 1 mL of 3.4 μM in 10 mM MOPS buffer, pH 7.4, was placed in a cuvette and the absorption spectra of the protein recorded (Perkin-Elmer UV/vis/NIR LAMBDA), at room temperature. To this sample 10 μL of copper solution was added, to a final concentration of 0.5 mM, and the absorbance spectra recorded. The spectra were once again buffer corrected.

2.2.5 pH Study

MOPS buffers ranging from pH 5.5 to 10.5 were prepared. A protein solution of 3 μM DsRed-Monomer in 10 mM MOPS buffer, pH 7.4, was mixed with the different pH buffers to obtain a final concentration of 1 μM at the desired pH. Fluorescence intensity was recorded for each of these samples, with and without copper (300 μM).

2.2.6 Metal-binding Prediction Studies

The amino acid sequence of DsRed-Monomer was examined via MetalMine [40], and Metsite [41]. MetalMine compares the target protein sequence with a compiled list of metal binding proteins and enzymes. Metsite looks for metal binding sites within the sequence computationally. MetSite uses a set of neural network classifiers trained to identify potential cation ion sites. MetSite uses relative residue position, to identify possible metal binding sites, and therefore does not require exact side-chain atom placement. This allows the results to be generated for predicted structures.

2.3 Results and Discussion

Recent studies from a number of laboratories have found that DsRed and its variants bind Cu^{2+} selectively, resulting in quenching of the natural fluorescence emission at its characteristic wavelength [14, 15, 17]. Copper ion-binding of DsRed has shown greater than 90 % fluorescence quenching reversibility with the addition of a metal ion chelator, such as EDTA [15]. This selectivity and reversibility increases the usability of these proteins in a variety of sensing applications. DsRed proteins can also serve as genetically encodable copper ion-binding fluorescent probes, which can be targeted to a specific subcellular compartment. Such work would open up new avenues of research. This copper-binding property of DsRed-Monomer has also been utilized for affinity purification of the protein, using metal chelating columns [16]. The copper-binding

selectivity observed for DsRed is unique since GFP, and a variety of other fluorescent proteins, do not show any inherent metal-binding properties.

Fluorescence quenching seen for DsRed proteins in the presence of copper has been shown to have no effect on the emission wavelength maximum. One variant of DsRed, DsRed2, has been examined as a highly selective and sensitive copper biosensor with a reported dissociation constant of 0.54 ± 0.09 μM [15]. Copper ion concentrations of 2.5 μM have shown greater than 90 % quenching with this protein. Further studies utilizing mutants of DsRed showed moderate quenching with copper concentrations of 10 μM [14]. Dissociation constants for these mutants, drFP583 (native DsRed) and Rmu13, were reported as 14.8 ± 1.7 and 10.9 ± 1.7 μM, respectively. These constants vary greatly from those reported for DsRed2 by Eli *et al*. Studies performed in our laboratory have demonstrated that DsRed-Monomer binds Cu^{2+} selectively. Additionally, DsRed-Monomer showed greater than 50 % quenching at concentrations of 3 μM copper [16]. Using DsRed-Monomer, a detection limit for copper was found, 0.8 μM [17]. All of the studies reported so far have focused on the use of DsRed in the construction of copper biosensors. However studies were lacking, which characterize the effect of copper-binding on DsRed-Monomer, in terms of the changes in spectral properties or the mechanism of this observed quenching. To investigate these properties we have performed a series of spectroscopic studies using DsRed-Monomer in the presence of Cu^{2+}.

Initially the copper dissociation constant for DsRed-Monomer was calculated, as a measure of the affinity for binding Cu^{2+}. This was calculated using the equation below [42].

$$\frac{\Delta F}{\Delta F_{\max}} = \frac{K_d + [P] + [Cu] \pm \sqrt{(K_d + [P] + [Cu])^2 - (4[P][Cu])}}{2[P]}$$

where ΔF is the change in the measured fluorescence, ΔF_{MAX} the maximum fluorescence change, [P] the total protein concentration, K_d the dissociation constant of the copper-binding site, and [Cu] the total concentration of copper. The curve of $\Delta F/\Delta F_{max}$ against

copper concentration was fitted using this equation (Figure 10). A detailed derivation of this equation is presented in Appendix B. From this data a dissociation constant of 1.7 ± 0.3 μM was calculated for DsRed-Monomer. This dissociation constant shows that DsRed-Monomer has a similar affinity for copper as that seen for DsRed2, and higher affinity than other DsRed variants, specifically, drFP583 and Rmu13. Other naturally available copper-binding proteins and peptides have reported K_d values ranging from 10^{-6} to 10^{-17} M [20, 23]. In comparison DsRed-Monomer, and other DsRed variants, appear to be relatively weak copper-binding proteins. However, the inherent fluorescence of these proteins and their high selectivity for copper ions can be an advantage over other copper-binding proteins for sensing applications.

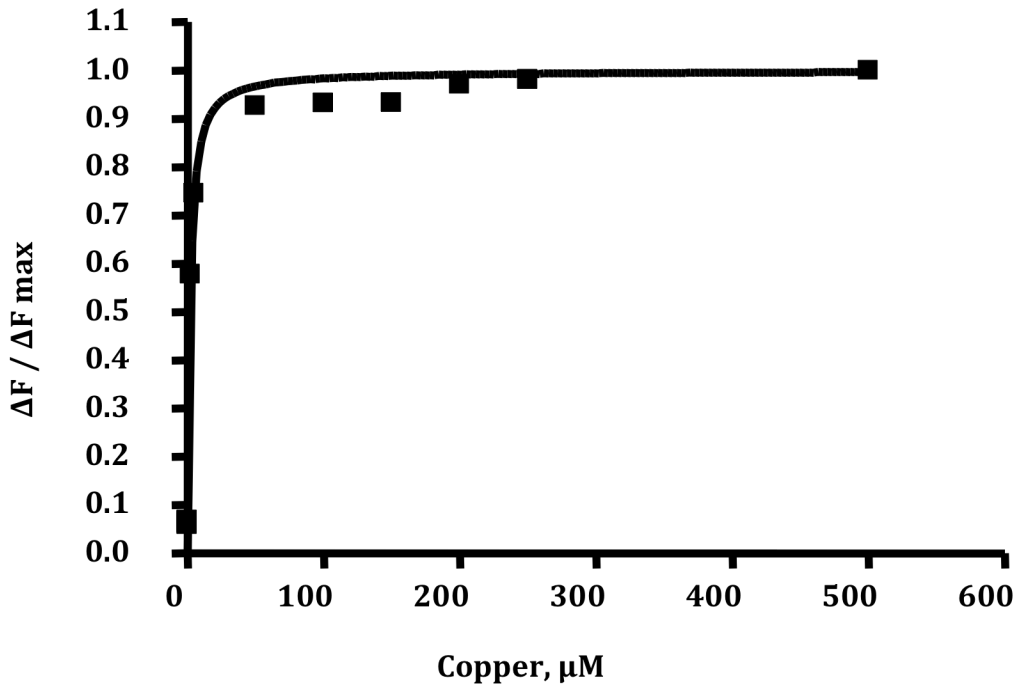

Figure 10: Plot of $\Delta F/\Delta F_{max}$ against copper concentration, where ΔF is the change in measured fluorescence and ΔF is the maximum fluorescence change

Fluorescence quenching was observed for DsRed-Monomer in the presence of Cu^{2+}. To investigate whether the mechanism of this quenching is a dynamic or static process we generated a Stern-Volmer plot [43] for DsRed-Monomer. This plot was generated by measuring the fluorescence of the protein upon the addition of copper at a

variety of points of temperatures (Figure 11). This plot showed a linear relationship, indicating that only one type of quenching was occurring. From the slope of this plot the Stern-Volmer constant (K_{sv}) was calculated, as displayed in Table 3 [43]. This constant showed an increase, with a decrease in temperature, indicating that a static quenching interaction is occurring between the protein and the copper ions. In static quenching the quencher forms a non-fluorescent ground-state complex with the fluorophore [43]. To further define the quenching seen between DsRed proteins and Cu^{2+}, the K_{sv} value, obtained from the Stern-Volmer plot was used to calculate the quenching rate constant, K_q, by the following equation

$$K_q = K_{sv} / \tau_0$$

where τ_0 represents the lifetime of the fluorophore of the protein, reported as 3.3 ns for DsRed [44]. The K_q value obtained for DsRed-Monomer from this study, 10^{12} to 10^{13} $M^{-1}s^{-1}$, is 100-fold larger than the maximum scatter collision quenching constant for quenchers (2.0×10^{10} $M^{-1}s^{-1}$) [45]. Therefore the K_q obtained for DsRed-Monomer indicates that the observed quenching of this protein in the presence of copper must be due to the formation of a complex, as observed in static quenching.

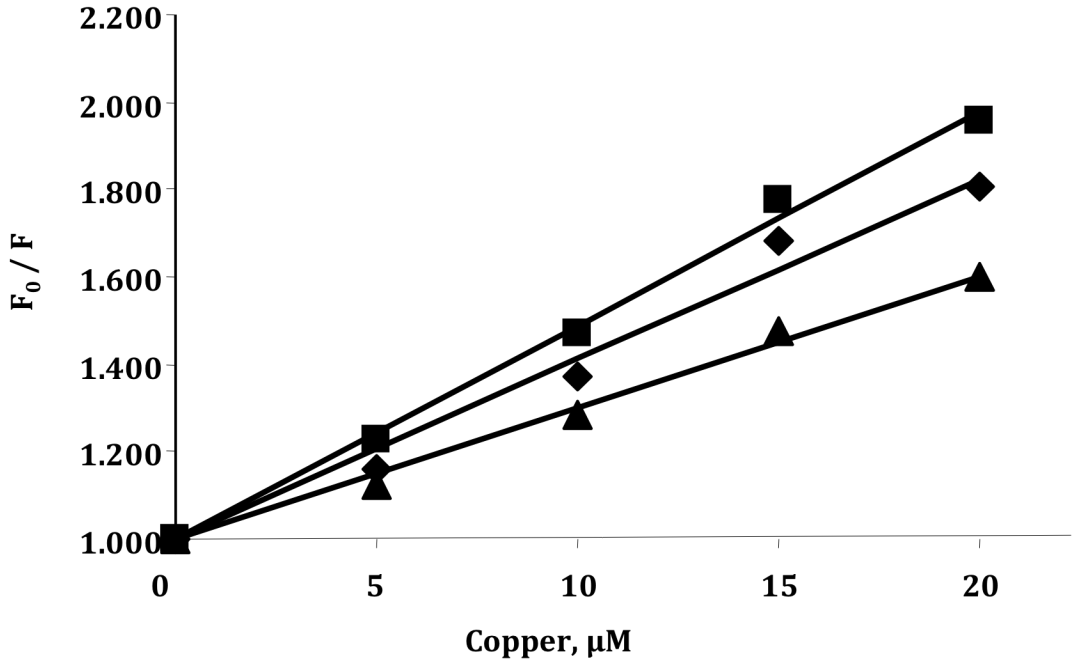

Figure 11: Stern-Volmer plots generated by adding Cu^{2+} to DsRed-Monomer followed by incubation at (square) 16 °C, (diamond) 25 °C, and (triangle) 30 °C

Table 3: Stern-Volmer constants (K_{sv}) determined from the slope of the Stern-Volmer plot and quenching rate constants determined using the equation $K_q = K_{sv}/\tau_0$ where K_{sv} is the Stern-Volmer constant and τ_0 is the lifetime of the fluorophore

T (°C)	K_{sv} (M^{-1})	K_q (M^{-1} s^{-1})
16	48,800	1.47×10^{-13}
25	41,200	1.24×10^{-13}
30	30,100	9.12×10^{-12}

To further validate that the mechanism of this fluorescence quenching in the presence of copper is static, we performed UV absorption scans of DsRed-Monomer, in the presence and absence of Cu^{2+}. Dynamic quenching affects only the excited states of the fluorophore whereas a static quenching process affects its' ground state [43]. Therefore the static quenching process leads to a change in the absorption spectra. The absorption spectra obtained for DsRed-Monomer in the presence of copper, showed that

the absorbance intensity was affected by the addition of copper, compared to the same protein concentration in the absence of copper (Figure 12). With a single equivalence of bound copper, the absorbance and the extinction coefficient of the protein decreased at its characteristic wavelength of 556 nm (Figure 12, Table 4). The overall shape and pattern of peaks was retained for the protein in the presence of copper compared to the peaks obtained for the protein alone. A static quenching process typically yields changes in the absorption profile [43, 45], however, this was not seen for DsRed-Monomer. The observed anomalous behavior seen for DsRed-Monomer can be explained as following. It is known, that in the case of proteins, only fluorophores located at the surface can be dynamically quenched whereas a static process quenches internal fluorophores. This dynamic process is excluded for internal fluorophores due to the higher hydrophobicity in the protein's interior. In the case of DsRed, the chromophore is well shielded inside a β-barrel and hence is not accessible for dynamic or collisional quenching. Taking this factor into consideration and the Stern-Volmer constants obtained in our study, we hypothesize that the fluorescence quenching of DsRed-Monomer in the presence of copper follows a sphere of action static quenching model. This indicates that the quencher forms a contact at a defined site on the protein, adjacent to the fluorophore, leading to the formation of a non-fluorescent species. This is further supported by the observation that the absorption spectral profile of this protein does not change in the presence of copper, only the intensities of the peaks were seen to change, as expected for a sphere of action static mechanism [43, 45]. In a static quenching model the quencher forms a non-fluorescent ground-state complex with the fluorophore. However, in a sphere of action static quenching model, the quencher forms a complex on a specific site on the surface of the protein, adjacent to the fluorophore. This close proximity, of the quencher to the fluorophore, at the moment of excitation leads to the formation of the non-fluorescent species. The radii of the solvent shells of both the fluorophore and the quencher define the maximum distance between the fluorophore and the quencher for this type of fluorescence quenching to occur. Based upon the interactions seen for the four chromophores within the tetrameric DsRed structure [6], we believe that this maximum distance would be within ~30 angstroms of the chromophore for such a quenching effect

to be seen. Since we hypothesize that in the case of DsRed proteins, copper ions form a complex with specific amino acid residues on the protein, further work was done to identify this binding site. This complex formation can lead to the formation of a non-fluorescent species in three ways, (i) by affecting the hydrogen-bonding network of the chromophore, (ii) by bringing copper close to the chromophore such that it contacts the excited-state of the chromophore, (iii) by causing conformational/structural changes in the protein.

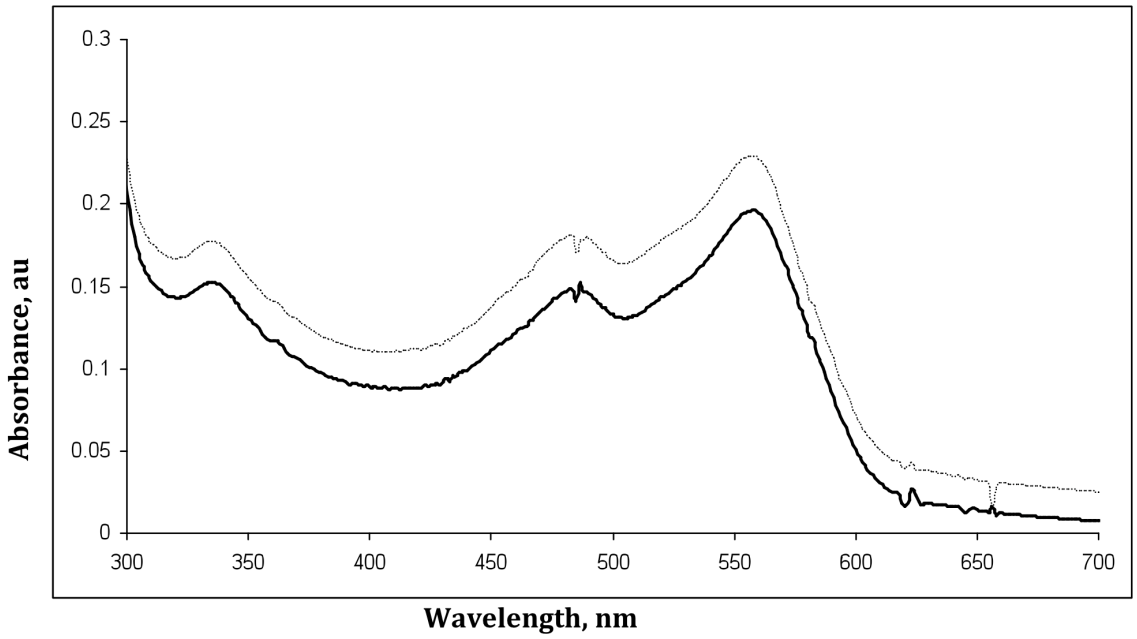

Figure 12: UV-Visible absorption spectra of DsRed-Monomer in the presence (—) and absence (---) of Cu^{2+}

Table 4: UV-Visible and CD spectral characteristics of DsRed-Monomer in the presence and absence of Cu^{2+}

DsRed-Monomer	ε ($M^{-1}cm^{-1}$)	α-helix (%)	β-sheet (%)	Random coil (%)
With Copper	62,700	5	47	48
Without Copper	57,600	5	47	48

We investigated whether the binding of copper to DsRed-Monomer caused any structural or conformational changes within the protein, leading to quenching of the fluorescence. To achieve this we monitored the far-UV CD spectra of the protein with and without copper. The spectra and the percentages of the secondary structure (Table 4) were found to be identical both in the presence and absence of copper. This result suggests that the observed quenching in DsRed-Monomer is not due to any structural or conformational changes in the protein upon copper-binding.

From the Stern-Volmer study and the CD spectroscopy results we can deduce that copper forms a complex with specific amino acid residues of DsRed-Monomer, while the structural and conformational integrity is maintained. To identify possible amino acid residues involved in this copper-binding we studied the effect of pH on this copper-binding, by monitoring any change in the fluorescence intensity of DsRed-Monomer with a change in pH, both in the presence and absence of copper. In the absence of copper the protein showed no pH dependence across a range of pH from 5 to 12, showing no change in fluorescence intensity. However in the presence of copper this plot showed a dramatic shift in fluorescence intensity from pH 6 to 8.5. The pK_a value of 7.3 calculated for DsRed-Monomer was obtained from this plot (Figure 13). This pK_a value suggests that either Cys or His residues may be involved in the copper-binding of DsRed-Monomer.

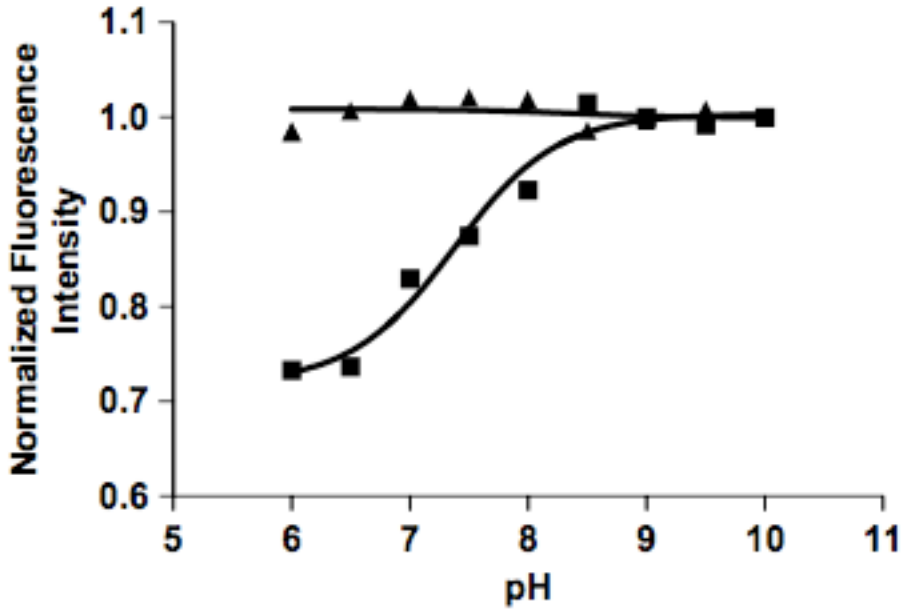

Figure 13: The plot represents the effect of pH change on the fluorescence intensity of DsRed-Monomer in the presence (squares) and absence (triangles) of Cu^{2+}

To further evaluate the identity and position of possible metal binding motifs within the structure and sequence of DsRed-Monomer, two computational programs were utilized. MetalMine and Metsite were used to help locate metal-binding sites within the DsRed-Monomer. Sequence identity comparison with known metal-binding proteins is a common method of locating metal-binding sites within a protein or enzyme. MetalMine evaluated the sequence of DsRed-Monomer compared to known copper-binding motifs, in an attempt to identify sequence homology. Furthermore, the x-ray crystal structure of a protein can be evaluated computationally to determine the possibility of metal-biding sites within a sequence. For DsRed-Monomer we utilized the Metsite website for such a computational study. The MetalMine sequence comparison did not indicate the presence of any known copper-binding motifs, within the sequence of DsRed-Monomer, comparable to known copper-binding proteins and enzymes. This suggests that the copper-binding site present in DsRed-Monomer is not one of the traditionally accepted binding motifs discussed in Chapter 1. This result is not surprising since the dissociation constant for DsRed-Monomer, 1.7 μM, is relatively low compared to those reported for traditional copper-binding proteins, 10^{-6} – 10^{-17} M. The Metsite predictive program,

however, did identify a number of possible metal binding sites with varying degrees of metal affinity. By comparing the results of the Metsite predictions with the X-ray crystal structure of DsRed-Monomer, two possible binding sites were identified that include two His residues, His25 and His216 (Figure 14). Both of these His residues are external to the beta barrel of DsRed-Monomer and have neighboring Gly residues, which could also assist in copper-binding. His25 has one set of neighboring Gly residues (Gly126-Gly20) which could assist in copper-binding. The His216 residues, on the opposite side of the beta barrel of DsRed-Monomer, has another set of Gly residues (Gly40-Gly35) in neighboring positions. Either of these sites may yield a GlyGlyHis copper-binding peptide, which, as described in the previous chapter, demonstrates one of the strongest copper-binding affinities, 10^{-17} M. However, the X-ray crystal structure suggests that these Gly residues will be internal to the beta barrel and not available for binding. These internally arranged Gly residues might still help the bound copper ions to come into contact with the chromophore as described in our quenching model, while their less than ideal positioning may explain the low dissociation constant seen for DsRed-Monomer. Alternatively, the low binding constant observed for DsRed-Monomer, compared to other known copper-binding proteins, may suggest that the His residues bind these copper ions alone or with only minor assistance from the neighboring residues.

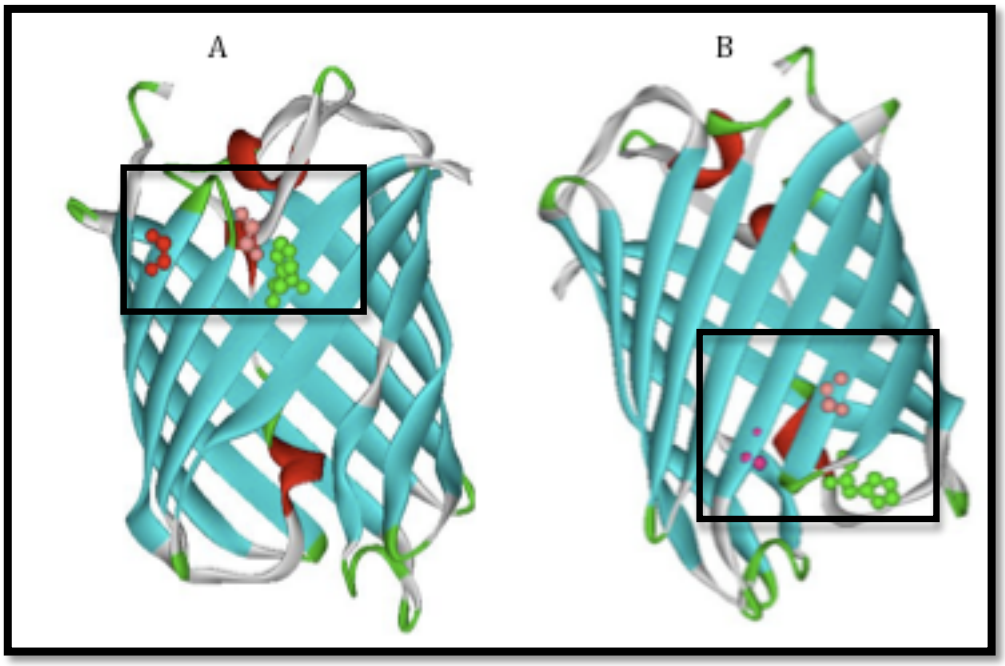

Figure 14: The possible copper-binding sites of DsRed-Monomer using the reported x-ray crystal structure [13] (A) His216 (green), Gly35 (red), Gly40 (peach), (B) His25 (green), Gly20 (peach), Gly126 (plum)

2.4 Conclusion

In summary, DsRed-Monomer has previously shown a unique selectivity for copper-binding. This copper-binding has been used in the development of affinity-based purification of DsRed and copper sensing applications [15, 16]. The work presented here has focused on biochemical; spectroscopic and computational studies to determine the mechanism of this observed fluorescence quenching in the presence of copper. The binding of copper to DsRed-Monomer appears to have no effect on the overall structure of this protein, as seen by far-UV CD spectral analysis. Deviations in the UV-visible absorbance values were seen in the presence of copper, however no shift in the absorbance peaks was observed in the presence of copper. Both the UV-visible and the Stern-Volmer constants suggest that the fluorescence quenching seen for DsRed-Monomer follows a sphere of action static quenching model, indicating the formation of a

complex between specific residues of the protein and copper ions. This binding brings the copper ion into close proximity to the excited state of the chromophore, creating a non-fluorescent species. Based on the pH study, either cysteine or histidine residues were identified to be involved in binding copper ions in DsRed-Monomer. Furthermore the Metsite results, when compared to the X-ray crystal structure of DsRed-Monomer, indicated the possible involvement of His25 or His216 in the copper-binding, possibly creating a GlyGlyHis binding site with neighboring Gly residues. The results presented here provide the groundwork for future investigations in identifying the copper-binding site in DsRed-Monomer. In that regard, site-directed mutagenesis, of His25 and His216, is envisioned to further evaluate their role in copper-binding.

CHAPTER 3. DUAL FUNCTION LABELING OF BIOMOLECULES BASED ON DSRED-MONOMER

3.1 Introduction

Genetically encoded tags are powerful tools for protein research. A variety of tags have been developed: fluorescent probes for imaging and visualization, affinity tags for isolation and purification and epitope tags for immunological detections. The ability to purify and visualize a protein of interest is of great importance to proteomics and biomolecular research [46-48]. Currently a number of affinity-based methods of protein purification are available, with either chemical or biological tags [49-51]. For efficient purification, either peptides or proteins are used as affinity tags [52-54]. However, a single affinity tag is now seldom used because of its limitations on purification effectiveness, but is rather used in tandem to achieve better results [55-57]. Additionally, for protein detection or localization, fluorescent probes such as fluorescent proteins, quantum dots, or fluorophores are fused to the protein as reporter tags [58-63]. Such systems require two separate tags to be fused to the target to accomplish protein purification and detection. This double tagging limits the flexibility in terms of available termini for protein fusions, making the ability to use a single tag for both purposes desirable. To address this issue we have designed a DsRed-Monomer fusion tag, which can be utilized to both purify a protein of interest and in fluorescence-based detection studies.

Prior to this work only a few reports had been published demonstrating methods that offer dual functionality of tags. Paramban *et al.* demonstrated the use of GFP for both localization and purification of a fused target protein. In order to utilize GFP as a purification tag this group engineered a 6-His tag into the loop region of GFP, between

Gln172 and Asp173 of the GFP [64]. The insertion of this histidine tag, however, lead to a 40 % loss of fluorescence but the remaining signal was sufficient for the detection of the fused target. This work was expanded by Kobayashi *et al*. [65] who engineered a "multifunctional GFP" with an 8-His tag and a streptavidin-binding peptide, for affinity purification, and a c-Myc tag for immunological detection. For this work the tags were engineered to be located between Asp173 and Gly174. Similarly, dye and antidye-antibody combinations have been used as dual function tags [66]. In a recent report, protein labeling was performed using the phosphopantetheinyltransferase (PPTase) to incorporate a stilbene reporter into a carrier protein fused to the target protein [67]. When the stilbene reporter binds to the anti-stillbene antibody, the fluorescence of the stilbene reporter group is turned on. The stilbene labeled fusion protein can then be purified using the antibody bound column. Such tags, however, present problems including high cost and low stability since they rely on immobilized antibodies.

The work presented in this chapter describes the use of site-specific tagging of a protein with DsRed-Monomer, for both purification and detection purposes. In this work, we have demonstrated that DsRed-Monomer can be employed, based upon its inherent fluorescence and copper-binding properties, as an efficient purification and visualization tag. As discussed in the preceding chapters, our group has reported on the natural, and selective, copper-binding affinity of DsRed-Monomer [17, 39]. We have utilized this copper-binding affinity to create an efficient, single-step, purification system for DsRed-Monomer [16]. Here we have used DsRed-Monomer as an affinity tag to purify a fusion partner. Furthermore, we show that this tag can also act as a reporter, utilizing DsRed-Monomer's natural fluorescence to perform bioassays. Using such tagging systems offers a number of advantages including the flexibility to attach the target protein to either termini and to perform site-specific genetic encoding, and to the achievement of efficient detection due to DsRed-Monomers excitation and emission in the red region of the spectrum. Protein-based affinity tags have also been shown to aid in the folding of the fusion partner, enhancing solubility, in comparison with peptide-based tags [52]. Finally the use of copper-immobilized columns for purification offers an inexpensive,

stable and reusable platform, compared to the antibody-immobilized columns utilized by other systems.

To demonstrate the ability of DsRed-Monomer to function as a dual-function tag and to show its flexibility in genetic fusions of proteins, we constructed a fusion protein of DsRed-Monomer. As a proof-of-concept study, a fusion protein between DsRed-Monomer and a model protein calmodulin (CaM) was constructed through the N-terminus of DsRed-Monomer. CaM is a Ca^{2+}-binding protein that is involved in the regulation of several cellular responses through its interaction with other proteins [68, 69]. In the absence of Ca^{2+}, the CaM has a collapsed conformation [70, 71]. In the presence of Ca^{2+}, CaM changes its conformation from a collapsed to a "dumbbell" configuration exposing its hydrophobic region that acts as a docking area for target peptides, proteins, and the tricyclic phenothiazene class of compounds [70, 72-75]. This CaM-DsRed-Monomer fusion protein was expressed in *E. coli* and purified using a copper-immobilized column. It was further employed as a fluorescent tag to evaluate the binding of a known CaM ligand, chlorpromazine, to this fusion protein [74, 75]. Furthermore, we demonstrated that this DsRed-Monomer tag could be separated from its fusion partner, CaM, by simply inserting a protease cleavage between the DsRed-Monomer and CaM.

3.2 Materials and Methods

3.2.1 Construction of Calmodulin-DsRed-Monomer Fusions

The PCR primers were designed to introduce the sequences for the restriction enzymes, *Sph*I and *Xma*I on the CaM gene (Table 5). The plasmid pVUC-1 was used as a template. The CaM gene obtained after PCR and the pDsRed-Monomer were digested with *Sph*I and *Xma*I followed by ligation of the CaM gene into pDsRed-Monomer plasmid to obtain pSKD104 (Figure 15). The plasmid pSKD104 was transformed into *E.*

coli ER2566 strain. The colonies were picked and miniprep was performed. DNA sequencing was utilized to determine the sequence of the fusion protein.

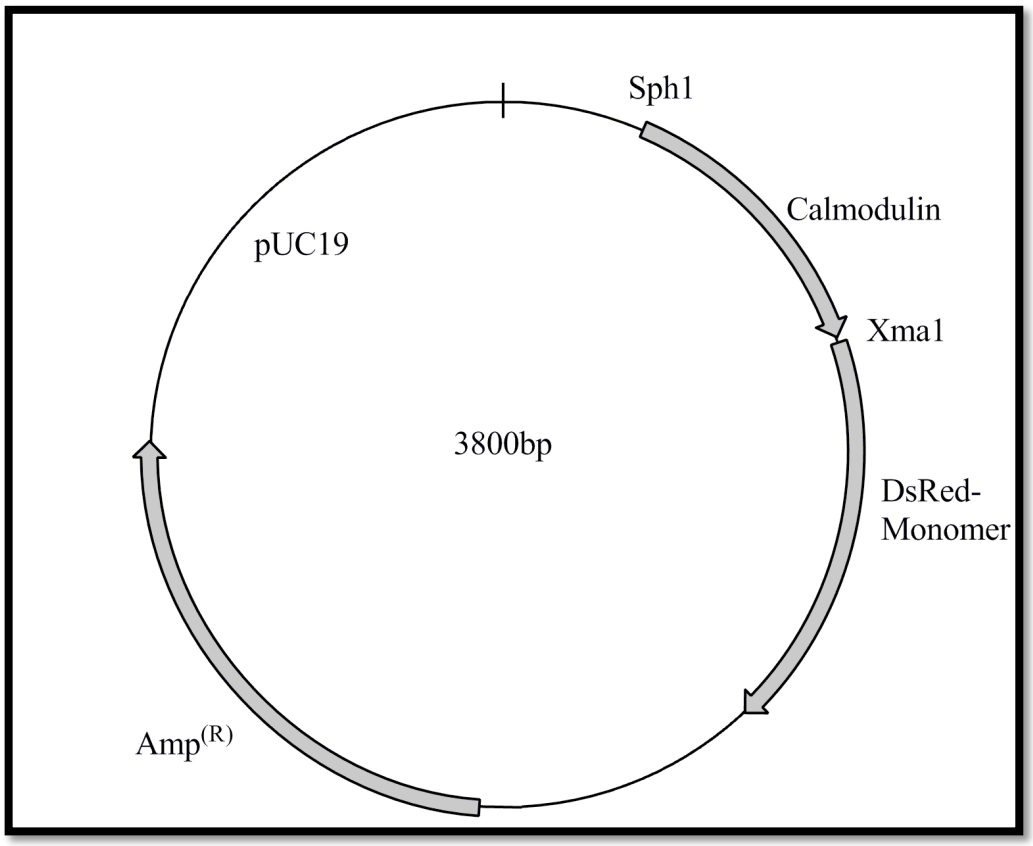

Figure 15: CaM-DsRed-Monomer plasmid map, ~3.8 kb

Table 5: PCR primers used to create Calmodulin-DsRed-Monomer fusion

Primer	Sequence
CaMSphI	ATATATGCATGCGATGGCTGATCAGCTGACTGACGAGCAG
CaMXmaI-Rev	ATATATCCCGGGCCTTAGCCATCATAACCTGAAACGAACTC
CaMXmaITEV-Rev	CCCGGG*CCCCCTGGAAGTACAGGTTTTCC*TTAGCCATCATAACCTGAACG

To construct the fusion gene, incorporating the TEV protease cleavage site between the calmodulin and DsRed-Monomer genes, the same forward primers,

restriction enzymes, and molecular biology techniques were used as above for the CaM-DsRed-Monomer fusion. However, a new reverse primer was designed (Table 5) which incorporated the TEV cleavage site, Glu-Asn-Leu-Tyr-Phe-Gln-Gly, before the *XmaI* restriction site. The DNA coding for TEV cleavage site is in italics and the DNA coding for *Xma*I is underlined. The PCR product was ligated into pDsRed-Monomer plasmid to obtain the plasmid pSKD104-TEV. This plasmid was transformed into *E. coli* JM107 strain.

3.2.2 Expression and Purification of Calmodulin-DsRed-Monomer Fusions

The fusion proteins of DsRed-Monomer were expressed in JM107 *E. coli* as previously described in Chapter 2 [76]. Briefly, 5 mL cultures of LB broth (containing 100 μg/mL ampicillin) with the prepared plasmids pSKD104 and pSKD104-TEV in *E. coli* were grown overnight. These cultures were transferred to 200 mL samples and grown to an OD_{420} of 0.5. Protein expression was induced by the addition of IPTG (0.5 mM), and grown overnight at 37 °C for CaM-DsRed-Monomer and at 30 °C for CaM-TEV-DsRed-Monomer. The cells were then collected by centrifugation at 4 °C, 4000 x g, for 15 min and sonicated using 20 s on 20 s off for 5 min. The crude fusion proteins were collected by centrifugation at room temperature, 4000 x g for 30 min. The crude fusion proteins were purified as described previously in Chapter 2 [77], utilizing a copper charged metal affinity column. Purity and concentration were found by SDS-PAGE gel electrophoresis and Bradford assay, respectively.

3.2.3 Protease Cleavage of Calmodulin from DsRed-Monomer

Promega ProTEV protease was used according to the manufacturer's recommendations with the supplied buffer to cleave the CaM from the purified CaM-TEV-DsRed-Monomer fusion protein. The reaction was allowed to continue for 24 h at 37 °C. Complete cleavage of CaM was verified by SDS-PAGE gel electrophoresis, with Coomassie staining.

3.2.4 Spectral Analysis of Fusion Protein

The fluorescence spectrum of CaM-DsRed-Monomer was collected. A volume of 200 μL of 1.0 μM CaM-DsRed-Monomer was placed into the well of a microtiter plate and the excitation and emission scans of the protein recorded. These scans were collected at room temperature using a Cary Eclipse fluorescence spectrophotometer.

3.2.5 Calmodulin Ligand-Binding Study

Initially, a dilution study was prepared for the CaM-DsRed-Monomer. Standard solutions of CaM-DsRed-Monomer fusion protein were prepared by serially diluting the stock solution of the protein in assay buffer 1 (30 mM Tris containing 10 mM calcium, pH 7.2). A volume of 100 μL of these solutions was mixed with 100 μL of assay buffer 1, placed in a microtiter plate, and the fluorescence intensity measured using an excitation maximum wavelength of 556 nm and emission wavelength maximum of 597 nm. All fluorescence intensities were obtained in triplicate.

A Dose-Response curve was generated for the fusion protein in the presence of chlorpromazine from the tricyclic phenothiazene class of drugs. Different concentrations of chlorpromazine were prepared by diluting in assay buffer 1. A volume of 100 μL of 1.0 μM CaM-DsRed-Monomer was mixed with 100 μL of chlorpromazine, at different concentrations. The fluorescence intensity was monitored corresponding to DsRed-Monomer excitation/emission wavelength. A control study was performed using DsRed-Monomer and chlorpromazine. In another control study, solutions of varying concentrations of chlorpromazine (1×10^{-3} to 1×10^{-6} M) were excited at 556 nm and the fluorescence emission monitored at 597 nm.

3.3 Results and Discussion

The results obtained from this study demonstrate the dual application of DsRed-Monomer. Reporter proteins, such as DsRed, are commonly fused to a target protein for fluorescence-based bioassay development. However, if the same reporter protein can also function as an affinity purification tag, then this will reduce the assay development time and simplify the assay development process. To demonstrate the versatility of DsRed-Monomer as a dual-function tag we have selected a calcium-binding, biologically relevant protein, calmodulin, as the fusion partner for this proof-of-concept study.

The DNA encoding for the calmodulin gene was fused to the gene coding for DsRed-Monomer using genetic engineering tools to construct a genetic fusion. Plasmid pSKD104 and pSKD104-TEV containing the fusion gene, and the fusion gene with a TEV protease cleavage site between the CaM and the DsRed-Monomer were transformed into *E. coli* cells and expressed. The fusion proteins were then purified using a copper-immobilized column, utilizing DsRed-Monomer as an affinity tag. Briefly, the crude fusion proteins were bound, via DsRed-Monomer's natural copper affinity, to immobilized copper ions on a metal affinity column. The purified fusion protein fractions were collected after wash steps by passing through an elution buffer, containing imidazole. The elution of the purified fusion proteins was monitored by the pink coloration of DsRed-Monomer, and by measuring the fluorescence of the collected fragments. The purity of the fusion proteins was verified by SDS-PAGE gel electrophoresis using Coomassie staining (Figure 16). The single band, at 41.5 kDa, demonstrates the efficiency of the CaM-DsRed-Monomer purification. We also performed an expression study to compare the effect of fusion of calmodulin to DsRed-Monomer on the expression yield. For this study we expressed wild-type calmodulin and CaM-DsRed-Monomer proteins under identical conditions. The conditions followed were the same as those used to express the fusion protein, described above. SDS-PAGE gel electrophoresis was performed that showed similar expression yields for calmodulin and CaM-DsRed-Monomer proteins (Figure 17). Additionally, the total protein yield for the two proteins was similar, as seen on this gel. For both of these proteins identical

expression and sonication protocols and volumes were used for both expressions. These observations indicate that the fusion of the target protein to DsRed-Monomer does not affect the expression of the target protein. The concentration of the purified protein was determined using Bradford assay. Percent recovery of the purified protein was estimated by passing a known quantity of purified fusion protein through the copper-immobilized column. The purification procedure was followed and the concentration of the eluted protein determined. The amount of eluted protein was compared to the amount of the protein initially loaded onto the column. The recovered protein was calculated to be ~96 % for the CaM-DsRed-Monomer fusion.

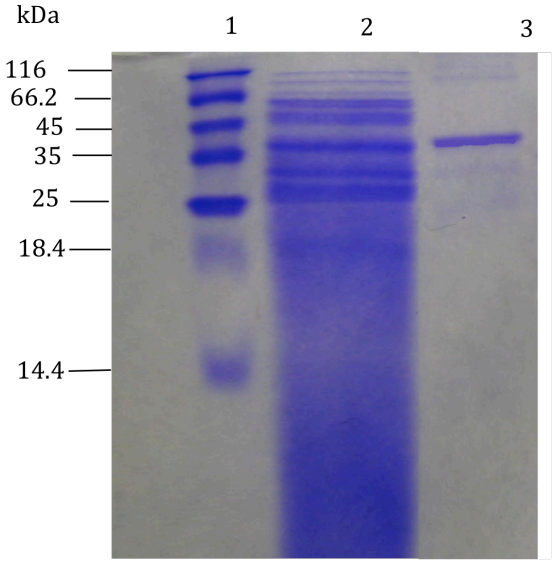

Figure 16: SDS-PAGE gel of CaM-DsRed-Monomer fusion protein molecular weight protein marker (lane 1), crude (lane 2), and purified (lane 3) CaM-DsRed-Monomer

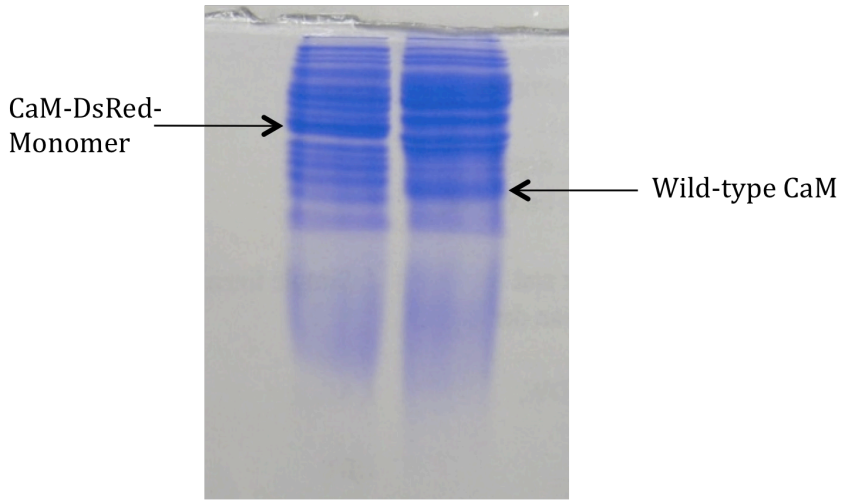

Figure 17: SDS-PAGE gel of expression yield comparison of CaM-DsRed-Monomer fusion protein and wild-type CaM, both expressed in *E. coli*

To demonstrate that the target protein can be separated after purification, from DsRed-Monomer, we incorporated a TEV protease cleavage site between the CaM and the DsRed-Monomer genes. The fusion protein was again purified on a copper immobilized column employing DsRed-Monomer as an affinity tag. The DsRed-Monomer was cleaved off easily and completely from the CaM-TEV recognition site-DsRed-Monomer fusion protein within a 24 h time period. This was verified, again, by SDS-PAGE gel electrophoresis (Figure 18), this gel shows two bands corresponding to calmodulin (~15 kDa) and DsRed-Monomer (~27 kDa). Therefore, it is reasonable to conclude that although DsRed-Monomer is a large affinity tag it can be efficiently separated from the target protein if desired.

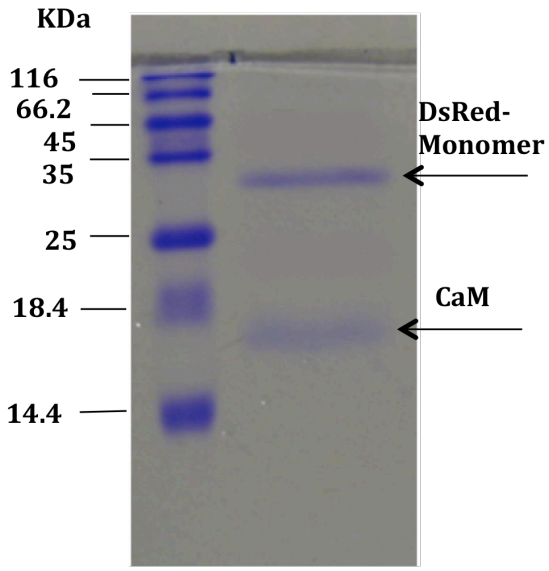

Figure 18: SDS-PAGE gel of protease cleavage of DsRed-Monomer from CaM-TEV recognition site-DsRed-Monomer, molecular weight protein marker (lane 1), separated CaM and DsRed-Monomer proteins (lane 2)

Although variants of DsRed have been employed as fusion tags in other studies, there have previously been no published reports on fusions of DsRed-Monomer. Therefore, the spectral characteristics of the fusion protein were evaluated to determine any effect of protein fusion on the DsRed-Monomer protein structure and fluorescence emission (Table 6). Fluorescence excitation and emission scans were performed for the CaM-DsRed-Monomer fusion protein, with an observed excitation and emission wavelength maximum of 556 nm and 597 nm, respectively. This observed fluorescence excitation and emission is indicative of DsRed-Monomer [16]. UV-visible absorbance spectrum of the fusion protein showed two peaks 480 nm and 556 nm, again, these are the representative peaks observed for DsRed-Monomer [77]. A comparison of the spectral properties of the fusion protein with DsRed-Monomer showed no effect of protein fusion on the DsRed-Monomer fluorescence activity. These studies indicate that the fusion of a protein to DsRed-Monomer does not affect the fluorescence excitation or emission wavelength maxima of the protein.

Table 6: Characteristics of DsRed-Monomer and the CaM fusion protein

	$\lambda_{excitation}$ (nm)	$\lambda_{emission}$ (nm)	Absorbance Max (nm)	ε ($M^{-1}cm^{-1}$)
DsRed-Monomer	556	597	480, 556	35,000
CaM-DsRed-Monomer	556	597	480, 556	59,000

The purification and spectroscopic analysis of the CaM-DsRed-Monomer fusion protein showed that a protein of interest could be fused to the DsRed-Monomer without affecting its copper-binding affinity, fluorescence or absorbance. This should prove useful in the visualization of fusion proteins, followed by their isolation. Furthermore, we wanted to demonstrate that a fusion with DsRed-Monomer could also be utilized in the optical detection of the interactions of a fused target protein with its ligands. In that respect, calmodulin is a well-studied protein with known ligands that are commercially available: therefore, we decided to study binding of CaM ligands to CaM-DsRed-Monomer fusion protein. This can be performed in two ways. The CaM-DsRed-Monomer fusion protein can be genetically encoded to study calmodulin interacting proteins or ligands *in vivo*, or the isolated fusion protein can be used to study calmodulin interacting molecules *in vitro*. It has been reported by other groups that fusions between GFP and calmodulin can be utilized in screening ligands that bind calmodulin [32, 33, 78] in solution-phase assay. On the basis of this, we performed a solution-based study by mixing CaM-DsRed-Monomer and a known representative CaM ligand, chlorpromazine. The addition of chlorpromazine resulted in a quenching of CaM-DsRed-Monomer fluorescence. This change in fluorescence can be attributed to the conformational change that occurs in calmodulin upon binding its ligand. It has been hypothesized that the conformational change in calmodulin may lead to a change in the microenvironment of the fused fluorescent proteins affecting their fluorescence output. A dose-response curve was generated for this assay by varying the amount of chlorpromazine added to the CaM-DsRed-Monomer fusion and relating this concentration to the change in fluorescence intensity (Figure 19). A detection limit of 5×10^{-6} M was obtained for chlorpromazine, which is comparable to that achieved with other reported fluorescence-based assays for

chlorpromazine [73, 78]. A control study was performed, by adding chlorpromazine to DsRed-Monomer protein, which did not result in fluorescence quenching (data not shown). In another control study, we evaluated the effect of fluorescence excitation at 556 nm on chlorpromazine, which is inherently fluorescent. For this study, solutions of varying concentrations of chlorpromazine were excited at 556 nm, and the resulting emission monitored at 597 nm. The fluorescence intensity obtained from these samples was the same as for the buffer blank, demonstrating no effect of fluorescence excitation on chlorpromazine. Overall, the study performed shows that the binding between calmodulin and its ligand can be monitored using the fluorescence of DsRed-Monomer. Furthermore, the observed fluorescence quenching is due to the specific binding of chlorpromazine to calmodulin. We hypothesize that binding of other phenothiazene-based CaM ligands would yield similar results and could be evaluated if desired. It should be noted that the fluorescence change observed upon binding of ligands to CaM might not be universally applicable to other target protein-ligand pairs. Nevertheless, the fluorescence of DsRed-Monomer could still be used in the evaluation of target-protein ligand pair using solid-phase competitive assay techniques.

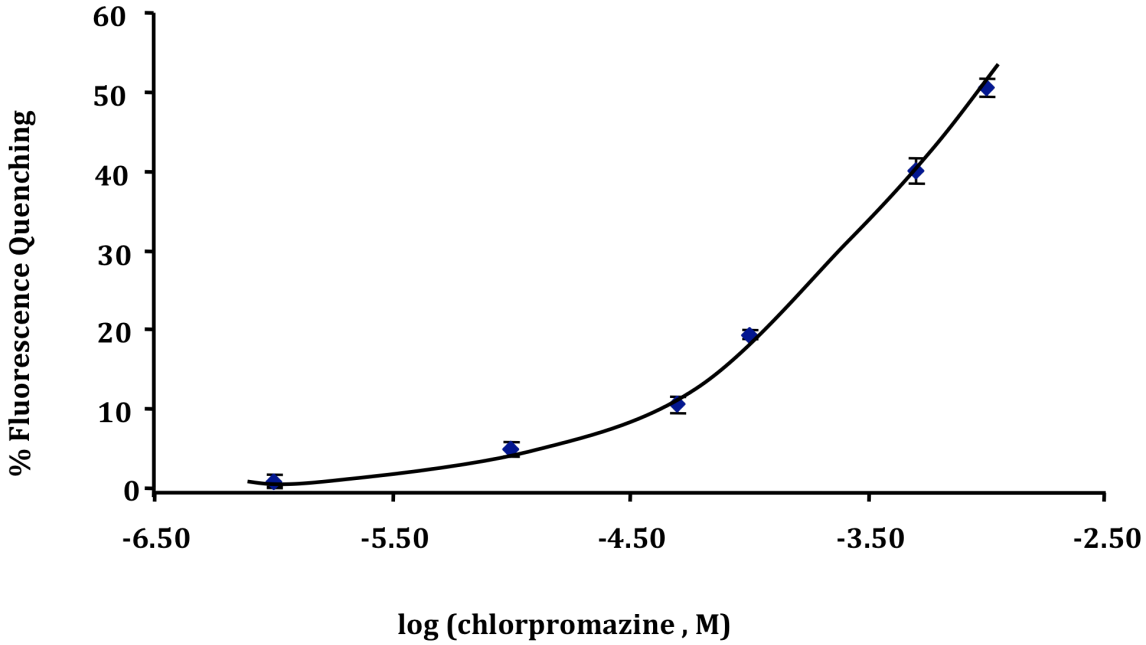

Figure 19: Dose-response curve for chlorpromazine generated by monitoring fluorescence change upon the addition of different concentrations of chlorpromazine to CaM-DsRed-Monomer fusion protein. Fluorescence was measured using 556 nm emission wavelength maximum

3.4 Conclusion

The work presented in this chapter, has demonstrated that DsRed-Monomer can be utilized as both an affinity and reporter tag. DsRed-Monomer offers a unique collection of properties, which allow its use in these roles, for both *in vivo* and *in vitro* protein analysis. We believe that in the future new vectors based on DsRed-Monomer could be designed that allows the insertion of any protein. The recombinant proteins produced could then be expressed in different organisms, monitored optically, purified, and employed in assay development. Further, if desired, protease cleavage sites can be incorporated into the fusion protein designs to isolate the target protein following purification. We did not experience any problems with the protease cleavage between DsRed-Monomer and the target protein. This technique is well developed and has been performed with DsRed previously [79-82]. Additionally, the DsRed-Tetramer/GFP pair

has been employed to design fluorescence resonance energy transfer assays for the detection of protease activity by inserting substrate for the protease between the genes of the two fluorescent proteins [80-82]. This is the first report of the fusion of a protein to DsRed-Monomer and its use as a label in the detection of protein-ligand binding. Through the work presented here we envision that DsRed-Monomer will, in future, be employed as a tag inserted directly into cells, expanding its utility in such biomolecular research.

CHAPTER 4. UTILIZING DSRED-MONOMER AS AN AFFINITY TAG TO ISOLATE PROTEIN-PROTEIN/PEPTIDE COMPLEXES

4.1 Introduction

Protein complexes mediate the majority of cellular processes. The ability to localize and isolate such complexes may provide key insights into protein functions. Purification of protein complexes, in combination with mass spectrometry, allows identification of interacting partners, and is becoming an important tool to define relationships between proteins [83, 84]. Since, currently, as little as 100 fmol of a protein can be evaluated by mass spectrometry, rapid characterization of a protein present in a complex mixture is easily accomplished. This characterization, however, requires that the protein complex be easily and selectively isolated in a reasonable quantity; hence protein characterization is frequently limited by the ability to isolate protein complexes of interest [85]. In this work we present a proof-of-concept study, which overcomes some of these challenges, by utilizing the copper-binding properties of DsRed-Monomer. Fusions of DsRed-Monomer were used to isolate protein-peptide and protein-protein complexes.

Affinity tags have been demonstrated as efficient tools for purifying protein complexes [86]. Additionally, the mild conditions used to elute these tags make them useful tools for purifying protein complexes, under native conditions. Affinity tags allow a diverse group of proteins and protein complexes to be purified using general and simple protocols. This simplicity and native condition elution, in contrast to highly customized procedures associated with conventional chromatography generally used for proteomics and structural genomics, are their primary advantages. Most of the commonly used protein and peptide affinity tags have been developed within the last 20 years and can be

categorized depending on the nature of the affinity tag and its target. Affinity tags have been designed, which utilize peptide or protein fusions, to bind small molecules on a solid support or chromatography resin [87]. Further affinity tags have utilized antibodies on a chromatography resin to bind a specific peptide [86].

A number of affinity purification approaches have been developed, including immunoaffinity, epitope tagging, and glutathione S-transferase (GST) pulldown. Among these, tandem affinity tag purification (TAP) has recently become the focus of native purification for protein complexes [56, 85, 88]. This strategy allows for fast purification of protein complexes with high yield. The TAP tag method involves the fusion of the tag to a target protein and the introduction of this construct into a host cell [85]. The TAP tag is composed of two IgG binding domains of *Staphylococcus aureus* protein A (ProtA) and a calmodulin binding peptide (CBP) with a TEV protease cleavage site between the IgG and CBP [85]. These TAP tags have been designed for both the N- and C-terminal fusion. This method of affinity purification has been optimized for the purification of a number of different proteins and protein complexes.

Fluorescent proteins have been widely applied for *in vivo* visualization of proteins however, isolation studies using fluorescent proteins have largely been ignored. GFP has been used to genomically tag more than 4000 proteins for large-scale analysis of protein localization in *Saccharomyces cerevisiae* [89]. GFP variants with an incorporated histidine tag have demonstrated the potential to serve both as a visualization and isolation tags. Such GFP fusions with a poly histidine tag have recently been utilized for isolation studies [64, 65]. Studies have also been reported which utilized GFP in immunoaffinity purifications [90-96]. Such work with GFP has further led to the design of GFP fusion tags that can visualize proteins in live cells and capture their interactions via immunoaffinity purification on magnetic beads coated with anti-GFP antibodies [97]. These immunoaffinity methods, however, rely on antibody-coated beads; such strategies present unique problems, including the high cost and limited stability of these antibodies.

Based on previous work in our laboratory [16], we believe that DsRed-Monomer's natural copper-binding affinity could provide an ideal partner for affinity purification of an interacting protein or peptide complex. This method offers advantages

over previous methods since it requires only one purification step, making it a faster method. Fusions of DsRed-Monomer have also been shown to retain full fluorescence emission, compared to GFP tags with an incorporated poly His tag. Additionally, this method uses a stable and inexpensive affinity column. In this chapter, we have demonstrated the use of fusions of DsRed-Monomer to isolate and purify a protein complex, utilizing the natural copper-binding affinity of DsRed-Monomer (Figure 20). Two fusions of DsRed-Monomer were used for this purification strategy, M13-DsRed-Monomer and CaM-TEV-DsRed-Monomer. The first of these fusions, M13-DsRed-Monomer, utilized the calmodulin-binding domain of skeletal muscle myosin light chain kinase (skMLCK) (residues 577-602), M13, fused to the N-terminus of DsRed-Monomer. This fusion was then used to isolate and purify CaM from a crude cellular sample. For this work crude calmodulin was combined with the crude M13-DsRed-Monomer fusion protein and allowed to bind. This complex was then isolated, via affinity chromatography, on a copper charged metal affinity column.

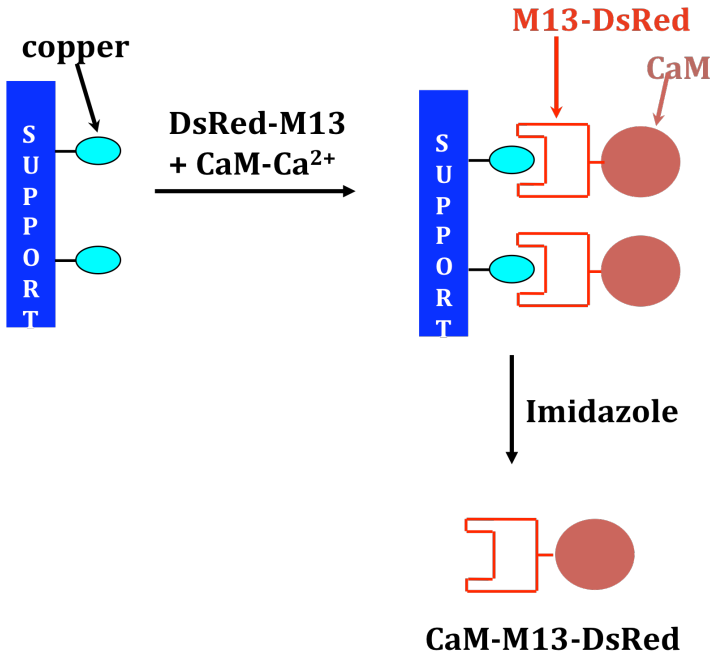

Figure 20: Schematic of protein complex isolation strategy

Additionally, we further utilized the CaM-TEV-DsRed-Monomer fusion, previously created and discussed in Chapter 3 [76], to isolate a CaM interacting protein,

caldesmon. Caldesmon is primarily an F-actin binding protein, isolated from smooth muscle cells. Such F-actin binding proteins are believed to be responsible for both the functional organization of microfilaments and their reorganization during normal functioning of cells [98]. The C-terminal region of this protein is also a primary binding site for the Ca^{2+}-CaM complex [99]. As seen for the CaM binding discussed in the previous chapter, the binding of caldesmon to CaM is also calcium dependent. The copper-binding affinity of DsRed-Monomer was used, again, to isolate this CaM-caldesmon complex. We have used the M13-DsRed-Monomer and CaM-TEV-DsRed-Monomer fusions to demonstrate the ability of DsRed-Monomer to isolate and purify interacting protein-protein and protein-peptide complexes.

4.2 Materials and Methods

4.2.1 M13-DsRed-Monomer and CaM-TEV-DsRed-Monomer Plasmid Construction

The plasmid pDsRed-Monomer was used as a template for the PCR reaction; primers were designed that encode the DNA sequence of the M13 peptide. Using four consecutive PCR reactions, the DNA sequence for the peptide, with a 5 amino acid linker (GGSGG), was inserted at the N-terminus of the DsRed-Monomer sequence present in the plasmid. These primers are displayed in Table 7. The product of each PCR was run on an agarose gel and the band of interest extracted for the subsequent PCR step. A final PCR was run to correct the reading frame of the DNA. This final product, plasmid pSKD105, was digested with Dpn1 for 1 h at 37 °C and transformed into ER2566 *E. coli*. The CaM-TEV-DsRed-Monomer fusion, plasmid pSKD104-TEV, was prepared as described in Chapter 3 [76].

Table 7: Primers for the insertion of the M13 peptide at the N-terminus of DsRed-Monomer

Primer	Sequence
Forward Primer PCR1	GCATTAGGTAGTGGTGGTCCCCGGGTACCGGTCGCC
Forward Primer PCR2	AATAGATTTAAAAAAATTAGTAGTAGTGGAGCATTAGGTGG TAGTGGT
Forward Primer PCR3	AGATGGAAAAAAAATTTTATTGCAGTAAGTGCAGCAAATAGA TTTAAAAAAATT
Forward Primer PCR4	ATATATAAGCTTGGTGGTAGTGGTGGTAAAAGAAGATGGAA AAAAAATTTT
Reverse Primer PCRRev	TATTATTATGAATTCGCTCTACTGGGAGCCGGAGTGGCGGGC
Forward Primer PCRcorrection	GACCATGATTACGCCAAGCTTGGGTGGTAGTGGTGGTAAAAG AAGATGG
Reverse Primer PCRcorrection Rev	CCATCTTCTTTTACCACCACTACCACCCAAGCTTGGCGTAATC ATGGTC

4.2.2 Fusion Protein Expression

The cells containing the plasmids (pSKD104-TEV, pSKD105, and pVUC-1) that encode for the DsRed-Monomer fusion proteins, and spinach CaM, were grown as previously described in LB containing ampicillin with shaking at 250 rpm at 37 °C to an OD_{600} of 0.5. The protein expression was induced using IPTG (0.5 mM) and the cells were allowed to grow for an additional 24 h at room temperature for the spinach CaM, and 5 h at 37 °C for the DsRed-Monomer fusions. The cells were harvested by centrifugation and the pellets resuspended in TBS (30 mM Tris, 300 mM NaCl, with 10 mM Ca^{2+}, pH 7.2) and sonicated using 20 s on and 15 s off for 3 min. The crude proteins were obtained by centrifugation (4000 x g for 30 min) at room temperature. The DsRed-

Monomer fusions were purified for spectroscopic studies using our previously developed copper purification method, described in Chapter 2 [16].

4.2.3 Caldesmon Extraction

Crude Caldesmon was prepared from fresh chicken gizzards [98]. A 20 g sample of trimmed smooth muscle from fresh chicken gizzards was collected and washed in cold water, containing 0.25 mM phenylmethylsulfonyl fluoride. The washed chicken gizzards were minced and suspended in six volumes of extraction buffer (0.3 M KCl, 1 mM EGTA, 0.5 mM $MgCl_2$, 0.25 mM phenylmethylsulfonyl fluoride, 50 mM imidazole-HCl, pH 6.9) at 4 °C, and blended at high speed until finely homogenized. The slurry was then heated in boiling water for five min, at least 2 min at 90 °C, and chilled on ice. The slurry was then centrifuged for 30 min at 47,000 x g, and the solid discarded. Ammonium sulfate was added to the supernatant to a concentration of 30 %, and the precipitate removed by centrifugation. Ammonium sulfate was again added to the supernatant to a final concentration of 50 %, and the precipitate collected by centrifugation. This precipitate was dissolved in 5 mL of buffer A (0.1 M NaCl, 0.1 mM EGTA, 0.1 mM DTT, 10 mM imidazole-HCl, pH 7.0). The crude caldesmon was run on an SDS-PAGE gel and buffer exchanged into TBS buffer (30 mM Tris, 300 mM NaCl) and then into Tris with calcium (30 mM Tris, 300 mM NaCl, 10 mM $CaCl_2$), for binding studies with DsRed-Monomer fusion protein.

4.2.4 Binding Studies Utilizing DsRed-Monomer Fusion Proteins

Crude M13-DsRed-Monomer, 2 mL, was combined with 2 mL crude CaM and mixed for 1 h at room temperature. The crude mixture was passed through a syringe filter onto a copper charged metal affinity column, and rotated for 1 h to allow the DsRed-Monomer to bind to the immobilized copper. The column was washed with multiple column volumes of TBS buffer (up to 10 mL). A volume of 5 – 10 mL of TBS buffer with increasing concentrations of imidazole (1 – 4 mM) were used to wash the

column. The CaM-M13-DsRed-Monomer complex was eluted with TBS containing 5 mM imidazole, until the entire red color band had been collected. A similar protocol was utilized to isolate the caldesmon-CaM-TEV-DsRed-Monomer complex. For this complex 500 μL of concentrated crude caldesmon, in TBS buffer with calcium, was combined with 500 μL CaM-TEV-DsRed-Monomer fusion, diluted to 5 mL with TBS buffer with calcium and mixed overnight at 4 °C. This complex was applied to a copper charged metal affinity column, rotated for 1 h and washed with increasing concentration of imidazole-containing TBS buffer with calcium. Each wash used a volume of 5 – 7 mL of buffer. The Caldesmon-CaM-TEV-DsRed-Monomer complex was eluted with TBS buffer containing 5 mM imidazole.

4.2.5 Spectroscopic Analysis of M13-DsRed-Monomer Fusion

The UV-visible and fluorescence spectra of the M13-DsRed-Monomer fusion were collected as previously described for CaM-TEV-DsRed-Monomer [76]. Briefly, A volume of 1 mL of (0.1 μM) the M13-DsRed-Monomer fusion was placed in a cuvette, and the absorption spectra of the fusion recorded at room temperature, using an Agilent 8453 UV-visible spectrometer from Agilent Technologies (Santa Clara, CA). For the fluorescence spectra, a 200 μL volume of the fusion protein was placed in a microtiter plate and the excitation and emission spectra obtained at room temperature using a Cary Eclipse Fluorescence Microtiter Plate Reader from Varian Inc. (Walnut Creek, CA). The absorbance, excitation, and emission wavelength of the CaM-TEV-DsRed-Monomer fusion protein are tabulated in Table 6, seen in Chapter 3 [76].

4.2.6 SDS-PAGE and Blot Analysis of Eluted Complexes

The purified CaM-M13-DsRed-Monomer and caldesmon-CaM-TEV-DsRed-Monomer complexes were run on an SDS-PAGE gel. For the dot blot analysis a volume of 1.5 μL of the purified CaM-M13-DsRed-Monomer complex was spotted onto a piece of nitrocellulose, dried, and incubated for 1 h, in Tris/Ca^{2+} buffer with 0.5 % skim milk,

at room temperature. The nitrocellulose was then washed three times for 5 min in PBS buffer, and incubated with the Tris/Ca^{2+} buffer containing a 1:500 dilution of a primary anti-CaM antibody for at least 30 min. This was again washed three times for 5 min with Tris/Ca^{2+} buffer and incubated for a further hour with a 1:5000 dilution of the secondary antibody. The nitrocellulose was again dried and then incubated with a horseradish peroxidase substrate. The same protocol was used for the caldesmon-CaM-TEV-DsRed-Monomer complex, utilizing an anti-caldesmon primary antibody. The Caldesmon-CaM-TEV-DsRed-Monomer complex was further subjected to western-blotting. The complex was run on a 10 % SDS-PAGE gel and transferred to a nitrocellulose membrane using electrophoretic blotting, 20 V, 100 mA for 4.5 h, in TOWBIN buffer (25 mM Tris, 192 mM glycine, 20 % (vol/vol) methanol, pH 8.3). The membrane was blocked for 1 h in the Tris/Ca^{2+} buffer with 5 % powered milk, and incubated overnight, at 4 °C, with the primary anti-caldesmon antibody (1:5000 dilution). The membrane was washed three times for 10 min with the Tris/Ca^{2+} buffer and incubated for a further hour with a 1:5000 dilution of the secondary antibody. The blot was, again, visualized with horseradish peroxidase substrate.

4.3 Results and Discussion

The work presented in this chapter demonstrates the use of DsRed-Monomer as an affinity tag for the isolation of protein-peptide and protein-protein complexes. DsRed-Monomer's natural copper-binding affinity has been utilized to purify itself, as well as genetically fused proteins and peptides, as discussed in Chapter 3 and in previous reports [16]. The fusions of DsRed-Monomer prepared here have allowed for the isolation of interacting protein complexes, again utilizing this natural copper-binding affinity. We have isolated a protein-peptide complex, CaM-M13, and a protein-protein complex, caldesmon-CaM, from a crude cellular extract using DsRed-Monomer as an affinity tag (Figure 20).

The M13-DsRed-Monomer fusion gene was prepared by PCR technique as described in the methods section. This gene was evaluated via DNA sequencing to verify the presence of the M13 peptide and the reading frame of the gene. This was further confirmed by the lack of red fluorescence seen for the expressed protein. A shift in the M13-DsRed-Monomer reading frame was observed due to wrong primer design. To correct this error another primer was designed. The sequencing results of the new plasmid showed that the M13 DNA sequence and the DsRed-Monomer gene were both present and in the correct reading frame. This gene was transformed and expressed in *E. coli*. The M13-DsRed-Monomer fusion protein was initially purified on a copper immobilized column and run on an SDS-PAGE gel to verify its purity (Figure 21). The spectral characteristics of the purified fusion protein were monitored. The UV-vis absorbance spectra, of M13-DsRed-Monomer, yielded results comparable to those seen for native DsRed-Monomer, with peaks at ~480 and ~556 nm. Additionally the excitation and emission wavelength maxima obtained for the purified M13-DsRed-Monomer, 556 and 597 nm, are the same as that reported for DsRed-Monomer previously in this work. The CaM-TEV-DsRed-Monomer fusion was prepared, expressed, purified, and spectrally evaluated as described in the previous chapter [76]. As previously reported this DsRed-Monomer fusion showed the same absorbance and excitation and emission wavelength maxima as DsRed-Monomer (Table 8). While these two DsRed-Monomer fusions were purified for spectral analysis, crude fusion proteins were used for the subsequent binding studies.

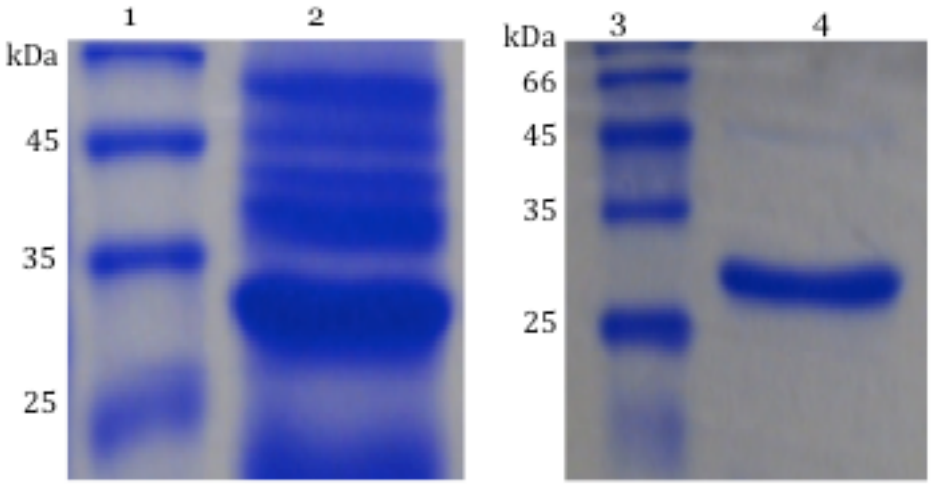

Figure 21: SDS-PAGE gel of purified M13-DsRed-Monomer, (lane 1) molecular weight protein marker, (lane 2) crude M13-DsRed-Monomer, molecular weight marker (lane 3), pure M13-DsRed-Monomer (lane 4)

Table 8: Characteristics of DsRed-Monomer and the CaM and M13 fusions

	$\lambda_{excitation}$ (nm)	$\lambda_{emission}$ (nm)	Absorbance Max (nm)
DsRed-Monomer	556	597	480, 556
CaM-TEV-DsRed-Monomer	556	597	480, 556
M13-DsRed-Monomer	556	597	480, 556

The spinach CaM encoded into the pVUC-1 plasmid was expressed in *E. coli* and run on an SDS-PAGE gel, a strong band was observed at ~15 kDa, indicative of the crude CaM (Figure 22). Initial control studies were done to determine if any copper-binding affinity existed for the CaM alone. Crude CaM was applied to an immobilized copper column, allowed to bind to the column for 1 h and washed with TBS buffer, containing no imidazole. Further washes were done with increasing imidazole concentrations (1 – 5 mM) and the whole series run on an SDS-PAGE gel. This gel showed that the CaM eluted in the initial wash step, prior to the addition of the imidazole, demonstrating that CaM has no copper-binding affinity. To isolate the CaM-M13-DsRed-Monomer

complex, 2 mL of both the crude spinach CaM and the M13-DsRed-Monomer fusion was mixed for at least an hour at room temperature. Since this CaM-M13 interaction is calcium dependent, all buffers used for the purification contained 10 mM $CaCl_2$. The binding time for the CaM-M13 complex formation was chosen based on a number of studies, these studies allowed an optimal time to be determined. Binding the CaM to the M13-DsRed-Monomer for less than 1 hour resulted in poor isolation of the CaM-M13 complex, whereas longer than 1 hour showed no noticeable improvement. The binding kinetics between the CaM protein and the M13 peptide would be much faster in an optimal cellular environment. However, in our studies performed in cellular extract, we believe that the environment is not ideal for binding, which may have resulted in the longer binding time seen for these studies. The crude complex mixture was applied to a copper charged metal affinity column, and bound for at least 1 h at room temperature. The column was washed with multiple column volumes of TBS buffer, containing calcium. Further washes were done with TBS with increasing concentrations of imidazole (from 1 to 4 mM). To elute the purified complex, 2 to 5 mL of a TBS buffer with 5 mM imidazole were passed through the column. Since the DsRed-Monomer has a vibrant red color the eluted complex was easily observed as it flowed off the column.

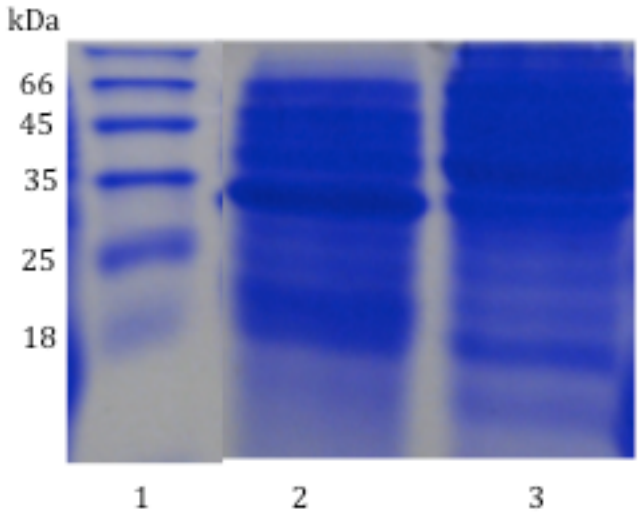

Figure 22: SDS-PAGE gel of crude fusion protein and crude CaM, molecular weight protein marker (Lane 1), crude CaM M13-DsRed-Monomer complex (Lane 2), and crude CaM (Lane 3)

The purity of the isolated complex was evaluated by SDS-PAGE gel electrophoresis, which yielded two bands, one at ~15 kDa, consistent with spinach CaM and one at ~29 kDa coinciding with M13-DsRed-Monomer (Figure 23). The eluted complex was further analyzed by dot blot assay, to confirm that the isolated protein is indeed CaM. A 1.5 μL sample of the purified complex, along with a 1.5 μL sample of the collected flow through from the initial wash steps of the purification, was spotted onto a nitrocellulose membrane, and incubated with an anti-CaM primary antibody. This was then incubated with a secondary antibody and then with a horseradish peroxidase. A strong blue color was observed within minutes of the addition of the peroxidase substrate, indicating the presence of CaM within the complex on the spot (Figure 24). The flow through from the initial wash steps of the purification was also blotted to determine if any of the CaM was washing off the column prior to its elution as the complex with M13-DsRed-Monomer.

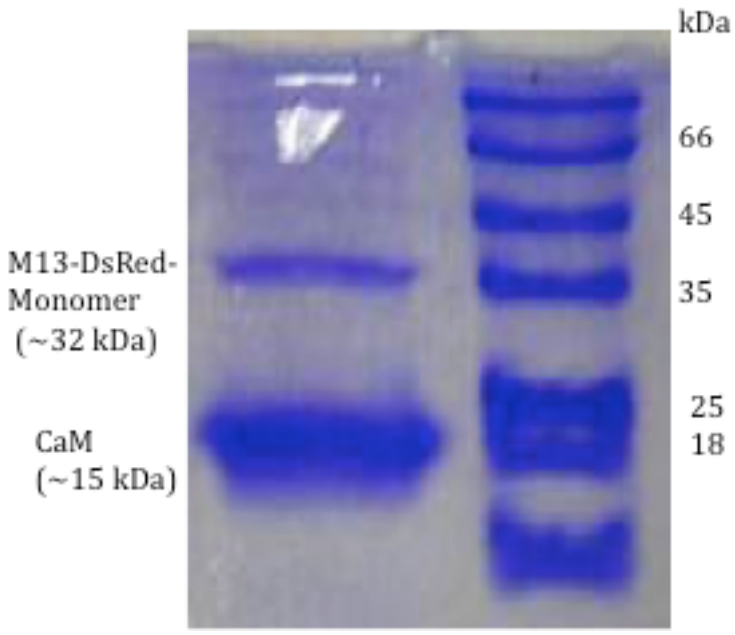

Figure 23: SDS-PAGE gel of isolated CaM-M13-DsRed-Monomer complex (lane 1), molecular weight protein marker (lane 2)

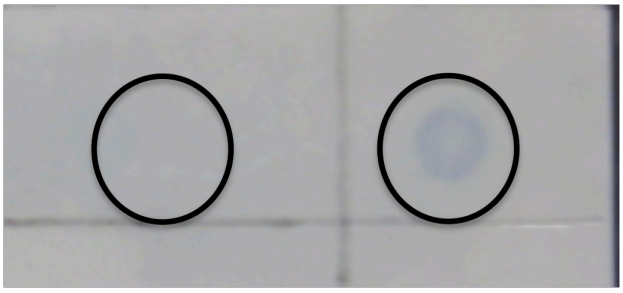

Figure 24: Dot blot assay of isolated CaM-M13-DsRed-Monomer (right panel) collected flow through from the initial wash step of the purification (left panel)

Using a similar protocol, the caldesmon-CaM-TEV-DsRed-Monomer complex was also isolated. For this study, crude caldesmon was extracted from smooth muscle, obtained from fresh chicken gizzards, and run on an SDS-PAGE gel (Figure 25). A control study was also conducted with the caldesmon protein to determine if it bound to the copper column in the absence of the CaM-TEV-DsRed-Monomer. This protein also eluted in the initial wash step, indicating that caldesmon does not bind to the copper column in the absence of CaM-DsRed-Monomer. To isolate the caldesmon-CaM complex, both crude proteins, caldesmon and CaM-TEV-DsRed-Monomer, were

combined, mixed overnight at 4 °C, and applied to a copper charged metal affinity column. As described previously, this binding time was determined by a series of time studies, which determined the optimal time required for the binding of the caldesmon-CaM complex. The complex was allowed to bind to the column for at least 1 hour and washed with multiple column volumes of TBS buffer. All TBS buffers used for this purification contained 10 mM $CaCl_2$, again, since the interaction between caldesmon and CaM is also calcium dependent. The column was washed with TBS buffer with increasing concentrations of imidazole (from 1 to 4 mM). The complex was eluted with TBS buffer containing 5 mM imidazole. The color of the DsRed-Monomer was again used to indicate when the complex had fully eluted. The collected elution was run on an SDS-PAGE gel and evaluated via dot blot as described for the CaM-M13-DsRed-Monomer (Figure 26). Although the caldesmon selected for this study was isolated from chicken gizzards, we expected it to bind to the spinach calmodulin. Calmodulin proteins, from a variety of sources, with differing amino acid sequence identity have been found to retain the necessary sequence required to form the binding site, for enzyme and protein binding [100]. For the isolated caldesmon-CaM complex a clear band was seen at ~90 kDa for the caldesmon protein and a second band at ~42 kDa for the CaM-TEV-DsRed-Monomer fusion. A further band seen at ~70 kDa is believed to represent a low molecular weight form of caldesmon [101, 102], also extracted from the chicken gizzards. In order to verify the identity of the caldesmon protein a dot blot assay was done, using the same protocol as for the CaM-M13-DsRed-Monomer complex. The dot blot, with the anti-caldesmon primary antibody, clearly showed the presence of caldesmon in the eluted protein complex (Figure 27). Again this dot blot was compared to the flow through from the initial wash of the column to determine if any of the caldesmon was being washed off before its elution with CaM-TEV-DsRed-Monomer. Utilizing the same anti-caldesmon primary antibody, the caldesmon-CaM-TEV-DsRed-Monomer complex was examined by western-blotting (Figure 28). This western-blotting showed only a single band, representing the high molecular weight caldesmon.

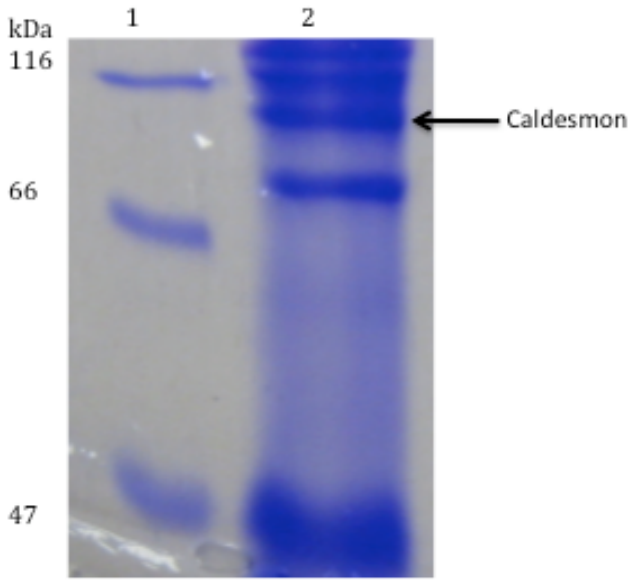

Figure 25: SDS-PAGE gel of crude caldesmon extracted from chicken gizzards (lane 2), molecular weight protein marker (lane 1)

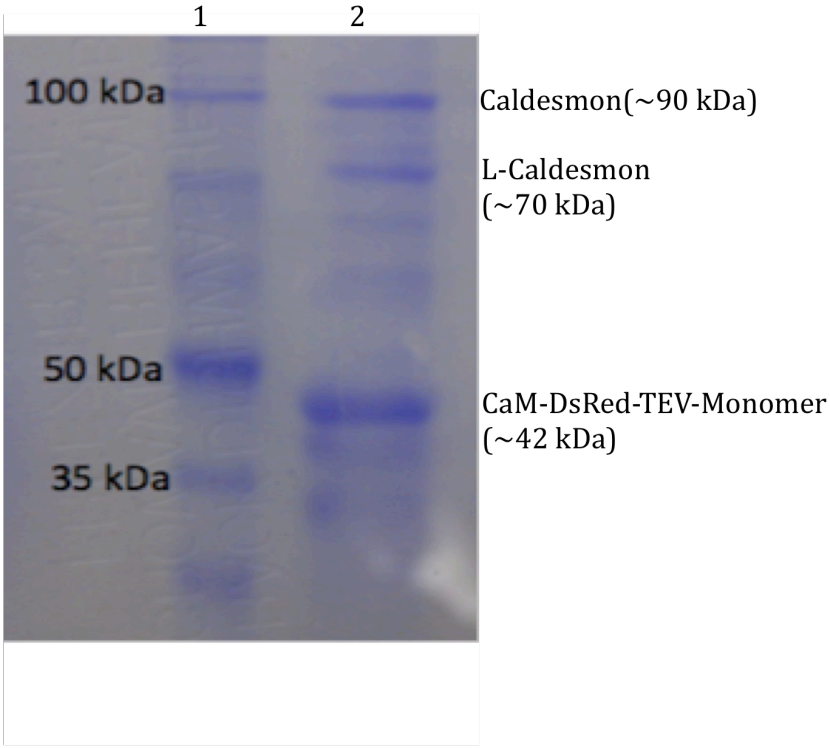

Figure 26: SDS-PAGE gel of isolated caldesmon-CaM-TEV-DsRed-Monomer complex (lane 2), molecular weight protein marker (lane 1)

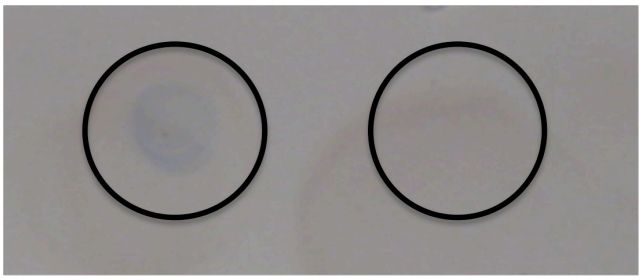

Figure 27: Dot blot assay of isolated caldesmon-CaM-TEV-DsRed-Monomer complex (left panel), collected flow through from the initial wash steps (right panel)

Figure 28: Western-blot of caldesmon-CaM-TEV-DsRed-Monomer

To identify this second band (~70 kDa) as a low molecular weight caldesmon, rather than a second calmodulin-binding protein, additional western-blotting studies are currently underway in our laboratory. Furthermore, as demonstrated in the previous chapter, the TEV cleavage site, coded between the CaM and DsRed-Monomer, could be utilized to separate the caldesmon-CaM complex from the DsRed-Monomer, for additional studies.

4.4 Conclusion

The work presented in this chapter demonstrates a proof-of-concept use of DsRed-Monomer, to isolate a protein-protein or protein-peptide complex. Two representative complexes were chosen for these studies, CaM-M13 and caldesmon-CaM. While both of these interactions are well understood, we envision that the method described here could be used to isolate unknown binding partners from a crude cellular matrix as well as for *in vivo* studies. The studies presented here address a number of problems identified for other isolation/purification tags, such as the expense and stability of antibodies for immunoaffinity, or the multiple tags required for TAP. DsRed-Monomer tags have been demonstrated here and in previous work to have no effect on protein expression, or folding, allowing their use in native environments. The natural copper-binding affinity of this protein also allows for a simple, one-step, purification on an inexpensive metal-affinity column. The fluorescence of DsRed-Monomer can also be utilized for tracking protein-protein complexes *in vivo*, for future studies. Additionally, the natural red color of the DsRed-Monomer protein, simplifies this purification, allowing the eluted complex to be visually observed during the purification.

CHAPTER 5. RED FLUORESCENT PROTEIN VARIANTS WITH INCORPORATED NON-NATURAL AMINO ACID ANALOGUES

5.1 Introduction

The discovery and mutation of DsRed has expanded the possible uses of fluorescent proteins beyond those demonstrated for the more commonly used GFP. While the bulk of the genetic modifications performed on DsRed, have been aimed at improving the many limitations observed for native DsRed [3, 4, 8, 12, 103, 104], as discussed in Chapter 1, recent studies have focused on the possibility of expanding the color pallet of its fluorescence. To date a few traditional mutagenesis studies have been done with DsRed and its variant, to shift the fluorescence excitation and emission wavelengths. Such studies have primarily focused on the amino acid residues in and around the chromophore of the protein. The chromophore of DsRed, as described in Chapter 1 of this work, is made up of a tri-peptide sequence of amino acids, specifically Gln-Tyr-Gly (residues 66-68) [7]. These residues form a fluorescently active chromophore autocatalytically through a three-step process, a cyclization reaction followed by two sequential dehydrogenations [26, 105]. The cyclization and initial dehydrogenation lead to a green emitting chromophore [106], this is shifted to a red emitting chromophore by the second dehydrogenation reaction. This second dehydrogenation extends the conjugated π-system of the chromophore which creates the red fluorescence [107]. Here we describe exploratory studies in the construction and characterization of variants of DsRed-Monomer with altered spectral properties by incorporating non-natural amino acids into the protein.

Rational mutagenesis has, so far, been a choice method to create variants of proteins with altered properties and to study structure-function relationships [3, 104]. In

this method, canonical amino acids are inserted into specific positions within the protein. For example, site-directed mutagenesis performed on mRFP1 resulted in the creation of variants with shifted excitation and emission wavelength maxima of up to 18 nm. These shifts have been attributed to altered electrostatic interactions with the chromophore of the protein [108]. However, incorporation of non-natural amino acids offers an alternative method, allowing for the addition of novel functional groups into proteins [104, 109-112]. For example, site-specific incorporation of non-natural amino acids has been used to create mutants of GFP [113-116], which show a variety of fluorescence shifts and properties. Specifically, incorporation of Trp analogues into GFP using a method of forced biosynthetic incorporation, has produced a number of "gold"-shifted fluorescent proteins [114]. In addition mutations at the Tyr66 position within the chromophore of GFP created mutants with no fluorescence or blue-shifted emission maximum depending on the analogue [115, 116]. Further incorporation of aromatic natural and non-natural amino acids into this same Tyr66 residue, of GFP, has shown a variety of emission shifts [115]. The fluorescence shifts observed for these mutants suggest the possibility of obtaining alternative, and biochemically appropriate fluorescent proteins by incorporating non-natural amino acid analogues into DsRed-Monomer.

Although incorporation of non-natural amino acids has been successfully demonstrated in GFP [117], prior to the work presented here, such studies had not previously been done on DsRed, its mutants, or any red fluorescent proteins. In this chapter we describe the incorporation of two Tyr analogues into DsRed-Monomer, creating variants with non-natural amino acid residues within the chromophore of the protein. The position of the Tyr67 residue, as part of the DsRed chromophore, prompted the use of tyrosine analogues in our study to shift the fluorescence of the protein. The non-natural amino acid analogues were incorporated into the protein by a system of forced biosynthetic incorporation [118], a simpler and quicker method than tRNA-based site-specific genetic incorporation. This method relies on the use of a minimal media, starved of the amino acid targeted for incorporation. The amino acid analogue of choice is added upon induction of the protein, allowing only the non-natural amino acid analogue to be incorporated into the final protein, in place of the native amino acid.

Hyun Bae *et al*. [114] showed that forced biosynthetic incorporation could be used for the overall incorporation of amino acid analogues into GFP. However, further studies showed that incorporation of non-natural amino acids into any position, outside of the chromophore had no effect on the spectral properties of GFP [114]. On the basis of this we selected fluoro- and amino- analogues of tyrosine for our study, specifically 3-fluoro-L-tyrosine and 3-amino-L-tyrosine [6]. Furthermore, X-ray crystal structure studies of DsRed has shown that the other Tyr residues within the protein do not interact with the chromophore and therefore should not affect the spectral properties of the protein [6]. The fluoro- analogue was selected due to its significantly different pKa than the hydroxy functional group. This has previously been used to alter the pKa of functional groups within the active site of enzymes, changing their catalytic properties [118, 119]. The addition of fluorinated amino acid analogues has also been found to affect the conjugation of the π-system of the chromophore and to cause limited changes in the bond lengths within such systems. In addition, this analogue may promote the formation of additional hydrogen bonds within the system [118, 119]. In contrast, the amino- group, on the 3-amino-L-tyrosine, should primarily affect the electrostatic charge within the aromatic ring of the tyrosine and allow either a different pattern of hydrogen bonding with surrounding amino acid residues, or contribute to the conjugation of the chromophore. The study here demonstrates that incorporation of non-natural amino acid analogues into DsRed-Monomer is a viable approach to alter the spectral characteristics of the protein. We envision that this study will open up the door to non-natural amino acid incorporation studies with red fluorescent proteins and its mutants.

5.2 Materials and Methods

5.2.1 Expression and Purification of DsRed-Monomer with Incorporated Non-Natural Amino Acids

The gene for DsRed-Monomer was digested with *Bam*HI and *Eco*RI and cloned into pRSetB to construct the plasmid pSKD1, as previously described. M9 minimal media [120, 121] containing 100 μg mL^{-1} ampicillin was prepared without tyrosine, tryptophan and phenylalanine. A 5 mL sample of the minimal media was inoculated with *E. coli*, JM107, containing the plasmid pSKD1 and incubated overnight in a shaker at 37 °C. The culture was transferred to a 200 mL sample of the minimal media and grown to an OD_{420} of 1.00 and induced with isopropyl-β-D-thiogalactoside (IPTG, 0.5 mM final concentration, from Sigma). Tryptophan, phenylalanine, and either tyrosine or the appropriate tyrosine analogue (1 mM final concentration of each amino acid, from Spectrum Chemicals) [118] was also added at that time. The cultures were grown for a further 5 h with shaking, 250 r.p.m., at 37 °C and collected by centrifugation, 4000 r.p.m., for 30 min at 4 °C. The pellet was dissolved in the PBS-binding buffer (100 mM Na_2PO_3, 50 mM NaCl, pH 7.0) and sonicated for 5 min to lyse the cells. The crude native DsRed-Monomer and the non-natural variants were purified on an immobilized copper charged sepharose column, as described in the previous chapter [16].

5.2.2 Determination of Protein Purity and Concentration

Protein purity was determined by running an SDS-PAGE assay with 12.5 % acrylamide gel at 150 V for 90 min at room temperature. Coomassie Brilliant Blue R-250 solution was used to stain the gels overnight and destained for at least 2 h. Protein concentration was determined by Bradford assay.

5.2.3 Spectral Analysis of Purified DsRed-Monomer with Incorporated Non-Natural Amino Acid and Comparison with Native DsRed-Monomer

Mass spectrometry analysis was performed by following the protocol of Gross *et al*. [5]. Approximately 2 nmol of purified protein was lyophilized and dissolved in 15 μL of sterilized water, 3 μL of guanidinium chloride (6 M) was added and the solution heated to 80 °C until it turned yellow. The solution was cooled to room temperature and 1 μL of HCl (0.33 M) was added followed by 10 μL of LysC endoprotease (0.05 μg/μL in 100 mM Tris, pH 9.2). The digestion proceeded for 22 h at 37 °C and was quenched with trifluoroacetic acid (0.1 % vol/vol). The mass spectra of each of the digested proteins were recorded on an Agilent 1100 Series LC/MSD, from Agilent Technologies (Santa Clara, CA) by direct injection, passing through the LC column

To obtain the fluorescence spectra, a volume of 200 μL (0.1 μM) of each of the non-natural mutants and the native DsRed-Monomer was placed into a microtiter plate, and excitation and emission scans of the proteins collected, using a Cary Eclipse Fluorescence Microtiter Plate Reader (Varian Inc, Walnut Creek, CA).

The UV-visible spectra were also collected. A volume of 1 mL (0.1 μM) of the two mutants and the native DsRed-Monomer was placed in a cuvette, and the absorption spectra recorded at room temperature, using an Agilent 8453 UV-visible spectrometer (Agilent Technologies, Santa Clara, CA)

The CD spectra of the proteins were also collected. The purified non-natural mutants and the native protein (250 μL, 0.1 μM) were placed in a 0.2 cm cell, and the adsorption spectrum was obtained at room temperature, using a Jasco Corporation spectropolarimeter (Tokyo, Japan).

Temperature and pH stability was also evaluated. Fluorescence spectra were recorded at 4 °C, room temperature (25 °C) and 37 °C for both the native protein and the two variants. Each protein was incubated for at least 2 h, at their respective temperature, prior to their spectra being collected. The pH of the proteins was adjusted from 4 to 11, with MOPS buffer, in increments of 1 pH unit, and the fluorescence emission of each protein recorded.

5.3 Results and Discussion

Fluorescent protein variants with differing spectral characteristics are highly desirable for biotechnology and cell biology studies. To obtain these variants a number of approaches including random mutagenesis, directed evolution, and non-natural mutagenesis have been successfully used. Previously in these studies GFP was primarily used as the scaffold. The availability of the red fluorescent protein, DsRed, provides a unique opportunity to further extend the spectral diversity of FPs. Thus far only mutagenesis of naturally available amino acids has been attempted with DsRed. Here we studied incorporation of non-natural amino acid analogues into DsRed-Monomer, to construct variants that yield alterations in the spectral characteristics of the protein. In our study, DsRed-Monomer and its variants with non-natural amino acids were expressed in minimal media using a method of forced biosynthetic incorporation. For this method the non-natural analogue was added to the culture media at a stage right before the protein expression. This method was chosen, for this study, rather than directed incorporation of non-natural amino acids because the latter method is complicated and time consuming, and the aim of this study was an initial demonstration of amenability of DsRed to non-natural mutagenesis.

The plasmid pSKD1 was transformed into *E. coli* cells and the proteins were expressed. During expression the time for the initial observation of color and the time to reach maximum fluorescence for the mutants were comparable to native DsRed-Monomer, in the minimal media. This indicates no change in the folding ability of the proteins upon mutation. Furthermore, we did not observe any formation of protein aggregates in the mutants as well as in the native DsRed-Monomer, implying no effect on the solubility of the proteins. The proteins were purified using an immobilized copper column, as previously discussed [16]. The purified proteins were run on an SDS-PAGE gel to verify purity (Figure 29). The non-natural variants of DsRed-Monomer were analyzed by spectroscopic and spectrometry techniques, and their characteristics were compared to those of native DsRed-Monomer prepared in the same manner.

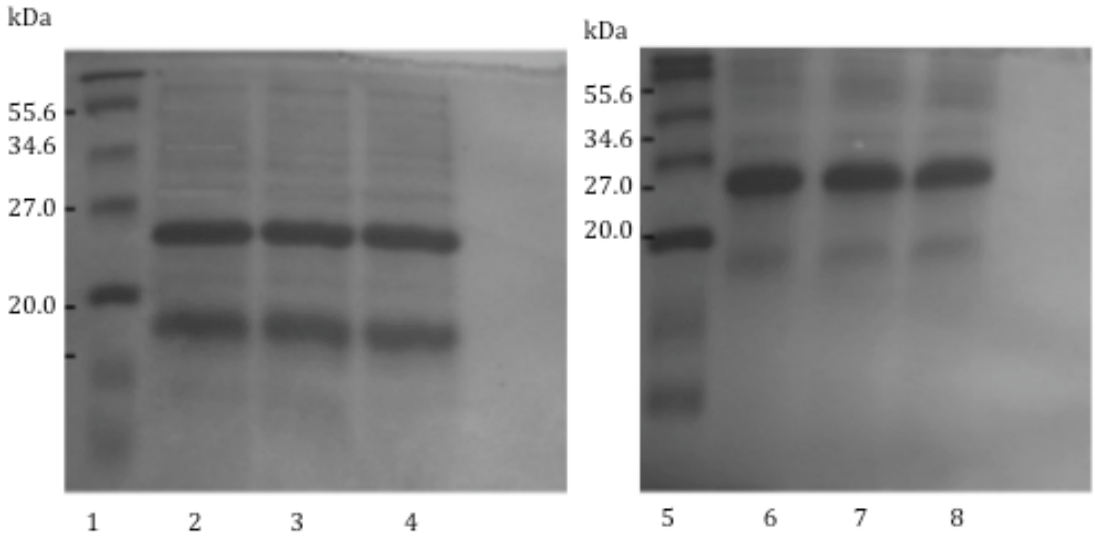

Figure 29: SDS-PAGE gel of crude (left panel) and purified (right panel) non-natural analogues of DsRed-Monomer. Molecular weight protein marker (lane 1 and 5), crude DsRed-Monomer (lane 2), crude 3-amino-L-tyrosine variant (lane 3), crude 3-fluoro-L-tyrosine variant (lane 4), pure DsRed-Monomer (lane 6), pure 3-amino-L-tyrosine variant (lane 7), and pure 3-fluoro-L-tyrosine variant (lane 8)

To verify the incorporation of the non-natural analogues into the chromophore of the protein, the mass spectra were collected for the DsRed-Monomer and for the non-natural mutants. The proteins were subjected to LysC digestion, which produced a peptide that included the chromophore of the protein, of mass 2185 for the native DsRed-Monomer [5]. The spectra of the non-natural variants showed the expected increases in mass, compared to the native protein (Table 9). A mass increase of approximately 15 was seen for the peptide of the amino- mutant compared to the chromophoric peptide obtained from the native protein. This increase coincides with the addition of an amino-group onto the aromatic ring of tyrosine, within the chromophore. The fluoro- mutant showed a mass increase of approximately 18 compared with the native protein, corresponding to the addition of fluorine onto the tyrosine ring. This mass analysis confirms the presence of non-natural amino acid analogues into the peptide forming the chromophore. Furthermore, the mass spectra of the mutants did not show any peak corresponding to the native DsRed-Monomer, suggesting the full incorporation of the non-natural analogues into the protein.

Table 9: Characteristics of DsRed-Monomer and its non-natural variants

	$\lambda_{excitation}$ (nm)	$\lambda_{emission}$ (nm)	ε ($M^{-1}cm^{-1}$)	Quantum Yield (%)	Mass of Chromophore peptide
DsRed-Monomer	556	603	59,000	0.04	2185
Amino-Variant	556	615	59,000	0.20	2199.6
Fluoro-Variant	556	591	47,000	0.13	2205

The fluorescence excitation and emission spectra of both the purified DsRed-Monomer and the purified non-natural mutants were recorded. The incorporated analogues showed no effect on the excitation spectra of the proteins, with the expected excitation maxima of 556 nm seen for each of the mutants. However, variations in peak intensity were seen, the amino- mutant showed the strongest fluorescence excitation intensity, with the fluoro- mutant intermediate, and native DsRed-Monomer the weakest. Spectral shifts, however, were observed in the emission spectra. The fluoro-tyrosine incorporated mutant showed a distinct blue shift of 12 nm (λ_{max} 591 nm) compared to native DsRed-Monomer (λ_{max} 603 nm), whereas the amino-tyrosine incorporated mutant showed a red shift of 12 nm (λ_{max} 615 nm) (Figure 30). These opposite shifts in emission wavelength maximum were expected since the two analogues would have opposite effects on the conjugated electron system of the chromophore. The addition of the amino- group will lead to a more expanded π-conjugated chromophore system [116], at the aromatic ring, because of the electron donation of this group. We expected that this would stabilize the conjugation in the chromophore leading to the observed red shift in the emission spectra. The fluoro- addition, however, would withdraw electrons from the conjugated system of the aromatic ring and chromophore in general. This reduction in the aromaticity of the Tyr phenyl ring may cause destabilization of the conjugation leading to the observed blue shift in emission. The absence of any secondary peaks or shoulders indicates 100 % incorporation of the non-natural amino acid of interest into the protein occurred. Any partial incorporation could have also given peaks or shoulder

similar to the native protein, which, were not observed. These results were obtained from a number of different expressions, and demonstrate the reproducibility of these observations. Emission spectra were recorded using the same concentration of all three proteins (data not shown); these spectra showed that the amino- mutant gave the most intense fluorescence followed by the fluoro- mutant and native DsRed-Monomer giving the lowest intensity emission at their respective emission wavelength maxima. Further studies showed that temperature insensitivity (between 4 and 37 °C) of the protein's fluorescence was maintained for the mutants compared with native DsRed-Monomer. The pH dependence of the fluorescence intensity of native DsRed-Monomer, the amino- and fluoro- variant was studied. The fluorescence intensity was found to be unaffected between pH 5 and 11. This is consistent with the results obtained by Baird *et al*. [3] that showed negligible dependence of DsRed-Monomer's fluorescence intensity on pH.

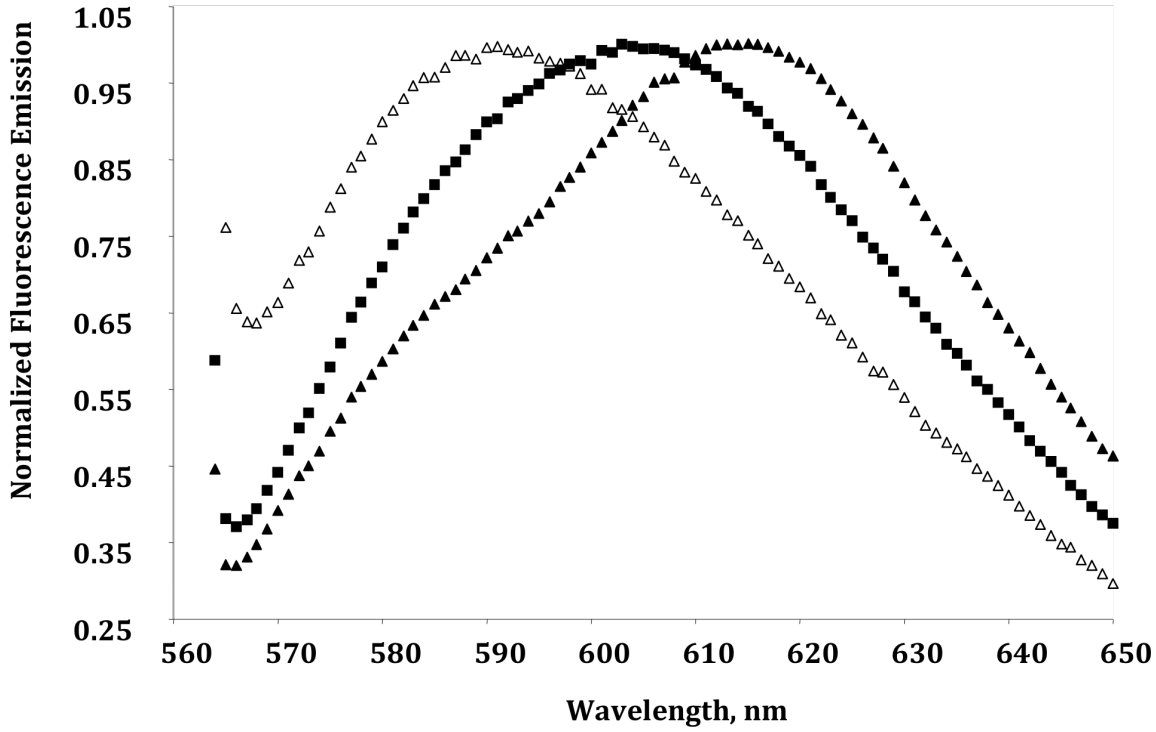

Figure 30: Normalized fluorescence emission spectra of DsRed-Monomer and non-natural mutants. (■) native DsRed-Monomer, (▲) 3-amino-L-tyrosine DsRed variant, (Δ) 3-fluoro-L-tyrosine DsRed variant

The UV-Visible spectra of the purified DsRed-Monomer and the purified non-natural mutants were recorded from 400 to 650 nm to further explore the spectral properties of these mutants. It has previously been reported [4, 122] that the UV absorption spectra of a monomeric DsRed, mRFP1, showed a strong peak at 556 nm corresponding to the red fluorescent species. The spectra also showed two additional peaks at ~480 and ~520 nm [1]. The peak at 480 nm has previously been attributed to a green-emitting intermediate for native (oligomerized) DsRed [3, 106]. The UV-visible spectra of DsRed-Monomer and the non-natural mutants (Figure 31) showed that the chromophore of all the proteins was absorbed strongly at the expected 556 nm and showed two additional peaks at 480 and 520 nm. An excitation study performed at 480 nm yielded only minimal fluorescence, on the order of 20 % of that seen at 603 nm. The same pattern of peaks was seen for all three proteins; however, the intensity of the absorbance peaks varied. Of the three proteins, the fluoro- variant showed the most pronounced peak at 480 nm. Within the spectra of the fluoro- mutant, the peak at 480 nm appeared more intense than the peak at 556 nm corresponding to the red fluorescent species. This suggests that incorporation of the fluoro- group may hinder the conjugation necessary for the red chromophore formation, locking the chromophore at an intermediate stage. This also may account for the decrease in fluorescence emission, seen for this protein compared to the amino- mutant. The amino- mutant showed the most pronounced peak at 556 nm, corresponding to emission from the major red fluorescent species. The 556 nm peak of the amino- mutant was also of highest absorbance units among the three proteins. This coincides with the fluorescence emission spectra of the proteins in which the amino- mutant showed the most intense fluorescence emission. This variant also showed an absorbance intermediate to both native DsRed-Monomer and the fluoro- variant, at 480 nm. The native DsRed-Monomer showed the lowered absorbance at both 480 and 556 nm; however the shoulder at 520 nm was more pronounced for this protein than for either of the variants. This shoulder was almost undetectable for the two variants. These fluorescence and absorbance observations further indicate that the position and electron density on Tyr67 are crucial for red chromophore formation in addition to the amino acids (Gln66 and Gly68) necessary for

the extended conjugation observed in DsRed. Further, Tyr67 can potentially be targeted to generate variants with far red-shifted emission wavelengths.

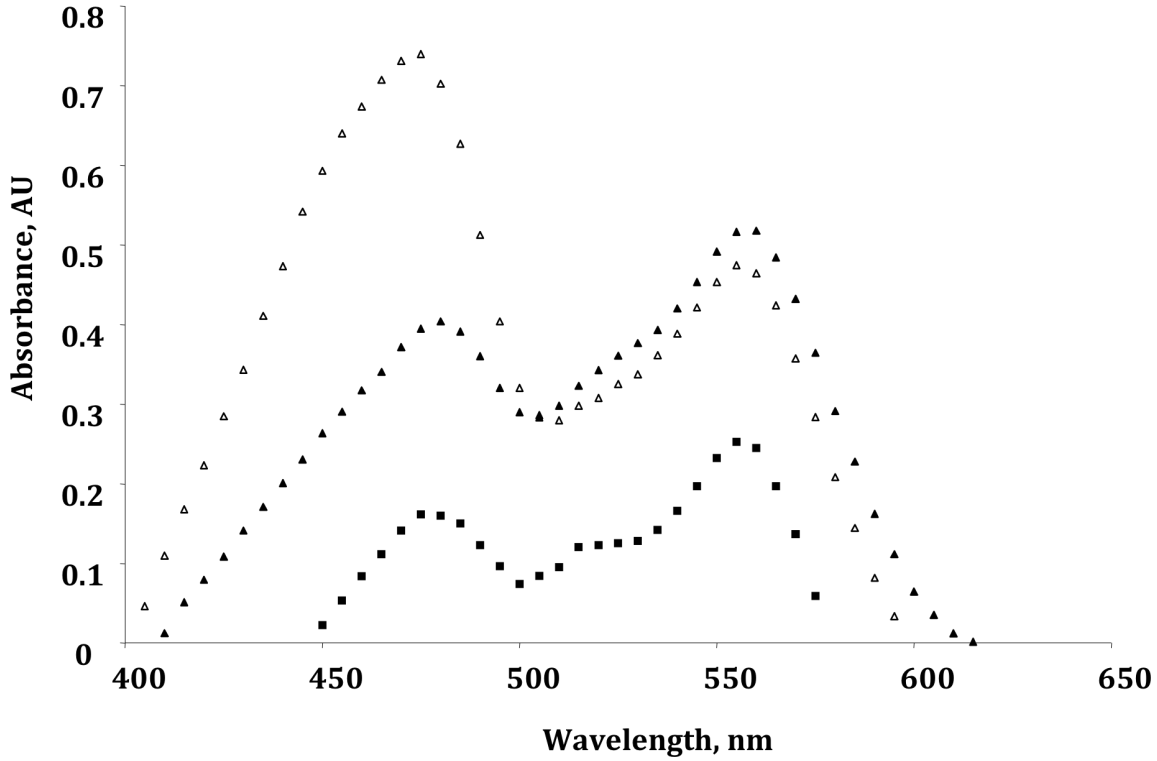

Figure 31: UV-Visible absorption spectra of DsRed-Monomer and non-natural mutants. (■) native DsRed-Monomer, (▲) 3-amino-L-tyrosine DsRed variant, (Δ) 3-fluoro-L-tyrosine DsRed variant

From the UV and fluorescence data, the extinction coefficients and quantum yields of DsRed-Monomer and each of the mutants were determined (Table 9). The quantum yield for all three proteins was calculated using DsRed-Express with a known quantum yield as the standard and by using the following equation [123]:

$$Q = Q_R\,(I/I_R)(OD_R/OD)(n^2/n_R^2)$$

where Q represents the quantum yield, I the intensity of the fluorescence, OD the optical density and n the refractive index. The values with subscript R correspond to the reference protein, DsRed-Express. This protein was chosen as the reference because it is the tetrameric form of DsRed-Monomer. For DsRed-Monomer, a surprisingly low

quantum yield of 0.05 was calculated. The quantum yield of the two variants appeared to be closer to the value of 0.4 reported for DsRed-Express. The quantum yields calculated here show that the variants obtained have improved brightness compared with the native DsRed-Monomer. This is an interesting observation since increases in quantum yield is obtained for both the amino- and fluoro- variants. This indicates that this increase is not due specifically to the presence of the fluoro- or amino- group on the Tyr. The quantum yield of DsRed-Monomer compared with DsRed-Express [4] is significantly lower. This has previously been attributed to the loss of shielding of the chromophore in the monomer. Therefore, we speculate that the presence of the amino- or fluoro- group on the Tyr ring, increasing the bulkiness of the Tyr, may improve this shielding of the chromophore in the mutated DsRed-Monomer, leading to the improved quantum yield observed here.

The far UV CD spectra of the native DsRed-Monomer and the non-natural variants were also recorded (Figure 32). This information was submitted for k2D analysis. These spectra showed that the overall secondary structural characteristics of the protein were maintained after the incorporation of the tyrosine analogues.

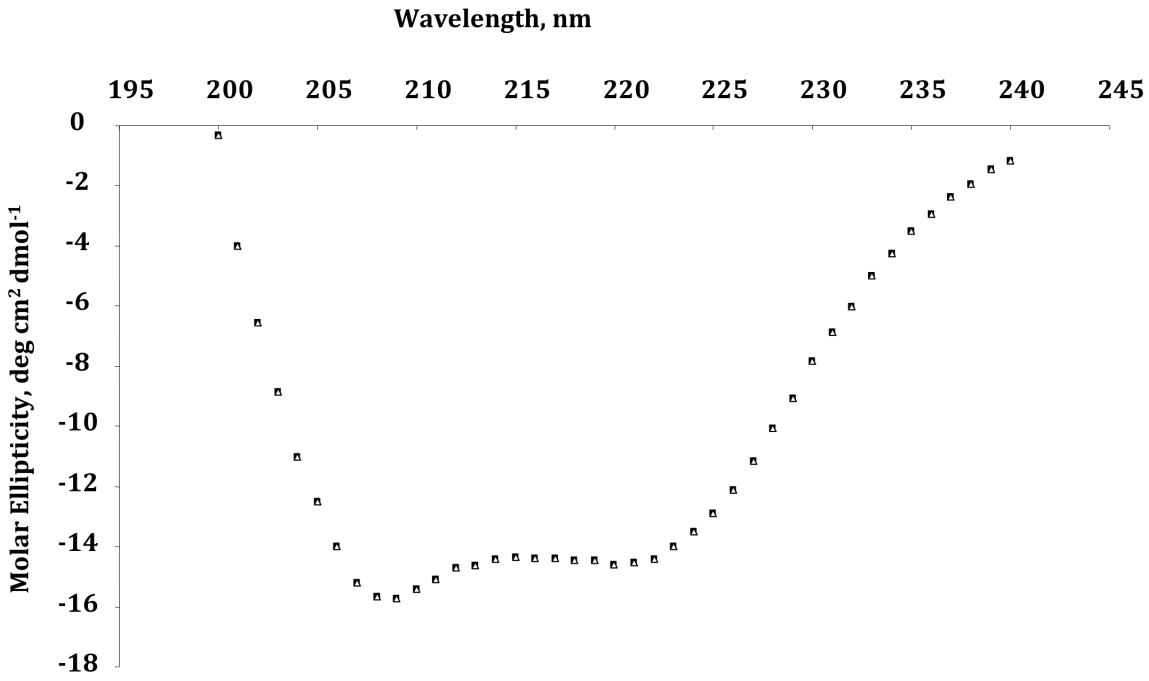

Figure 32: CD spectra of DsRed-Monomer and non-natural mutants. (■) native DsRed-Monomer, (▲) 3-amino-L-tyrosine DsRed variant, (Δ) 3-fluoro-L-tyrosine DsRed variant. Some data sets are not visible due to the exact overlap of all data points

5.4 Conclusion

The incorporation of non-natural amino acid residues into the chromophore of DsRed-Monomer caused a shift in the fluorescence emission. The fluoro- variant showed a 12 nm blue shift and the amino- variant a 12 nm red shift in fluorescence emission. The incorporation of these tyrosine analogues was verified by mass analysis of the peptide containing the chromophore. These variants also displayed improvements in their quantum yields and fluorescence emission intensities, compared to the native DsRed-Monomer. In addition, the absorption spectra of all three showed the same pattern of peaks, with variations in their relative intensities. The incorporation of the tyrosine analogues into the chromophore of DsRed-Monomer appears to have no effect on the overall structure of the variants. The studies performed by us demonstrate that the spectral properties of red fluorescent proteins can be altered by non-natural mutagenesis.

The variants produced in our study can be purified and used as labels for *in vitro* multicolor applications. Furthermore, the studies performed show that the Tyr in the chromophore, of DsRed-Monomer, can be manipulated to produce variants with unique properties. For *in vivo* applications, such variants can be produced using modified tRNAs that code for non-natural amino acids.

CHAPTER 6. CONCLUSIONS AND FUTURE DIRECTIONS

6.1 Conclusions and Future Directions

The work presented in this thesis has focused on the biochemical applications of a red fluorescent protein, DsRed-Monomer. In this work both DsRed-Monomer's natural fluorescence and its unique copper-binding affinity, which results in fluorescence quenching, have been exploited. This unique metal-binding affinity has previously been utilized for the purification of DsRed-Monomer and in the development of copper sensing systems. In this thesis work we have performed studies to identify the mechanism of this fluorescence quenching seen for DsRed-Monomer in the presence of copper. Through a series of studies, as described in Chapter 2, which included determining the copper dissociation constant, spectroscopic studies in the presence and absence of copper, the effect of pH on this copper-binding affinity, and computational studies, we were able to shed light on the fluorescence quenching mechanism of DsRed-Monomer and hypothesized possible copper-binding residues within the protein. These studies suggested that, upon copper-binding, a sphere of action static quenching mechanism results in the observed fluorescence quenching. These studies, specifically the pH and computational studies, indicated the possible involvement of His and/or Cys residues in this copper-binding. Further studies with this protein will be required to formally identify the copper-binding site of DsRed-Monomer and other RFP variants. Based on our studies within this chapter, two specific His residues, His25 and His216, could be targeted for future studies. These studies will include site-directed mutagenesis and chemical modifications, which can be monitored by fluorescence quenching assay, to study their effect on the DsRed-Monomer's copper-binding affinity. The copper-binding site, once identified, can be subjected to further rational mutagenesis with the aim of

improving the copper-binding affinity constant for DsRed-Monomer, while retaining this unique copper specificity. Such improvements of this affinity (K_D), to nM levels, would allow for improved use of DsRed-Monomer as an affinity tag for isolation and purification, while retaining the ability to elute this tag under relatively mild conditions. By understanding this quenching mechanism and identifying the copper-binding site of DsRed-Monomer, we believe that improvements can be made in the copper-binding affinity. Such improvements may enhance the utility of DsRed-Monomer as an affinity tag for purification and isolation assays as well as offering possible expansion to the uses of the fluorescence of this protein.

Another work in this thesis focused on the use of DsRed-Monomer for both purification and detection of a fusion partner, exploiting the copper-binding affinity and the fluorescence of the protein. We designed and created, via molecular biology techniques, an N-terminal fusion of DsRed-Monomer with a protein, calmodulin. Using DsRed-Monomer's natural copper-binding affinity we were able to purify this fusion partner, calmodulin, on an immobilized copper column. The calmodulin fusion partner was then separated from the DsRed-Monomer tag, via proteolytic cleavage, of a TEV site encoded between calmodulin and the DsRed-Monomer tag. Additionally, we used DsRed-Monomer's fluorescence to design a detection assay for a calmodulin-binding ligand, chlorpromazine. We observed a decrease in fluorescence emission with increasing concentrations of chlorpromazine. We attributed this to the binding of chlorpromazine to calmodulin, causing a structural change in the calmodulin and subsequently the environment of the DsRed-Monomer, resulting in this decrease in the fluorescence emission. We would like to continue to explore this type of DsRed-Monomer fusion assay by expanding the selection of fusion partners. Such work would utilize an additional set of fusion partners to explore this method to purify other target proteins. We would also like to expand on the use of the fluorescence-based detection assay, of such DsRed-Monomer fusion proteins, by demonstrating the viability of developing further assays for studying target protein-ligand pair binding. The use of this assay in a cellular environment is also of interest to the continuation of this work, since

the work to date has utilized a buffer matrix only. For this work we would express DsRed-Monomer fusions *in vivo* where a target ligand is also present.

The aim of our next work was to utilize DsRed-Monomer's natural copper-binding affinity, in the design of an isolation tag, for interacting peptide-protein or protein-protein complexes. This work utilized N-terminal fusions of DsRed-Monomer with either a peptide or protein bait partner. One such fusion of DsRed-Monomer was designed, utilizing molecular biology, to fuse a peptide to the N-terminus of the DsRed-Monomer protein. For this work the M13 peptide from skeletal muscle myosin light chain kinase, a calmodulin-binding peptide, was selected as the fusion partner. Initial studies with this fusion were done to demonstrate DsRed-Monomers use as an affinity tag to isolate a peptide-protein complex, calmodulin-M13, via copper-affinity purification. In this study DsRed-Monomer's natural fluorescence was not specifically used in a detection sense, however, it did simplify the purification as the red band could be observed eluting off the column. The previously discussed calmodulin-DsRed-Monomer fusion was also used in these studies to explore the use of a protein-DsRed-Monomer fusion as an affinity tag for isolating protein-protein complexes. In this work we demonstrated isolation of a caldesmon-calmodulin complex, again using DsRed-Monomer's copper-affinity. The current study has been performed using a cellular extract as a matrix; however, we can also employ DsRed-Monomer as an affinity tag to isolate protein-protein interacting complexes in an *in vivo* system. In the future we envision using these, and other, DsRed-Monomer fusions to isolate unknown binding partners in *in vivo* studies. Again such work will require expressing the DsRed-Monomer-target protein fusions within cells, to which an interacting protein binds. This complex once isolated, using the copper-based affinity of DsRed-Monomer, can be subjected to mass spectrometry analysis for identification of interacting proteins or ligands.

The final study in this thesis demonstrates the amenability of this protein to non-natural mutagenesis. These studies were aimed at increasing the color pallet of possible fluorescent reporters and tags. Here we focused on the three amino acids residues, which form the internal chromophore of DsRed-Monomer. Utilizing forced biochemical

incorporation we replaced the tyrosine residues within the sequence of DsRed-Monomer with either a fluoro- or amino- variant. These non-natural variants of DsRed-Monomer were spectroscopically analyzed, showing a shift in the observed fluorescence emission. The fluoro- variant showed a 12 nm blue shift and the amino- variant showed a 12 nm red shift, compared to DsRed-Monomer expressed in the minimal media. This work demonstrated the ability to shift the fluorescence emission, and other spectral characteristics, of DsRed-Monomer via non-natural mutagenesis. We envision these variants being used in the future as reporter tags, such as those discussed in the previous chapters of this and in other works for native DsRed-Monomer. Such reporters have been designed for both *in vitro* and *in vivo* studies. We believe that non-natural variants of this, and other fluorescent proteins, will be efficient tools for such methods, as well as for two-color labeling studies. Future non-natural mutagenesis studies will focus on the incorporation of additional non-natural Tyr analogues into the chromophore of the protein, as well as non-natural Gln and Gly analogues. Additionally, we will explore the use of modified tRNAs for efficient, site-specific incorporation of non-natural amino acids into DsRed-Monomer.

Since it's discovery DsRed and its variants have been utilized in a number of biochemical applications, the work presented in this thesis aims to expand these applications of one such variant, DsRed-Monomer. The initial studies, described in this work, aimed at defining the mechanism of copper-induced fluorescence quenching will ideally lead to a better understanding and future improvements of this protein's copper-based fluorescence behavior and of the copper-affinity. Further, we have explored biochemical applications for this protein, based upon both copper-binding affinity and fluorescence. We have demonstrated the amenability of this protein to N-terminal fusion with both peptides and proteins, with no effect on its overall structure or spectroscopic properties. Additionally, we have shown that DsRed-Monomer can serve as an affinity tag for efficient purification of target proteins, as a fluorescent reporter tag for interacting ligands, and as a tag to isolate interacting protein complexes. We envision that these findings can be potentially expanded to various biochemical studies and applications. Furthermore, we believe that the expansion of the color pallet of DsRed-Monomer

demonstrated here by non-natural mutagenesis could be of great interest for future multicolor labeling studies.

LIST OF REFERENCES

LIST OF REFERENCES

1. Matz, M.V., A.F. Fradkov, Y.A. Labas, A.P. Savitsky, A.G. Zaraisky, M.L. Markelov, and S.A. Lukyanov, *Fluorescent proteins from nonbioluminescent Anthozoa species.* Nat Biotechnol, 1999. **17**(10): p. 969-73.
2. Matz, M., D. Shagin, E. Bogdanova, O. Britanova, S. Lukyanov, L. Diatchenko, and A. Chenchik, *Amplification of cDNA ends based on template-switching effect and step-out PCR.* Nucleic Acids Res, 1999. **27**(6): p. 1558-60.
3. Baird, G.S., D.A. Zacharias, and R.Y. Tsien, *Biochemistry, mutagenesis, and oligomerization of DsRed, a red fluorescent protein from coral.* Proc Natl Acad Sci U S A, 2000. **97**(22): p. 11984-9.
4. Campbell, R.E., O. Tour, A.E. Palmer, P.A. Steinbach, G.S. Baird, D.A. Zacharias, and R.Y. Tsien, *A monomeric red fluorescent protein.* Proc Natl Acad Sci U S A, 2002. **99**(12): p. 7877-82.
5. Gross, L.A., G.S. Baird, R.C. Hoffman, K.K. Baldridge, and R.Y. Tsien, *The structure of the chromophore within DsRed, a red fluorescent protein from coral.* Proc Natl Acad Sci U S A, 2000. **97**(22): p. 11990-5.
6. Yarbrough, D., R.M. Wachter, K. Kallio, M.V. Matz, and S.J. Remington, *Refined crystal structure of DsRed, a red fluorescent protein from coral, at 2.0-A resolution.* Proc Natl Acad Sci U S A, 2001. **98**(2): p. 462-7.
7. Tubbs, J.L., J.A. Tainer, and E.D. Getzoff, *Crystallographic structures of Discosoma red fluorescent protein with immature and mature chromophores: linking peptide bond trans-cis isomerization and acylimine formation in chromophore maturation.* Biochemistry, 2005. **44**(29): p. 9833-40.

8. Yanushevich, Y.G., D.B. Staroverov, A.P. Savitsky, A.F. Fradkov, N.G. Gurskaya, M.E. Bulina, K.A. Lukyanov, and S.A. Lukyanov, *A strategy for the generation of non-aggregating mutants of Anthozoa fluorescent proteins.* FEBS Lett, 2002. **511**(1-3): p. 11-4.

9. Terskikh, A.V., A.F. Fradkov, A.G. Zaraisky, A.V. Kajava, and B. Angres, *Analysis of DsRed Mutants. Space around the fluorophore accelerates fluorescence development.* J Biol Chem, 2002. **277**(10): p. 7633-6.

10. Terskikh, A., A. Fradkov, G. Ermakova, A. Zaraisky, P. Tan, A.V. Kajava, X. Zhao, S. Lukyanov, M. Matz, S. Kim, I. Weissman, and P. Siebert, *"Fluorescent timer": protein that changes color with time.* Science, 2000. **290**(5496): p. 1585-8.

11. Fradkov, A.F., Y. Chen, L. Ding, E.V. Barsova, M.V. Matz, and S.A. Lukyanov, *Novel fluorescent protein from Discosoma coral and its mutants possesses a unique far-red fluorescence.* FEBS Lett, 2000. **479**(3): p. 127-30.

12. Shaner, N.C., R.E. Campbell, P.A. Steinbach, B.N. Giepmans, A.E. Palmer, and R.Y. Tsien, *Improved monomeric red, orange and yellow fluorescent proteins derived from Discosoma sp. red fluorescent protein.* Nat Biotechnol, 2004. **22**(12): p. 1567-72.

13. Strongin, D.E., B. Bevis, N. Khuong, M.E. Downing, R.L. Strack, K. Sundaram, B.S. Glick, and R.J. Keenan, *Structural rearrangements near the chromophore influence the maturation speed and brightness of DsRed variants.* Protein Eng Des Sel, 2007. **20**(11): p. 525-34.

14. Eli, P. and A. Chakrabartty, *Variants of DsRed fluorescent protein: Development of a copper sensor.* Protein Sci, 2006. **15**(10): p. 2442-7.

15. Sumner, J.P., N.M. Westerberg, A.K. Stoddard, T.K. Hurst, M. Cramer, R.B. Thompson, C.A. Fierke, and R. Kopelman, *DsRed as a highly sensitive, selective, and reversible fluorescence-based biosensor for both Cu(+) and Cu(2+) ions.* Biosens Bioelectron, 2006. **21**(7): p. 1302-8.

16. Rahimi, Y., S. Surestha, and S.K. Deo, *Metal Affinity-Based Purification of a Red Fluorescent Protein.* Chromatographia, 2007. **65**: p. 429-433.

17. Rahimi, Y., S. Shrestha, T. Banerjee, S. K. Deo *Study of Metal Binding to DsRed-Monomer", "Bioluminescence and Chemiluminescence: Chemistry, Biology and Applications.* World Scientific, 2006.
18. Adman, E.T., *Copper protein structures.* Adv Protein Chem, 1991. **42**: p. 145-97.
19. Kaufman Katz, A., Liat Shimoni-Livny, Oshrit Navon, Charles W. Bock, and Jenny P. Glusker, *Copper-Binding Motifs: Structural and Theoretical Aspects.* Helvetica Chimica Acta, 2003. **86**: p. 1320-1338.
20. Regan, L., *The design of metal-binding sites in proteins.* Annu Rev Biophys Biomol Struct, 1993. **22**: p. 257-87.
21. Nar, H., A. Messerschmidt, R. Huber, M. van de Kamp, and G.W. Canters, *Crystal structure analysis of oxidized Pseudomonas aeruginosa azurin at pH 5.5 and pH 9.0. A pH-induced conformational transition involves a peptide bond flip.* J Mol Biol, 1991. **221**(3): p. 765-72.
22. Wells, M.A., G.S. Jackson, S. Jones, L.L. Hosszu, C.J. Craven, A.R. Clarke, J. Collinge, and J.P. Waltho, *A reassessment of copper(II) binding in the full-length prion protein.* Biochem J, 2006. **399**(3): p. 435-44.
23. Walter, E.D., M. Chattopadhyay, and G.L. Millhauser, *The affinity of copper binding to the prion protein octarepeat domain: evidence for negative cooperativity.* Biochemistry, 2006. **45**(43): p. 13083-92.
24. Davies, P., F. Marken, S. Salter, and D.R. Brown, *Thermodynamic and voltammetric characterization of the metal binding to the prion protein: insights into pH dependence and redox chemistry.* Biochemistry, 2009. **48**(12): p. 2610-9.
25. Hay, R.W., M.M. Hassan, and C. You-Quan, *Kinetic and thermodynamic studies of the copper (II) and nickel(II) complexes of glycylglycyl-L-histidine.* J Inorg Biochem, 1993. **52**(1): p. 17-25.
26. Verkhusha, V.V.a.K.A.L., *The Molecular Properties and Applications of Anthozoa Fluorescent Proteins and Chromoproteins.* Nat Biotechnol, 2004. **22**: p. 289-296.

27. Fradkov, A.F., V.V. Verkhusha, D.B. Staroverov, M.E. Bulina, Y.G. Yanushevich, V.I. Martynov, S. Lukyanov, and K.A. Lukyanov, *Far-red fluorescent tag for protein labelling.* Biochem J, 2002. **368**(Pt 1): p. 17-21.

28. Shrestha, S. and S.K. Deo, *Anthozoa red fluorescent protein in biosensing.* Anal Bioanal Chem, 2006. **386**(3): p. 515-24.

29. Erickson, M.G., D.L. Moon, and D.T. Yue, *DsRed as a potential FRET partner with CFP and GFP.* Biophys J, 2003. **85**(1): p. 599-611.

30. Bizzarri, R., C. Arcangeli, D. Arosio, F. Ricci, P. Faraci, F. Cardarelli, and F. Beltram, *Development of a novel GFP-based ratiometric excitation and emission pH indicator for intracellular studies.* Biophys J, 2006. **90**(9): p. 3300-14.

31. Galietta, L.J., P.M. Haggie, and A.S. Verkman, *Green fluorescent protein-based halide indicators with improved chloride and iodide affinities.* FEBS Lett, 2001. **499**(3): p. 220-4.

32. Baird, G.S., D.A. Zacharias, and R.Y. Tsien, *Circular permutation and receptor insertion within green fluorescent proteins.* Proc Natl Acad Sci U S A, 1999. **96**(20): p. 11241-6.

33. Miyawaki, A., J. Llopis, R. Heim, J.M. McCaffery, J.A. Adams, M. Ikura, and R.Y. Tsien, *Fluorescent indicators for Ca2+ based on green fluorescent proteins and calmodulin.* Nature, 1997. **388**(6645): p. 882-7.

34. Jayaraman, S., P. Haggie, R.M. Wachter, S.J. Remington, and A.S. Verkman, *Mechanism and cellular applications of a green fluorescent protein-based halide sensor.* J Biol Chem, 2000. **275**(9): p. 6047-50.

35. Wachter, R.M., D. Yarbrough, K. Kallio, and S.J. Remington, *Crystallographic and energetic analysis of binding of selected anions to the yellow variants of green fluorescent protein.* J Mol Biol, 2000. **301**(1): p. 157-71.

36. Fox, J.H., J.A. Kama, G. Lieberman, R. Chopra, K. Dorsey, V. Chopra, I. Volitakis, R.A. Cherny, A.I. Bush, and S. Hersch, *Mechanisms of copper ion mediated Huntington's disease progression.* PLoS One, 2007. **2**(3): p. e334.

37. Macreadie, I.G., *Copper transport and Alzheimer's disease.* Eur Biophys J, 2008. **37**(3): p. 295-300.

38. Richardson, D.R. and Y. Suryo Rahmanto, *Differential regulation of the Menkes and Wilson disease copper transporters by hormones: an integrated model of metal transport in the placenta.* Biochem J, 2007. **402**(2): p. e1-3.

39. Rahimi, Y., A. Goulding, S. Shrestha, S. Mirpuri, and S.K. Deo, *Mechanism of copper induced fluorescence quenching of red fluorescent protein, DsRed.* Biochem Biophys Res Commun, 2008. **370**(1): p. 57-61.

40. *MetalMine*. Available from: http://metalmine.naist.jp/metalmine009/index.html.

41. *Metsite*. Available from: http://bioinf4.cs.ucl.ac.uk:3000/metsite.

42. Taira, K. and S.J. Benkovic, *Evaluation of the importance of hydrophobic interactions in drug binding to dihydrofolate reductase.* J Med Chem, 1988. **31**(1): p. 129-37.

43. Lakowicz, J.R., *Principles of Fluorescence Spectroscopy, third ed.* 2006, New York: Springer.

44. Bowen, B. and N. Woodbury, *Single-molecule fluorescence lifetime and anisotropy measurements of the red fluorescent protein, DsRed, in solution.* Photochem Photobiol, 2003. **77**(4): p. 362-9.

45. Jiang, C.Q. and T. Wang, *Study of the interactions between tetracycline analogues and lysozyme.* Bioorg Med Chem, 2004. **12**(9): p. 2043-7.

46. O'Rourke, N.A., T. Meyer, and G. Chandy, *Protein localization studies in the age of 'Omics'.* Curr Opin Chem Biol, 2005. **9**(1): p. 82-7.

47. Chen, I., M. Howarth, W. Lin, and A.Y. Ting, *Site-specific labeling of cell surface proteins with biophysical probes using biotin ligase.* Nat Methods, 2005. **2**(2): p. 99-104.

48. Hu, Y., X. Huang, G.Y. Chen, and S.Q. Yao, *Recent advances in gel-based proteome profiling techniques.* Mol Biotechnol, 2004. **28**(1): p. 63-76.

49. Meredith, G.D., H.Y. Wu, and N.L. Allbritton, *Targeted protein functionalization using His-tags.* Bioconjug Chem, 2004. **15**(5): p. 969-82.

50. Zhang, Z., P.J. Edwards, R.W. Roeske, and L. Guo, *Synthesis and self-alkylation of isotope-coded affinity tag reagents.* Bioconjug Chem, 2005. **16**(2): p. 458-64.

51. Whetstone, P.A., N.G. Butlin, T.M. Corneillie, and C.F. Meares, *Element-coded affinity tags for peptides and proteins.* Bioconjug Chem, 2004. **15**(1): p. 3-6.

52. Waugh, D.S., *Making the most of affinity tags.* Trends Biotechnol, 2005. **23**(6): p. 316-20.

53. Cull, M.G. and P.J. Schatz, *Biotinylation of proteins in vivo and in vitro using small peptide tags.* Methods Enzymol, 2000. **326**: p. 430-40.

54. Larive, C.K., S.M. Lunte, M. Zhong, M.D. Perkins, G.S. Wilson, G. Gokulrangan, T. Williams, F. Afroz, C. Schoneich, T.S. Derrick, C.R. Middaugh, and S. Bogdanowich-Knipp, *Separation and analysis of peptides and proteins.* Anal Chem, 1999. **71**(12): p. 389R-423R.

55. Braud, S., M. Moutiez, P. Belin, N. Abello, P. Drevet, S. Zinn-Justin, M. Courcon, C. Masson, J. Dassa, J.B. Charbonnier, J.C. Boulain, A. Menez, R. Genet, and M. Gondry, *Dual expression system suitable for high-throughput fluorescence-based screening and production of soluble proteins.* J Proteome Res, 2005. **4**(6): p. 2137-47.

56. Burckstummer, T., K.L. Bennett, A. Preradovic, G. Schutze, O. Hantschel, G. Superti-Furga, and A. Bauch, *An efficient tandem affinity purification procedure for interaction proteomics in mammalian cells.* Nat Methods, 2006. **3**(12): p. 1013-9.

57. Tropea, J.E., S. Cherry, S. Nallamsetty, C. Bignon, and D.S. Waugh, *A generic method for the production of recombinant proteins in Escherichia coli using a dual hexahistidine-maltose-binding protein affinity tag.* Methods Mol Biol, 2007. **363**: p. 1-19.

58. Miyawaki, A., A. Sawano, and T. Kogure, *Lighting up cells: labelling proteins with fluorophores.* Nat Cell Biol, 2003. **Suppl**: p. S1-7.

59. Chapman, S., K.J. Oparka, and A.G. Roberts, *New tools for in vivo fluorescence tagging.* Curr Opin Plant Biol, 2005. **8**(6): p. 565-73.

60. Dubertret, B., P. Skourides, D.J. Norris, V. Noireaux, A.H. Brivanlou, and A. Libchaber, *In vivo imaging of quantum dots encapsulated in phospholipid micelles.* Science, 2002. **298**(5599): p. 1759-62.

61. Lidke, D.S., P. Nagy, R. Heintzmann, D.J. Arndt-Jovin, J.N. Post, H.E. Grecco, E.A. Jares-Erijman, and T.M. Jovin, *Quantum dot ligands provide new insights into erbB/HER receptor-mediated signal transduction.* Nat Biotechnol, 2004. **22**(2): p. 198-203.

62. Patterson, G.H. and J. Lippincott-Schwartz, *A photoactivatable GFP for selective photolabeling of proteins and cells.* Science, 2002. **297**(5588): p. 1873-7.

63. Adams, S.R., R.E. Campbell, L.A. Gross, B.R. Martin, G.K. Walkup, Y. Yao, J. Llopis, and R.Y. Tsien, *New biarsenical ligands and tetracysteine motifs for protein labeling in vitro and in vivo: synthesis and biological applications.* J Am Chem Soc, 2002. **124**(21): p. 6063-76.

64. Paramban, R.I., R.C. Bugos, and W.W. Su, *Engineering green fluorescent protein as a dual functional tag.* Biotechnol Bioeng, 2004. **86**(6): p. 687-97.

65. Kobayashi, T., N. Morone, T. Kashiyama, H. Oyamada, N. Kurebayashi, and T. Murayama, *Engineering a novel multifunctional green fluorescent protein tag for a wide variety of protein research.* PLoS One, 2008. **3**(12): p. e3822.

66. Watt, R.M. and E.W. Voss, Jr., *Mechanism of quenching of fluorescein by anti-fluorescein IgG antibodies.* Immunochemistry, 1977. **14**(7): p. 533-51.

67. Shute, T.S., M. Matsushita, T.J. Dickerson, J.J. La Clair, K.D. Janda, and M.D. Burkart, *A site-specific bifunctional protein labeling system for affinity and fluorescent analysis.* Bioconjug Chem, 2005. **16**(6): p. 1352-5.

68. Trewhella, J., *The solution structures of calmodulin and its complexes with synthetic peptides based on target enzyme binding domains.* Cell Calcium, 1992. **13**(6-7): p. 377-90.

69. Daunert, S., L.G. Bachas, V. Schauer-Vukasinovic, K.J. Gregory, G. Schrift, and S. Deo, *Calmodulin-mediated reversible immobilization of enzymes.* Colloids Surf B Biointerfaces, 2007. **58**(1): p. 20-7.

70. Kuboniwa, H., N. Tjandra, S. Grzesiek, H. Ren, C.B. Klee, and A. Bax, *Solution structure of calcium-free calmodulin.* Nat Struct Biol, 1995. **2**(9): p. 768-76.

71. Babu, Y.S., C.E. Bugg, and W.J. Cook, *Structure of calmodulin refined at 2.2 A resolution.* J Mol Biol, 1988. **204**(1): p. 191-204.

72. Schauer-Vukasinovic, V., Cullen, L., and Daunert, S., *Rational design of a calcium sensing system based on induced conformational changes of calmodulin* J. Am. Chem. Soc., 1997. **1119**: p. 11102-11103.

73. Douglass, P.M., L.L. Salins, E. Dikici, and S. Daunert, *Class-selective drug detection: fluorescently-labeled calmodulin as the biorecognition element for phenothiazines and tricyclic antidepressants.* Bioconjug Chem, 2002. **13**(6): p. 1186-92.

74. Watt, S.J., A. Oakley, M.M. Sheil, and J.L. Beck, *Comparison of negative and positive ion electrospray ionization mass spectra of calmodulin and its complex with trifluoperazine.* Rapid Commun Mass Spectrom, 2005. **19**(15): p. 2123-30.

75. Dikici, E., Deo, S.K., and Daunert, S., *Drug detection based on the conformational changes of calmodulin and the fluorescence of its enhanced green fluorescent protein fusion partner.* Anal. Chim. Acta 500, 2003: p. 237-245.

76. Goulding, A.M., Y. Rahimi, S. Shrestha, and S.K. Deo, *Dual function labeling of biomolecules based on DsRed-Monomer.* Bioconjug Chem, 2008. **19**(11): p. 2113-9.

77. Goulding, A., S. Shrestha, K. Dria, E. Hunt, and S.K. Deo, *Red fluorescent protein variants with incorporated non-natural amino acid analogues.* Protein Eng Des Sel, 2008. **21**(2): p. 101-6.

78. Dikici, E., Deo, S.K., and Daunert, S., *Drug detection based on the conformational changes of calmodulin and the fluoresence of its enhanced green fluorescent protein fusion partner* Anal. Chim. Acta 2003. **500**: p. 237-245.

79. Martin, M.M. and F. Jean, *Single-cell resolution imaging of membrane-anchored hepatitis C virus NS3/4A protease activity.* Biol Chem, 2006. **387**(8): p. 1075-80.

80. Hsu, Y.Y., Y.N. Liu, W. Wang, F.J. Kao, and S.H. Kung, *In vivo dynamics of enterovirus protease revealed by fluorescence resonance emission transfer (FRET) based on a novel FRET pair.* Biochem Biophys Res Commun, 2007. **353**(4): p. 939-45.

81. Kohl, T., K.G. Heinze, R. Kuhlemann, A. Koltermann, and P. Schwille, *A protease assay for two-photon crosscorrelation and FRET analysis based solely on fluorescent proteins.* Proc Natl Acad Sci U S A, 2002. **99**(19): p. 12161-6.

82. Mizuno, H., A. Sawano, P. Eli, H. Hama, and A. Miyawaki, *Red fluorescent protein from Discosoma as a fusion tag and a partner for fluorescence resonance energy transfer.* Biochemistry, 2001. **40**(8): p. 2502-10.

83. Shevchenko, A., O.N. Jensen, A.V. Podtelejnikov, F. Sagliocco, M. Wilm, O. Vorm, P. Mortensen, H. Boucherie, and M. Mann, *Linking genome and proteome by mass spectrometry: large-scale identification of yeast proteins from two dimensional gels.* Proc Natl Acad Sci U S A, 1996. **93**(25): p. 14440-5.

84. Blackstock, W.P. and M.P. Weir, *Proteomics: quantitative and physical mapping of cellular proteins.* Trends Biotechnol, 1999. **17**(3): p. 121-7.

85. Puig, O., F. Caspary, G. Rigaut, B. Rutz, E. Bouveret, E. Bragado-Nilsson, M. Wilm, and B. Seraphin, *The tandem affinity purification (TAP) method: a general procedure of protein complex purification.* Methods, 2001. **24**(3): p. 218-29.

86. Lichty, J.J., J.L. Malecki, H.D. Agnew, D.J. Michelson-Horowitz, and S. Tan, *Comparison of affinity tags for protein purification.* Protein Expr Purif, 2005. **41**(1): p. 98-105.

87. Hochuli, E., H. Dobeli, and A. Schacher, *New metal chelate adsorbent selective for proteins and peptides containing neighbouring histidine residues.* J Chromatogr, 1987. **411**: p. 177-84.

88. Rigaut, G., A. Shevchenko, B. Rutz, M. Wilm, M. Mann, and B. Seraphin, *A generic protein purification method for protein complex characterization and proteome exploration.* Nat Biotechnol, 1999. **17**(10): p. 1030-2.

89. Huh, W.K., J.V. Falvo, L.C. Gerke, A.S. Carroll, R.W. Howson, J.S. Weissman, and E.K. O'Shea, *Global analysis of protein localization in budding yeast.* Nature, 2003. **425**(6959): p. 686-91.

90. Loiodice, I., A. Alves, G. Rabut, M. Van Overbeek, J. Ellenberg, J.B. Sibarita, and V. Doye, *The entire Nup107-160 complex, including three new members, is targeted as one entity to kinetochores in mitosis.* Mol Biol Cell, 2004. **15**(7): p. 3333-44.

91. Obuse, C., O. Iwasaki, T. Kiyomitsu, G. Goshima, Y. Toyoda, and M. Yanagida, *A conserved Mis12 centromere complex is linked to heterochromatic HP1 and outer kinetochore protein Zwint-1.* Nat Cell Biol, 2004. **6**(11): p. 1135-41.

92. Iijima, M., Y.E. Huang, H.R. Luo, F. Vazquez, and P.N. Devreotes, *Novel mechanism of PTEN regulation by its phosphatidylinositol 4,5-bisphosphate binding motif is critical for chemotaxis.* J Biol Chem, 2004. **279**(16): p. 16606-13.

93. Cheeseman, I.M., S. Niessen, S. Anderson, F. Hyndman, J.R. Yates, 3rd, K. Oegema, and A. Desai, *A conserved protein network controls assembly of the outer kinetochore and its ability to sustain tension.* Genes Dev, 2004. **18**(18): p. 2255-68.

94. Kops, G.J., Y. Kim, B.A. Weaver, Y. Mao, I. McLeod, J.R. Yates, 3rd, M. Tagaya, and D.W. Cleveland, *ZW10 links mitotic checkpoint signaling to the structural kinetochore.* J Cell Biol, 2005. **169**(1): p. 49-60.

95. Cheeseman, I.M., I. MacLeod, J.R. Yates, 3rd, K. Oegema, and A. Desai, *The CENP-F-like proteins HCP-1 and HCP-2 target CLASP to kinetochores to mediate chromosome segregation.* Curr Biol, 2005. **15**(8): p. 771-7.

96. Flory, M.R., A.R. Carson, E.G. Muller, and R. Aebersold, *An SMC-domain protein in fission yeast links telomeres to the meiotic centrosome.* Mol Cell, 2004. **16**(4): p. 619-30.

97. Cristea, I.M., R. Williams, B.T. Chait, and M.P. Rout, *Fluorescent proteins as proteomic probes.* Mol Cell Proteomics, 2005. **4**(12): p. 1933-41.

98. Bretscher, A., *Smooth muscle caldesmon. Rapid purification and F-actin cross-linking properties.* J Biol Chem, 1984. **259**(20): p. 12873-80.

99. Stafford, W.F., J.M. Chalovich, and P. Graceffa, *Turkey gizzard caldesmon molecular weight and shape.* Arch Biochem Biophys, 1994. **313**(1): p. 47-9.

100. Lukas, T.J., D.B. Iverson, M. Schleicher, and D.M. Watterson, *Structural Characterization of a Higher Plant Calmodulin : Spinacia Oleracea.* Plant Physiol, 1984. **75**(3): p. 788-795.

101. Walker, G., W.G. Kerrick, and L.Y. Bourguignon, *The role of caldesmon in the regulation of receptor capping in mouse T-lymphoma cell.* J Biol Chem, 1989. **264**(1): p. 496-500.

102. Alexanian, A.R., J.R. Bamburg, H. Hidaka, and D. Mornet, *Calcium-dependent regulation of interactions of caldesmon with calcium-binding proteins found in growth cones of chick forebrain neurons.* Cell Mol Neurobiol, 2001. **21**(5): p. 437-51.

103. Gavin, P., R.J. Devenish, and M. Prescott, *An approach for reducing unwanted oligomerisation of DsRed fusion proteins.* Biochem Biophys Res Commun, 2002. **298**(5): p. 707-13.

104. Noren, C.J., S.J. Anthony-Cahill, M.C. Griffith, and P.G. Schultz, *A general method for site-specific incorporation of unnatural amino acids into proteins.* Science, 1989. **244**(4901): p. 182-8.

105. Pakhomov, A.A., N.V. Pletneva, T.A. Balashova, and V.I. Martynov, *Structure and reactivity of the chromophore of a GFP-like chromoprotein from Condylactis gigantea.* Biochemistry, 2006. **45**(23): p. 7256-64.

106. Cotlet, M., J. Hofkens, S. Habuchi, G. Dirix, M. Van Guyse, J. Michiels, J. Vanderleyden, and F.C. De Schryver, *Identification of different emitting species in the red fluorescent protein DsRed by means of ensemble and single-molecule spectroscopy.* Proc Natl Acad Sci U S A, 2001. **98**(25): p. 14398-403.

107. Wall, M.A., M. Socolich, and R. Ranganathan, *The structural basis for red fluorescence in the tetrameric GFP homolog DsRed.* Nat Struct Biol, 2000. **7**(12): p. 1133-8.

108. Shu, X., N.C. Shaner, C.A. Yarbrough, R.Y. Tsien, and S.J. Remington, *Novel chromophores and buried charges control color in mFruits.* Biochemistry, 2006. **45**(32): p. 9639-47.

109. Hohsaka, T., Y. Ashizuka, H. Taira, H. Murakami, and M. Sisido, *Incorporation of nonnatural amino acids into proteins by using various four-base codons in an Escherichia coli in vitro translation system.* Biochemistry, 2001. **40**(37): p. 11060-4.

110. Hohsaka, T. and M. Sisido, *Incorporation of non-natural amino acids into proteins.* Curr Opin Chem Biol, 2002. **6**(6): p. 809-15.

111. Link, A.J., M.L. Mock, and D.A. Tirrell, *Non-canonical amino acids in protein engineering.* Curr Opin Biotechnol, 2003. **14**(6): p. 603-9.

112. Liu, W., A. Brock, S. Chen, S. Chen, and P.G. Schultz, *Genetic incorporation of unnatural amino acids into proteins in mammalian cells.* Nat Methods, 2007. **4**(3): p. 239-44.

113. Taki, M., T. Hohsaka, H. Murakami, K. Taira, and M. Sisido, *A non-natural amino acid for efficient incorporation into proteins as a sensitive fluorescent probe.* FEBS Lett, 2001. **507**(1): p. 35-8.

114. Hyun Bae, J., M. Rubini, G. Jung, G. Wiegand, M.H. Seifert, M.K. Azim, J.S. Kim, A. Zumbusch, T.A. Holak, L. Moroder, R. Huber, and N. Budisa, *Expansion of the genetic code enables design of a novel "gold" class of green fluorescent proteins.* J Mol Biol, 2003. **328**(5): p. 1071-81.

115. Wang, L., J. Xie, A.A. Deniz, and P.G. Schultz, *Unnatural amino acid mutagenesis of green fluorescent protein.* J Org Chem, 2003. **68**(1): p. 174-6.

116. Kajihara, D., T. Hohsaka, and M. Sisido, *Synthesis and sequence optimization of GFP mutants containing aromatic non-natural amino acids at the Tyr66 position.* Protein Eng Des Sel, 2005. **18**(6): p. 273-8.

117. Hendrickson, T.L., V. de Crecy-Lagard, and P. Schimmel, *Incorporation of nonnatural amino acids into proteins.* Annu Rev Biochem, 2004. **73**: p. 147-76.

118. Brooks, B., R.S. Phillips, and W.F. Benisek, *High-efficiency incorporation in vivo of tyrosine analogues with altered hydroxyl acidity in place of the catalytic tyrosine-14 of Delta 5-3-ketosteroid isomerase of Comamonas (Pseudomonas) testosteroni: effects of the modifications on isomerase kinetics.* Biochemistry, 1998. **37**(27): p. 9738-42.

119. Minks, C., R. Huber, L. Moroder, and N. Budisa, *Noninvasive tracing of recombinant proteins with "fluorophenylalanine-fingers".* Anal Biochem, 2000. **284**(1): p. 29-34.

120. Neidhardt, F.C., P.L. Bloch, and D.F. Smith, *Culture medium for enterobacteria.* J Bacteriol, 1974. **119**(3): p. 736-47.

121. Lu, P., M. Jarema, K. Mosser, and W.E. Daniel, *lac repressor: 3-fluorotyrosine substitution for nuclear magnetic resonance studies.* Proc Natl Acad Sci U S A, 1976. **73**(10): p. 3471-5.

122. Verkhusha, V.V., H. Otsuna, T. Awasaki, H. Oda, S. Tsukita, and K. Ito, *An enhanced mutant of red fluorescent protein DsRed for double labeling and developmental timer of neural fiber bundle formation.* J Biol Chem, 2001. **276**(32): p. 29621-4.

123. Povrozin, Y., Terpetschnig, E, *Measurement of Fluorescent Quantum Yields on ISS Instrumentation Using Vinci.* ( ): p. .

124. Bevis, B.J. and B.S. Glick, *Rapidly maturing variants of the Discosoma red fluorescent protein (DsRed).* Nat Biotechnol, 2002. **20**(1): p. 83-7.

125. {Rahimi, *Metal Affinity-Based Purification of a Red Fluorescent Protein* Chromatographia, 2007. **65**(7-8): p. 1612-1112.

APPENDICES

Appendix A: Creation of DsRed-Monomer

The major problems associated with native DsRed have involved the intermediate/parasitic green fluorescence, low extinction coefficient, and the tendency for oligomerization. The previous section of this chapter described how the former two have been addressed through directed evolution and site-directed mutagenesis. However the problem of oligomerization presented more challenges. The native DsRed protein is primarily negatively charged, with the exception of a short length at the N- terminal region which contains a group of positively charged amino acid residues. This positively charged region was thought to be the most likely cause of the high molecular weight aggregates, primarily tetramers, seen with this protein [124]. It also appears to be possible for each tetramer to form up to four salt bridges with adjacent tetramers, forming stable polymeric structures. Since the isolation of DsRed, a number of groups have attempted to resolve the problem of aggregation, the results of which will be discussed below.

It has long been known that native DsRed formed extensive oligomers both *in vitro* and *in vivo*, however the exact behavior of the protein and degree of aggregation were not fully understood. Baird *et al*. [3] explored this oligomerization of native DsRed by comparing SDS-PAGE gels of boiled and un-boiled samples of DsRed. The un-boiled samples showed a band at >110 kDa, while after boiling this band was no longer seen. This suggested that an oligomerized form of the protein was present in the un-boiled sample. This was further studied by analytical equilibrium centrifugation, which showed molecular weights corresponding to a tetrameric form of the protein. To determine if this aggregation was seen *in vivo*, the oligomerization was further explored by a FRET study in mammalian cells and a two-hybrid assay in yeast. Both of these confirmed that native DsRed forms a tetramer *in vivo*.

The aggregation of native DsRed was reduced by Bevis *et al*. [124] both *in vivo* and *in vitro* by decreasing the net positive charge at the N- terminal region of the protein. As previously observed, native DsRed is unusually basic. These basic patches on the surface of the protein interact with acidic patches on a second unit of DsRed (or other

macromolecules) forming high order aggregates. By eliminating the cluster of positive charges near the N- terminus through point mutations, these interactions can be minimized. A decrease in the strength of these oligomeric interactions was observed upon mutation; however complete elimination of aggregation was not achieved.

The first commercially available non-aggregating mutant of DsRed was generated by Yanushevich *et al*. [8]. This group focused on minimizing the aggregation of a number of fluorescent proteins, including three DsRed mutants; E57 [9], E5 [10] and ds/drFP616 [11]. Following the example of Bevis' and Baird's groups [3, 124], this work focused on the fully charged N- terminal residues. A series of mutants of E57, containing R2A, K5E, and K9T substitutions in different combinations were created. Of these mutations, R2A appeared to have the strongest impact on the overall aggregation of the proteins. One mutant, E57-NA, with all three mutations, showed no aggregation. This mutant also showed spectroscopic properties similar to E57; with similar maturation time, brightness of colonies, and excitation/emission wavelength maxima. This mutant was the first commercially available monomer of DsRed, specifically called DsRed2. These mutations were generated for both E5 and ds/drFP616 with similar results, creating mutants which appear to be monomeric on SDS-PAGE gels. Additionally these mutants appeared to retain the spectral properties of the respective parent mutant, E5 and ds/drFP616.

An improved monomeric DsRed was generated by Campbell *et al*. [4]. Initially a dimer of DsRed was prepared by a single point mutation, I125R. This mutant gave poor red fluorescence with an increased green component and a much longer maturation time. To improve the fluorescence of this dimer directed evolution was used to identify mutants with the desired properties. Dimer2, with 16 additional mutations, was isolated from this pool of mutants. Of the 17 mutations present in the final dimer, eight are internal to the β-barrel, three are aggregation reducing R2A, K5E, and N6D, two are at the AB interface of two single units I125R, V127T, and the final four are surface mutations. Using this dimer2, a tandem dimer, tdimer2 [125], was generated. A polypeptide linker was used to attach two dimer2 units, such that critical dimer interactions were satisfied by this tandem linker. Linkers of 9, 12, 13, or 22 amino acid

residues were used to form these tandem dimers. All of these tandem dimers, showed essentially the same behavior except the clone with the 9 residue linker, which was slower to mature. The tandem dimer with the 12 residue linker, tdimer2 [125], was chosen for further study. This tandem dimer showed excitation and emission wavelength maxima identical to that of dimer2, with an extinction coefficient twice that of dimer2, due to the presence of the two absorbing chromophores per polypeptide chain. tdimer2 [125] became the focus of forming a true DsRed monomer. By a series of directed evolution steps targeting H162 and A164 of the tandem dimer a first generation monomer, mRFP0.1, was identified. This monomer was further mutated, by directed evolution, through six generations yielding mRFP1, with a total of 33 amino acid substitutions, relative to DsRed. Of these substitutions 13 are internal to the β-barrel, three are aggregation reducing mutants R2A, K5E, and N6D, three are AB interface mutations I125R, V127T and I180T, ten are AC interface mutations R153E, H162K, A164R, L174D, Y192A, Y194K, H222S, L223T, F224G, and L225A, and the remaining four are non-specific beneficial mutations. Both the dimers and monomers generated by this group appear to overcome the major problem, which previously prevented the formation of a stable non-aggregating form of DsRed. Decreasing the charge of the N-terminal region of the protein had the greatest effect on the protein's aggregation and oligomerization.

Shaner *et al*. [12] reported a further improvement in mRFP1 [4]. mRFP1 was subjected to many rounds of directed evolution, the resulting colonies were screened both manually and by fluorescence-activated cell sorting (FACS)-based screening. This screening isolated many mutants with differing emission maxima, increased tolerance to N- and C- terminal fusions, improved extinction coefficients, higher quantum yields, and high photostability. However none of these mutants showed improvements in all of these properties. A second approach was examined by substituting residues around the chromophore of the protein, Gln66, Tyr67, and Gly68. One clone from this library, mRFP1.1, with a Q66M substitution, showed a minor fluorescence shift of 5 nm, in both excitation and emission, and more complete maturation. This mutant was further modified, to reduce its sensitivity to the N- terminal fusion, by replacing the first seven

amino acid residues with the corresponding residues from enhanced GFP, MVSKGEE followed by a spacer, consisting of residues NNMA (6a-6d). Additionally the last seven residues at the C- terminus were also appended to that of GFP, creating mRFP1.3. This fluorescent mutant of mRFP1 was not affected by the N- terminal fusion. The clone mRFP1.4 was generated by the addition of two more point mutations, V7I and M182K, which showed improved folding of the protein's chromophore. An additional substitution of M163Q resulted in a complete loss of green fluorescence. The final optimized monomer, mCherry, included the additional mutations R17H, T195V, D196N, and N6aD. Further mutations, at the 66 position of both mRFP1.1 and mRFP1.4, along with additional rounds of directed evolution, yielded a series of fluorescently shifted mutants: mTangerine, mHoneydew, mOrange, and mStrawberry. Each of these monomers showed an improvement in a specific area of fluorescent protein research, offering an improved quantum yield, extinction coefficient, or fluorescence intensity; however mCherry is the most promising overall. The fluorescence excitation and emission wavelength maximum of mCherry showed a significant red shift to 587 nm and 610 nm, respectively. This mutant also showed shorter maturation times than native DsRed and mRFP1. However mCherry showed quantum yields, extinction coefficients, and brightness of colonies comparable to mRFP1. Through directed evolution on the dimer, dimer2 [4], a promising new dimer mutant, dTomato, was generated. The dTomato mutant showed higher tolerance to N- and C- terminal fusion, as seen for mCherry. Since tandem dimers of DsRed reduced its oligomerization [4], a tandem dimer, tdTomato, was generated from the dTomato mutant. Both dTomato and tdTomato showed improved maturation kinetics. Additionally, both showed limited parasitic green fluorescence and a minor red shift in excitation and emission wavelength maxima to 554 nm and 581 nm.

A DsRed monomer is now commercially available from Clontech, denoted as DsRed-Monomer. This monomer contains 45 amino acid substitutions in native DsRed. This protein overcame the oligomerization seen with native DsRed, which has been confirmed by a number of methods including gel filtration chromatography that showed a single uniform peak. The retention time obtained for this peak is consistent with a 28

kDa molecular weight. The spectral and maturation properties of this protein are comparable to those of the commercially available tetrameric DsRed, DsRed-Express, also from Clontech. This protein displays a fluorescence excitation and emission wavelength maxima of 556 nm and 586 nm respectively.

The DsRed monomers generated by both directed evolution and site-specific mutagenesis of amino acid residues have an ideal set of properties for biological and analytical applications. The high quantum yields and extinction coefficients of these monomers have allowed for further uses of this protein to be explored and developed. Additionally the faster maturation and lack of oligomerization seen with these monomers should be an advantage for their use as fusion tags.

Appendix B: Derivation of Dissociation Constant Equation

The equilibrium constant for dissociation is a function of the ratios of the dissociation and association rates, k_{on} and k_{off}. k_{on} is often limited only by diffusion, so k_{off} is the discriminator for differential binding. K_D can be measured if the concentration of the protein-ligand complex ([PD]) and either the free concentration of the protein ([P]) or the ligand ([D]) can be measured experimentally, for example through titration. In practice [PD] is rarely measured, rather a spectroscopic change, such as fluorescence, upon binding of ligand to protein is measured.

- $K_D = \frac{[P][D]}{[PD]} = \frac{k_{off}}{k_{on}}$

  Bound fraction of protein/ligand, from conservation of mass

  $[P] = [P_T] - [PD]$

  $[D] = [D_T] - [PD]$

- $K_D = \frac{([P_T] - [PD])([D_T] - [PD])}{[PD]}$

- $0 = [P_T][D_T] - (K_D + [D_T] + [P_T])\,[PD] + [PD]^2$

- $[PD] = \frac{(K_D + [D_T] + [P_T]) - \sqrt{(K_D + [D_T] + [P_T])^2 - 4[D_T][P_T]}}{2}$

  F_P – Signal from free protein

  F_{PD} – Signal from the complex

  F – Total fluorescence signal

- $F = F_P[P] + F_{PD}\,[PD]$

- $F = F_p([P_T] - [PD]) + F_{PD}\,[PD]$

- $F = F_P \left(1 - \frac{[PD]}{[P_T]}\right) + F_{PD}\frac{[PD]}{[P_T]}$
- $F = F_P - F_P\frac{[PD]}{[P_T]} + F_{PD}\frac{[PD]}{[P_T]}$
- $F = F_P + (F_{PD} - F_P)\frac{[PD]}{[P_T]}$
- $F = F_P + (F_{PD} - F_P)\frac{(K_D + [D_T] + [P_T]) \pm \sqrt{(K_D + [D_T] + [P_T])^2 - 4[D_T][P_T]}}{2[P_T]}$
- $\frac{\Delta F}{\Delta F_{\max}} = \frac{F - F_P}{F_{PD} - F_P} = \frac{(K_D + [D_T] + [P_T]) \pm \sqrt{(K_D + [D_T] + [P_T])^2 - 4[D_T][P_T]}}{2[P_T]}$

VITA

VITA

ANN MARIE GOULDING

EDUCATION

- 2010 (August Graduation): PhD, Chemistry, Purdue University, Indianapolis
  Thesis title: "Biochemical Applications of DsRed-Monomer Utilizing Fluorescence and Metal-Binding Affinity"
  Advisor: Dr Sapna K. Deo
- 2004: BS, Chemistry, Purdue University, Indianapolis, IN

EXPERIENCE

- Teaching Assistant, 2005-2009
  Purdue University, Indianapolis
  Courses: General Chemistry Laboratory I and II
- Research Assistant, 2004-2005
  Purdue University, Indianapolis
  Advisor: Dr Paul L. Dubin
  Investigated the effects of polyelectrolyte structural variables on binding to proteins and micelles

LABORATORY SKILLS

- Experience with fluorescence spectrophotometer, luminescence reader, HPLC, UV-Vis, circular dichroism spectropolarimeter, affinity chromatography, turbidimetric titration, dynamic light scattering, mass spectrometry, western blotting techniques
- Experience with DNA gel electrophoresis, SDS-PAGE
- Recombinant DNA and mutagenesis experience
- Bacterial protein expression and purification techniques
- Experience working with fluorescent and bioluminescent proteins and enzymes

RESEARCH SKILLS

2005-present Purdue University, Indianapolis. Advisor: Dr Sapna K. Deo

- Designed and created novel mutants of fluorescent proteins, utilizing non-natural amino acids, with improved spectroscopic properties
- Explored the metal binding affinity of red fluorescent proteins and metal binding mechanism
- Designed and created molecular fusions, via molecular biology techniques, of fluorescent proteins for isolating, purifying, and exploring protein-protein and protein-peptide interactions
- Developed split fluorescent and bioluminescent proteins for protein complementation assays
- Developed bioluminescent-based detection assays for microRNA
- Bioconjugation experience employing various cross linkers

2004-2005 Purdue University, Indianapolis. Advisor: Dr Paul L. Dubin

- Explored micelle and protein binding to polymers of varying charge density and heterogeneity, via turbidimetric titration and dynamic light scattering studies

PUBLICATIONS

1. Goulding, Ann M., Suresh Shrestha, and Sapna K. Deo, "Exploring Protein-Protein and Protein-Peptide Interactions Using DsRed-Monomer Fusions", *To be submitted*
2. Hunt, Eric A., Ann M. Goulding and Sapna K. Deo, "Direct Detection and Quantification of microRNAs", *Analytical Biochemistry* Vol. 387(1) **(2009)** 1-12
3. Goulding, Ann M., Yasmeen Rahimi, Suresh Shrestha, and Sapna K. Deo, "Dual Function Labeling of Biomolecules Based on DsRed-Monomer" *Bioconjugate Chemistry* Vol. 19 **(2008)** 2113-2119
4. Rahimi, Yasmeen, Ann M. Goulding, Suresh Shrestha, Sweetie Mirpuri, and Sapna K. Deo, "Mechanism of Copper Induced Fluorescence Quenching of Red Fluorescent Protein, DsRed", *Biochemical and Biophysical Research Communications* Vol. 370 **(2008)** 57-61

5. Goulding, Ann M., Suresh Shrestha, Karl Dria, Eric Hunt, and Sapna K. Deo, "Red Fluorescent Protein Variants with Incorporated Non-natural Amino Acid Analogues", *Protein Engineering, Design and Selection* Vol. 21 **(2008)** 101-106
6. Cooper, Christy L., Ann M. Goulding, A. Basak Kayitmazer, Serge Ulrich, Serge Stoll, Sibel Turksen, Shin-ichi Yusa, Anil Kumar, and Paul L. Dubin, "Effects of Polyelectrolyte Chain Stiffness, Charge Mobility, and Charge Sequence on Binding to Proteins and Micelles", *Biomacromolecules* Vol. 7 **(2006)** 1025-1035

BOOK CHAPTER

- Deo, Sapna K., Kyle A. Cissell, Ann M. Goulding, Yasmeen Rahimi, Suresh Shrestha, Biochemistry, structure, and engineering of red fluorescent proteins, Chapter 6, in: "Luciferases and Fluorescent Proteins Technology: Principles and Advances in Biotechnology and Bioimaging," V. R. Viviani and Y. Ohmiya, Eds., *Research Signpost Press, (***2007)**

PRESENTATIONS

1. Goulding, Ann M., Suresh Shrestha, and Sapna K. Deo, "Exploring Protein-Protein Interactions Using DsRed-Monomer Fusions", 62nd Pittsburgh Conference (PITTCON) February 28 - March 5, 2010, Orlando, FL
2. Goulding, Ann M., Kyle A. Cissell, and Sapna K. Deo, "MicroRNA Detection by Renilla Luciferase Split Reporter Complementation Assay", 61st Pittsburgh Conference (PITTCON) March 10-13, 2009, Chicago, IL
3. A. Goulding, Suresh Shrestha, Yasmeen Rahimi, Eric Hunt, and Sapna K. Deo* "Ligand Fishing and Protein Purification Using DsRed-Monomer" Local ACS Meeting, Oct 16, 2008, Muncie, IN
4. A. Goulding, S Shrestha, Y. Rahimi, and Sapna K Deo "DsRed-Based Protein Labeling system: Application in Affinity Purification and Fluorescent Analysis", 60th Pittsburgh Conference (PITTCON) March 2-9, 2008, New Orleans, LA
5. A. Goulding, S. Shrestha, E. Hunt, and S. K. Deo "Variants of DsRed-Monomer with Differing Emission Wavelengths" 39th ACS Central Regional Meeting (CERMACS), May 21-23, 2007, Covington, KY

6. A. Goulding, S. Shrestha, and S. K. Deo "Spectral Evaluation of Red Fluorescent Protein Variants" In Vitro Biology Meeting, June 9-13, 2007, Indianapolis, IN
7. A. Goulding, S. Shrestha, Y. Rahimi, E. Hunt, and S. K. Deo "DsRed-Monomer as Bifunctional Tag", 234th ACS National Meeting, September 9-14, 2007, Boston, MA
8. A. Goulding, S. Shrestha, and S. K. Deo "Biochemical Characteristics of Red Fluorescent Protein Variants with Incorporated Non-natural Amino Acid Analogues" 232nd ACS National Meeting, September 9-14, 2006, San Francisco, CA